Politecnico di Torino

Faculty of Engineering
Master’s Degree in Civil Engineering
Academic Year 2021/2022

Master’s Degree Thesis

Residual safety assessment of corroded offshore steel structures

Supervisor:
Prof. Francesco TONDOLO

Candidate:
Matteo NICCOLI

July 2022

Contents

Abstract

A large number of offshore platform are currently located in our seas, however many of these are destined to have a shorter useful life than they were designed for. This is due to the high rate of deterioration to which they are subject in the marine environment.

In particular, corrosion is a major contributor to the degradation of marine and offshore structures. Therefore it is necessary to understand what kind of corrosion occurs on these structures and what are the environmental factors that determine it.

Finally, the aim of this thesis is to predict long-term corrosion in order to calculate the loss of resistance of aging structures and thus avoid ultimate failure.

1. Structural deterioration of steel constructions

1.1 The degradation phenomena

Although the degradation phenomena almost never act separately it is necessary to conduct all alteration processes to a synthetic and clear system. This makes it possible to recognize the possible acting causes, the various related mechanisms and the final effects on the system within the often complex and articulated manifestations. In this way it will be easier to choose the most appropriate type and methods of intervention.

The natural environment carries out in itself, regardless of human activity, an action tending to transform over time the structure, morphology and chemical composition of the materials exposed to it. The root cause of deterioration is the process that leads to a gradual weakening of the material's structures exposed to the environment.

We speak of "chemical degradation" when the environment acts on the material in order to alter the composition. Chemical alteration occurs mainly due to the presence of water. To this must be added the action of acids which is the factor capable of strongly influencing the aggressiveness of the attack.

On the other hand, under the heading "physical degradation" we use to classify those cases in which environmental factors exert an action on the structures of the materials that subject them to mechanical stress of such intensity as to break them up.

Furthermore, the main causes of alteration of the materials also include the forms of degradation of biological origin. The agents responsible for the biodeterioration of the material are numerous and diversified (they belong to both the plant and animal world).

By restricting the field to steel, the main form of degradation is certainly corrosion. The corrosion process is explained by the tendency of metal, to return to the state of the original mineral from which it was obtained, undergoing a reduction of its own free energy. In fact, the behaviour of metals is conditioned by their atomic structure, which tends to lose electrons; the atoms of the element bind in an orderly manner, letting the outermost electrons freely circulate among them, forming the so-called "atomic glue" and determining the thermal and electrical conductivity of the material, as well as its ability to bind to other elements.

The inevitable formation of a surface patina on the metal exposed to air derives from this last characteristic, resulting from the reaction between metal and oxygen or other environmental component.

Corrosion of metallic material can be divided into two types according to the nature of the phenomena: wet and dry corrosion.

- In wet corrosion, the mechanism is an electrochemical type in which the corrosion process is the product of an anodic dissolution process of a metallic material (with the release of electrons) process in which chemical particles are present in the environment. Thus, wet corrosion can be described by the laws of thermodynamics and kinetics of electrochemistry. Wet corrosion occurs in the presence of water; therefore, it can occur in case of immersion of the metal and also of condensation.
- In dry corrosion, a chemical type is used instead of a mechanism. This phenomenon is described by the laws of thermodynamics and kinetics of heterogeneous reactions. The oxidation that generates the patina is the most natural case of dry corrosion.

1.2 Detecting corrosion

The following quotation from Fontana and Greene’s classic textbook on corrosion engineering originally published in 1967 summarizes a training principle that has been reused extensively by many instructors and that is central in all modern training manuals on the subject:

“It is convenient to classify corrosion by the forms in which it manifests itself, the basis for this classification being the appearance of the corroded metal. Each form can be identified by mere visual observation. In most cases the naked eye is sufficient, but sometimes magnification is helpful or required. Valuable information for the solution of a corrosion problem can often be obtained through careful observation of the corroded test specimens or failed equipment.” [1]

It is now widely accepted that much can be deduced from examination of materials which have failed in service and that it is often possible by visual examination to decide which corrosion mechanisms have been at work and what corrective measures are required. In another widely used NACE document, Paul Dillon and his co-authors have grouped the eight forms of corrosion depicted graphically in Scheme 1 in the following three categories:

Group I: Corrosion problems readily identifiable by visual examination.

1. Uniform corrosion is characterized by an even, regular loss of metal from the corroding surface.

2. Localized corrosion during which all or most of the metal loss occurs at discrete areas. In this scheme crevice corrosion is said to be a particular form of pitting usually due to localized differences in the environment (pitting, crevice).

3. Galvanic corrosion occasioned by electrical contact between dissimilar conductors in an electrolyte.

Group II: Corrosion damage that may require supplementary means of examination for identification.

4. Velocity effects include erosion–corrosion, a form of attack caused by high velocity flow; cavitation caused at even higher flow by the collapse of bubbles formed at areas of low pressure in a flowing stream; and fretting that is caused by vibratory relative motion of two surfaces in close contact under load (erosion–corrosion, cavitation, fretting).

5. Intergranular corrosion at the grain boundaries in the metal structure (intergranular, exfoliation).

6. Dealloying corrosion due to the selective dissolution of one component of an alloy.

Group III: Corrosion specimens for these types should usually be verified by microscopy of one kind or another.

7. Cracking phenomena includes corrosion fatigue, a mechanical phenomenon enhanced by nonspecific corrosive environments, and environmental cracking, in which a brittle failure is induced in an otherwise ductile material under tensile stress in an environment specific for the alloy system (stress corrosion cracking, fatigue).

8. High-temperature corrosion (scaling, internal attack).

9. Microbial effects caused by certain types of bacteria or microbes when their metabolism produces corrosive species in an otherwise innocuous

environment, or when they produce deposits which can lead to corrosion attack.

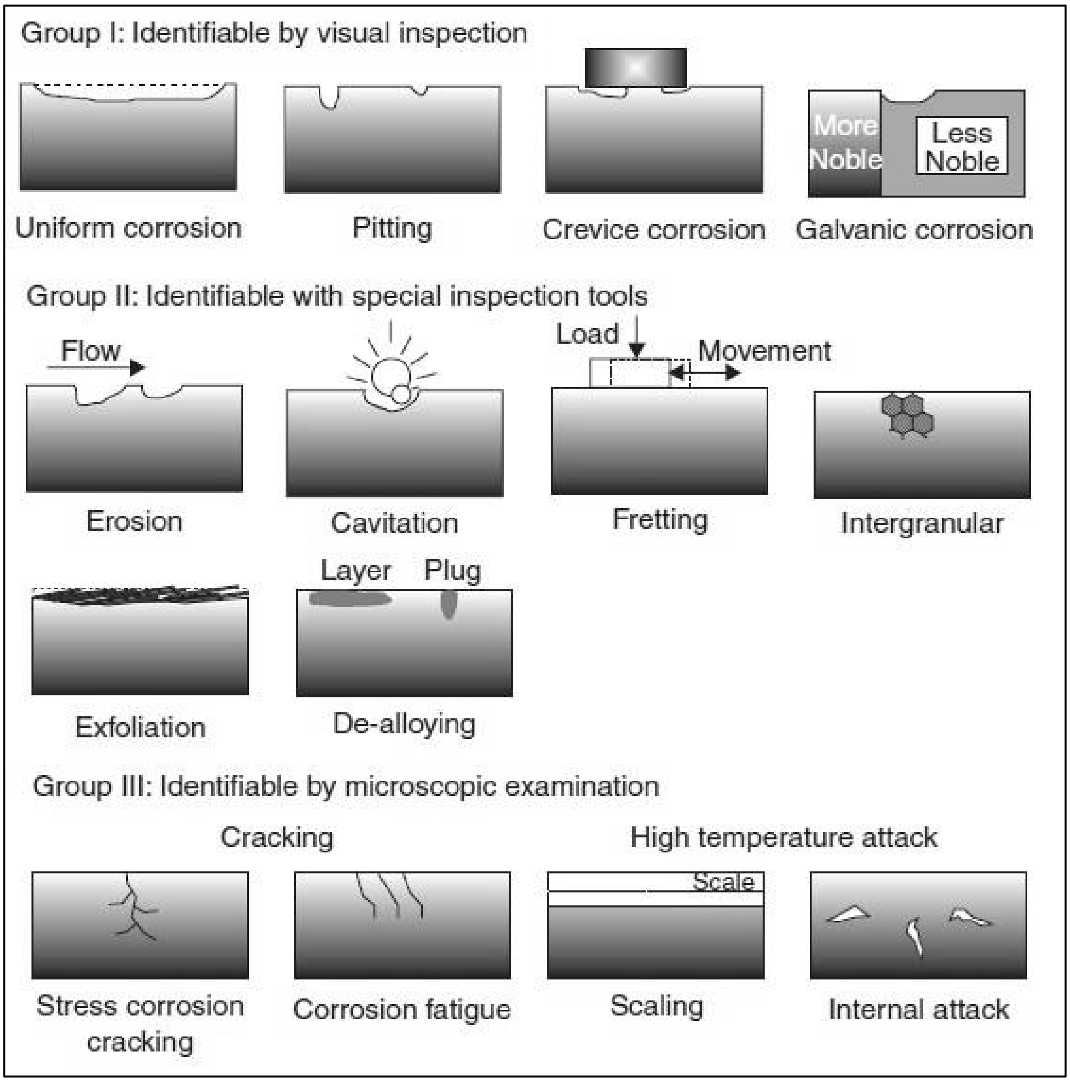

Table 1.1 - Main forms of corrosion attack regrouped by ease of identification [1].

These corrosion forms could also have been organized on the basis of other factors than their visible appearance or inspectability. The degree of localization, for example, would be a way to organize corrosion problems as a function of the surface selectivity of attack.

Another method to organize corrosion problems would be by using metallurgical features of importance such as the grain structure of a metallic material. A common type of corrosion attack for which the grain structure is important is intergranular or intercrystalline corrosion during which a small volume of metal is preferentially removed along paths that follow the grain boundaries to produce what might appear to be fissures or cracks. Intergranular and transgranular corrosion sometimes are accelerated by tensile stress. In extreme cases, the cracks proceed entirely through the metal, causing rupture or perforation. This condition is known as stress corrosion cracking (SCC).

While the types of corrosion identified in Scheme 1 are described individually in the following sections it should be recognized at the onset that during any damaging corrosion process these types often act in synergy. The unfolding of a crevice situation, for example, will typically create an environment favorable for pitting, intergranular attack, and even cracking.
The actual importance of each corrosion type will also differ between systems, environments, and other operational variables.

1.3 Types of corrosion

There are various types of corrosion, some are very common and can be seen in day-to-day life, while there others are rarely seen except in very specific combinations of material and environments. Let's see how they differ [2].

a) Atmospheric Corrosion
b) Erosion Corrosion
c) Selective Corrosion
d) Uniform Corrosion

e) Pitting Corrosion

f) Fretting Corrosion

g) Stress Corrosion

h) Inter-granular Corrosion

i) Corrosion Fatigue

a) Atmospheric Corrosion

Atmospheric corrosion is a type of wet corrosion caused by the action of electrolytes. The initial stage of atmospheric corrosion is characterized by the formation of a layer of thin-film electrolyte (see Figure 1.1a). This layer can be formed by rain, dew, and condensation of high RH (Revie, 2011). In moderate climates, this film is formed due to condensation, which typically occurs in the morning, when the metal surface is cooler than the surrounding air and the relative humidity goes above a certain threshold. In this case, moisture present in the atmosphere, rainwater, etc. acts as electrolytes triggering corrosion of the exposed metal surface.

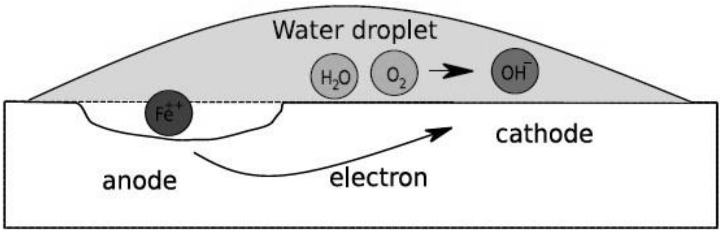

Fig. 1.1a - Schematic representation of atmospheric corrosion of steel

Fig 1.1b - Atmospheric Corrosion

b) Erosion Corrosion

Erosion corrosion is caused by mechanical abrasion due to the relative movement between metal surfaces and corrosive fluids. In this case, the surface of metal gets deteriorated gradually by the abrasion of fast-moving fluids and cavities are also formed. This type of corrosion commonly seen in metal tubes carrying moving fluids in it.

Fig 1.2 - Erosion Corrosion

c) Selective Corrosion

Selective corrosion occurs in alloys where one of the component metals is de-alloyed by the corrosive environment. This type of corrosion can be seen in brass alloy pipes where zinc is commonly used as another component and here zinc is de-alloyed. Similarly in the case of copper-nickel alloy tubes where nickel is de-alloyed by selective corrosion.

Fig 1.3 - Selective Corrosion of Brass Pipe

d) Uniform Corrosion

In case of uniform corrosion, a uniform layer of rust is formed on the surface of metals and it is extended over the whole surface area of metal. This type of corrosion can be seen in metals which are not protected by surface coating.

Aluminium, zinc, lead, etc. are some metals commonly affected by uniform corrosion.

Fig 1.4 - Uniform Corrosion

e) Pitting Corrosion

Pitting is the formation of rust pits or holes on the surface. Pitting corrosion is a localized form of corrosion where the corrosion is limited to small areas. The shapes of rust pits may not be similar but in most of the cases, they are hemispherical in shape. Figure 5a shows the most common forms of pit.

Pitting corrosion occurs when the protective oxide layer of the surface gets damaged or due to structural defects in metal. It is considered more dangerous because it causes the failure of structure with a relatively low overall loss of material. It can be observed in steel, aluminium, nickel alloys, etc.

Pitting can consist in various stages: passive film breakdown (passive films are present on the surface of the stainless steels in the presence of oxygen), pit initiation, metastable pitting, pit growth and pit stifling. Any of these stages may be considered to be critical. Pitting corrosion capitalizes on breakdown in the protective layer, either natural or applied, and provides a nucleation point for the formation of pits in the presence of an electrolyte containing an aggressive anion. Once the passive film breaks down and a pit initiates, there is a possibility that a single pit will grow.

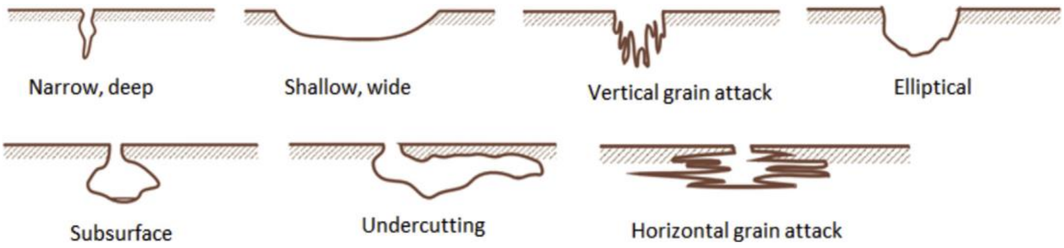

Fig 1.5a - Sketch of common pit shapes

Fig 1.5b - Pitting Corrosion

f) Fretting Corrosion

Fretting corrosion occurs at the contact area of the two materials which are joined together. This is developed when the contact area is subjected to slips and vibrations. This type of corrosion can be seen in bolted and riveted joints, clamped surface, etc.

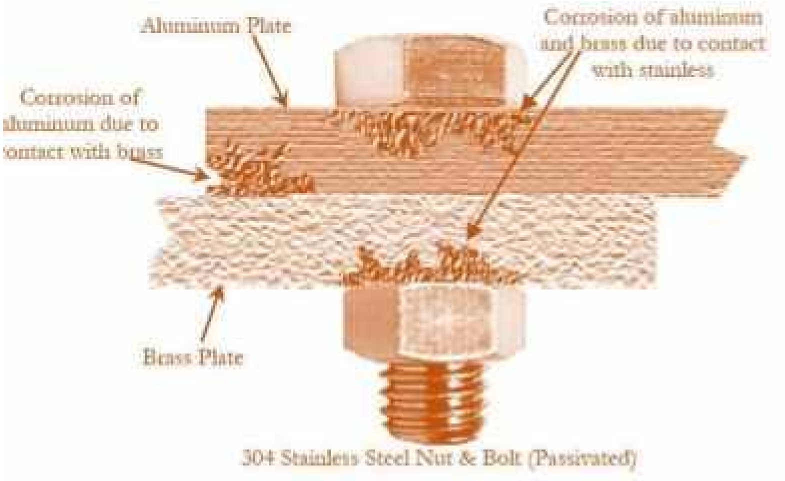

Fig 1.6 - Fretting Corrosion

g) Stress Corrosion

Stress corrosion caused by the combined action of a corrosive environment and mechanical stress on the surface of the material. In its initial stage, small cracks are developed and these finally leads to failure of the whole structure. This type of corrosion can be seen in stainless steel when they are stressed in chloride environments, in brass materials when they are stressed in the presence of ammonia, etc.

Fig 1.7 - Stress Corrosion

h) Inter-granular Corrosion

Inter-granular corrosion is the corrosion that occurs along the grain boundaries and the grains are not affected in this case. It is caused when there is a noticeable difference in reactivity against impurities exists between grain boundaries and grains. This difference in reactivity occurs due to defective welding, heat treatment stainless steels, copper, etc.

Fig 1.8 - Inter-granular Corrosion

i) Corrosion Fatigue

Fatigue of materials is defined as the failure of a material due to repeated application of stress. When the fatigue of metal is developed in the corrosive environment then it called corrosion fatigue. This can be prevented by improving the fatigue resistance of a material.

Fig 1.9 - Corrosion Fatigue

1.4 Corrosion principles

To understand corrosion of a metal it is important to know the path taken to refine that metal from its natural form (ore) to its usable form, and subsequent processing and any heat treatment that may have been applied to the material to make it useful [3].

Thermodynamics, the science of the flow of energy, explains a specific corrosion process and indicates if corrosion is possible in a given metal and environment. The flow of energy in the corrosion process is in the form of electrical energy. The rate of corrosion is similarly predicted by the kinetics.

As we know, with the exception of a few naturally occurring metals, most engineering materials are found in the form of ores, often metal oxides found in nature. A lot of energy is spent in the extraction process of these usable metals from their ores. Hematite ($Fe2O3$) is an ore of iron, and bauxite ($Al2O3*H2O$) is an ore of aluminum, there are some more complex ore like that of Nickel ore kupfer-nickel, smaltite ores are a combination of sulphur and arsenic which are roasted to form an oxide which is then reduced to the metal by hydrogen and purified by the Mond process to obtain nickel that engineers can use. Copper is found as pure metal; that is the reason copper is usually free from corrosion, but it is also extracted from various ores like Ruby ore ($Cu2O$), Copper Glance ($Cu2S$), or Pyrite ($CuFeS2$). It may be pointed out that copper obtained from nature and copper extracted from ores would display different potentials.

A lot of energy is put into the extraction of engineering metals. Some metals that are extracted as free metals from the earth and do not require additional energy to convert the natural form to make it usable are very low in corrosion galvanic energy. These metals are called Nobel metals.

In the galvanic table, Table 1.2, metals are listed from the more negative potentials (Active) to more positive (Noble).

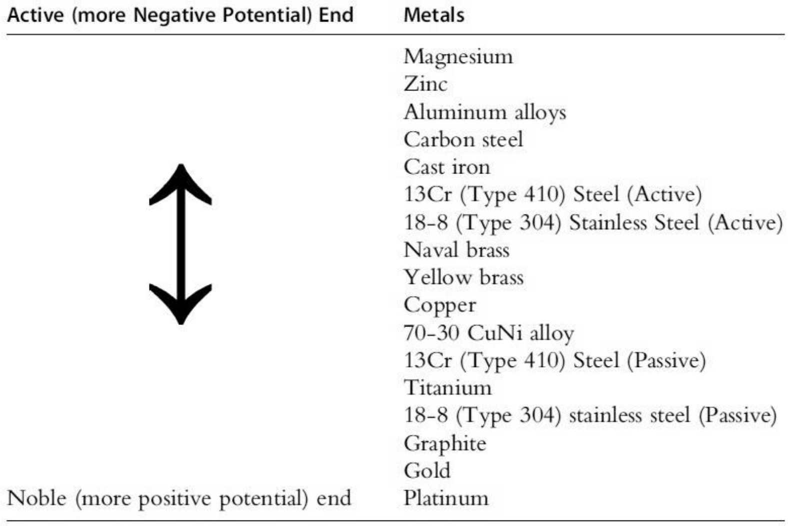

Active (more Negative Potential) End	**Metals**
	Magnesium
	Zinc
	Aluminum alloys
	Carbon steel
	Cast iron
	13Cr (Type 410) Steel (Active)
↕	18-8 (Type 304) Stainless Steel (Active)
	Naval brass
	Yellow brass
	Copper
	70-30 CuNi alloy
	13Cr (Type 410) Steel (Passive)
	Titanium
	18-8 (Type 304) stainless steel (Passive)
	Graphite
	Gold
Noble (more positive potential) end	Platinum

Table 1.2 - Galvanic Series

In the galvanic series table, a new term, “potential,” is introduced in relation to corrosion; it is one way of measuring the energy difference between two metals. Electrons flow from a higher energy state anode, which is a negative, to a low energy electrode, a cathode. The potential difference between two electrodes facilitates the flow of electrons. If a voltmeter of sufficient sensitivity is attached across the flow circuit, the potential difference between anode and cathode can be measured. The potential of each metal in reference to another is a unique number, these numbers by themselves do not establish a standard by which to measure and compare all possible potential differences and thus it is not of much practical use except in relation to the two metals. One unified scale is needed to compare and establish a universal reference for understanding the potential difference of various metals.

For this purpose, a standard electrode is used; a reference electrode is so constructed that its potential is reproducible. There are a number of standard electrodes that are used as reference electrodes.

For most common engineering materials corrosion is electrochemical in nature and occurs in an aqueous environment. The aqueous environment is the electrolyte in the corrosion process, through which the electron travels from anode to cathode (i.e., high-potential to low-potential metal). The corrosion process involves the removal of electrons (oxidation) of metal and the consumption of those electrons is termed reduction reactions, often indicated by the presence of oxygen or reduction of water from the aqueous environment, electrolyte, etc. The following reactions illustrate these points.

1. The basic process at an anodic site is the release of iron (Fe) from the steel surface into the environment:

   $Fe \rightarrow Fe^{++} + 2e^-$ (removal of electrons - oxidation process, ananodic reaction)

2. During the process, two electrons ($2e^-$) are generated which must be consumed by the environment (in aerated systems) and can be expressed as:

   $O_2 + 2H_2O + 4e^- \rightarrow 4OH^-$ (presence of oxygen - reduction and evolution of hydrogen ions, a cathodic reaction)

3. A summary of these half reactions can be expressed as:

   $2H_2O + 2e^- \rightarrow H_2 + 2OH^-$ (aqueous environment - reduction and evolution of hydrogen ions of water, a cathodic reaction)

$Fe(OH)_2$, iron oxide, can be oxidized to form the red-brown $Fe(OH)_3$ commonly referred to as rust. The corrosion three stages of cells are shown in Figure 1.10.

These reactions can occur within a metal itself (Half-Cell) even though they are not physically separated; when they are physically separated the reaction is referred to as a corrosion cell. From the above basic description of corrosion, we can deduce that a corrosion cell must have the following four components to be active.

1. An anode (the location from where electrons are emitted and corrosion with metal loss occurs).

2. A cathode (the location where electrons collect).

3. A metallic path (often the structure itself provides that metallic path).

4. An electrolyte, in which the anode and cathode are immersed (the electrolyte could be any moist surface or immersion in any conducting fluid, water, or soil).

If we remove any one of these four essential elements from the corrosion cell, the corrosion action will stop.

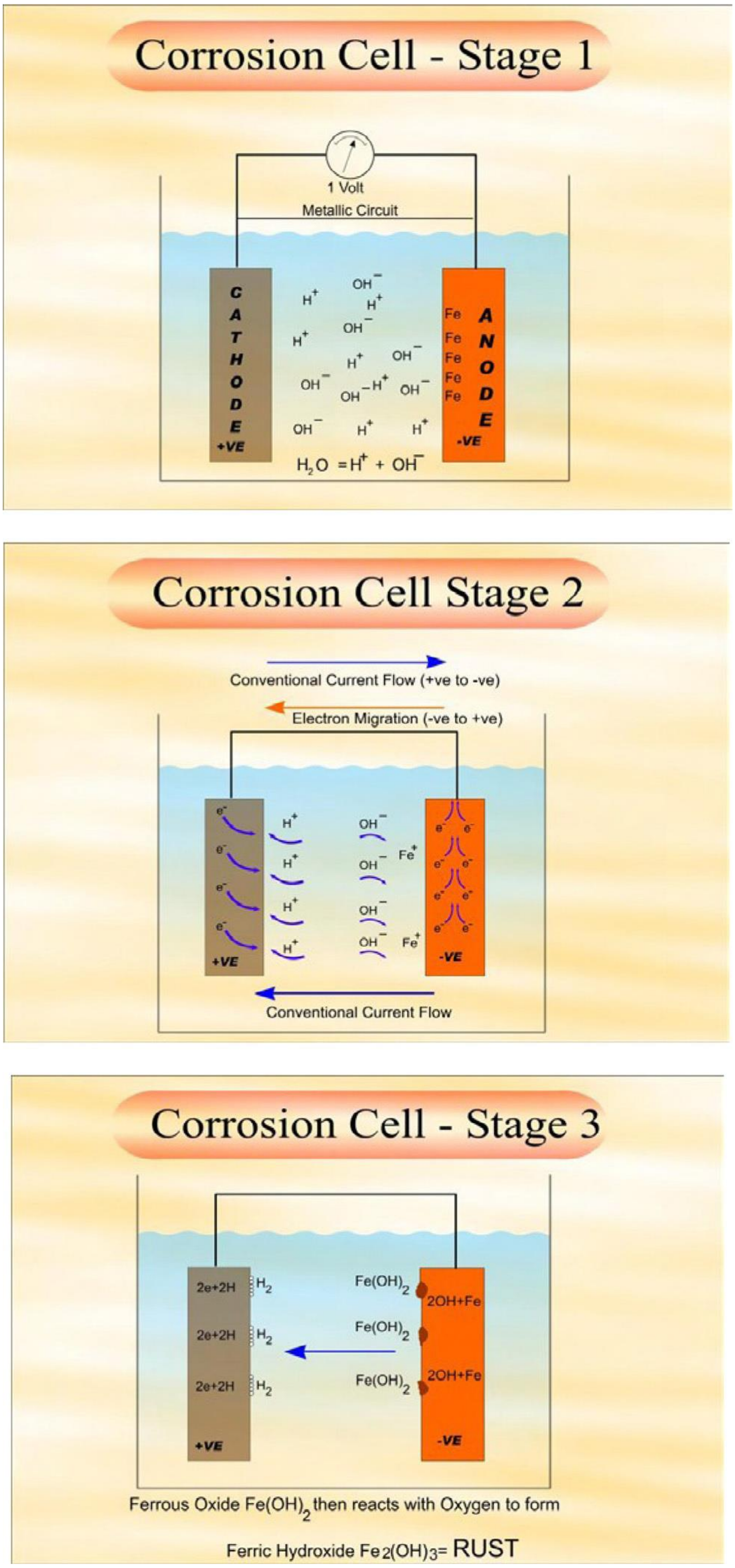

Corrosion Cell - Stage 1

$H_2O = H^+ + OH^-$

Corrosion Cell Stage 2

Conventional Current Flow (+ve to -ve)

Electron Migration (-ve to +ve)

Conventional Current Flow

Corrosion Cell - Stage 3

Ferrous Oxide $Fe(OH)_2$ then reacts with Oxygen to form

Ferric Hydroxide $Fe_2(OH)_3$= RUST

Fig. 1.10 - Three stages of corrosion cells [3]

The oxidation reaction is an anodic reaction in which the metal loss occurs, while the reduction reaction is a cathodic reaction. Both these reactions are electrochemical in nature and are essential for corrosion to occur. The oxidation loss at the anode must be balanced with consumption of emitted electrons at the cathodic end. This charge neutrality is very essential for the corrosion process to occur and continue. If, however, this is not maintained and the accumulation of large negative charges between the metal and electrolyte occurs, then gradually the reaction reduces and eventually stops the corrosion process. This is utilized to an advantage in a cathodic protection system as we discuss in later chapters, where the process of providing Cathodic Protection is used to prevent metals from corrosion.

1.5 Electrochimical mechanism of corrosion

In a corrosion reaction, a partial electrochemical step occurs which is influenced by the electrical variables that include the current flowing (I), potential difference (voltage V), electrolyte to metal interface, and the extent of electrical resistance to electrical current flow [3].

In an aqueous media, the action is similar to a dry cell, where the carbon electrode in the center and the zinc cap is separated by sodium chloride (Na_4Cl) electrolyte. In this cell the carbon electrode in the positive pole, at the carbon electrode chemical reduction occurs and at negative pole is the zinc electrode where oxidation takes place. In this reaction, metallic zinc is changed into zinc ions, thus corroding the zinc electrode. The rate of corrosion is linked to the rate of electricity produced. This relationship is quantitative and it is explained with the help of Faraday’s law:

$$W = kIt \tag{1.1}$$

where: W is the weight of metal reacting; k is a constant for the metal, for zinc this value is 3.39×10^{-4} g/C (gram per coulomb); t is the time in seconds; and I is the flow of current in amperes.

One coulomb is the measure of electricity produced by the flow of 1 amp, for 1 s.

In the dry cell example, the metal zinc is in an active cell, the metal is constantly corroding; however, if the circuit is broken and the current stops flowing, the zinc stops corroding. Any other metal surface in a similar situation behaves similarly, that is, the metal surface corrodes if it is in the electrical circuit and stops corroding if removed from that electrical circuit. If the metal is embedded with impurities, the current can flow from one spot to another within that metal as an electrical cell is created within the metal itself. This phenomenon of electrical circuits in the presence of an electrolyte is called local action cell or simply local cell. Any process that reduces the presence of impurities in a metal improves the corrosion resistance of that metal. This explains why purified aluminum and magnesium are more resistant to corrosion in seawater than several of their commercial versions.

But this does not mean that pure metals do not corrode. As we have briefly pointed out, the local action cell causes corrosion, but this local cell can be caused not only by inherent impurities but also by the variations of structure within the metals, temperature, and environment. The best examples of these are the corrosion cells between the parent metal and weld metal, the corrosion of high-purity iron in air saturated with water which is nearly the same as commercial grades of iron in water.

The electrochemical aspect of corrosion gives us an opportunity to detect and mitigate the corrosion of structures. We can monitor the potential difference measured in volts and the currents associated with the existing corrosion process.

The energy difference between anode and cathode can help us determine if there exists a corrosion cell. This is, in fact, the measure of electrical potential between two points. The energy difference causes a potential difference which causes the flow of electrons. If a voltmeter is inserted in the circuit, we can measure the potential difference in volts.

2. Corrosion impact on offshore platforms

2.1 Fundamentals of offshore structures

In this thesis we want to investigate the structural degradation in offshore structures, for which the marine environment represents the most unfavourable environmental condition towards steel corrosion.

Offshore structures are types of systems built for oil and natural gas production in general. An offshore platform, or offshore drilling rig is a large structure with good drilling facilities for exploring, extracting, storing, and processing oil and natural gas contained in rock formations below the seabed. Many oil platforms will have facilities to accommodate the workforce [5].

It is estimated that as time progresses in the world, offshore construction technology will advance further. Among the reasons for this is the increasing trend of energy needs in the world, the decrease in energy reserves on land, and the loss of new oil deposits and new funding sources can be listed. Until the 1950s, shipbuilding and fishing technology were the first to come to mind when it came to offshore technology. However, today, oil and natural gas research on the open sea and parallel to this, extraction of these natural resources from the bottom of the oceans has become much more critical. The economic benefits of oil and natural gas production under the sea are significant. Mostly oil and natural gas drilling, for their extraction, processing, and transportation of the extracted raw material, it is necessary to design and manufacture tools and equipment that were not used until then. In this context, new technologies were needed, and studies on this subject have intensified.

There is an essential need for marine structures today, and their number is increasing day by day in this direction. Since 1940, offshore structures have been built as fixed structures. The water depth of these fixed offshore structures is also increasing.

Typical offshore structures today would include [28]:

- Fixed platforms: Fixed platforms are the offshore production mainstay with economic water-depth limits of about 450 m.
- Compliant towers: Floating platforms permanently anchored to the bottom. May be considered for water depths of about 450 to 900 m.
- Tension-leg platforms: These structures are attached to the ocean bottom with tendons held in tension. They are used in 450 to 2100 m water depths.
- Spars: Buoyant structures shaped like a spar (a single, large-diameter cylinder), with a functional deck mounted on top. They are used in 2100 to 10000 m water depths.
- Semi - submersible production units: They can permanently be moored in a field usually producing from subsea facilities.
- Floating production, storage, and offloading (FPSO) systems: Ship shaped vessels with storage and some treatment facilities. Serves both floating and subset production arrays. May be used in water depths ranging up to and beyond 3048 m.
- Pipeline systems: Steel pipelines transporting oil and gas in various diameters and operating in various water depths.

Figure 2.1 graphically shows various types of offshore structures and their typical locations in relation to the shore and depth of waters in which they are installed.

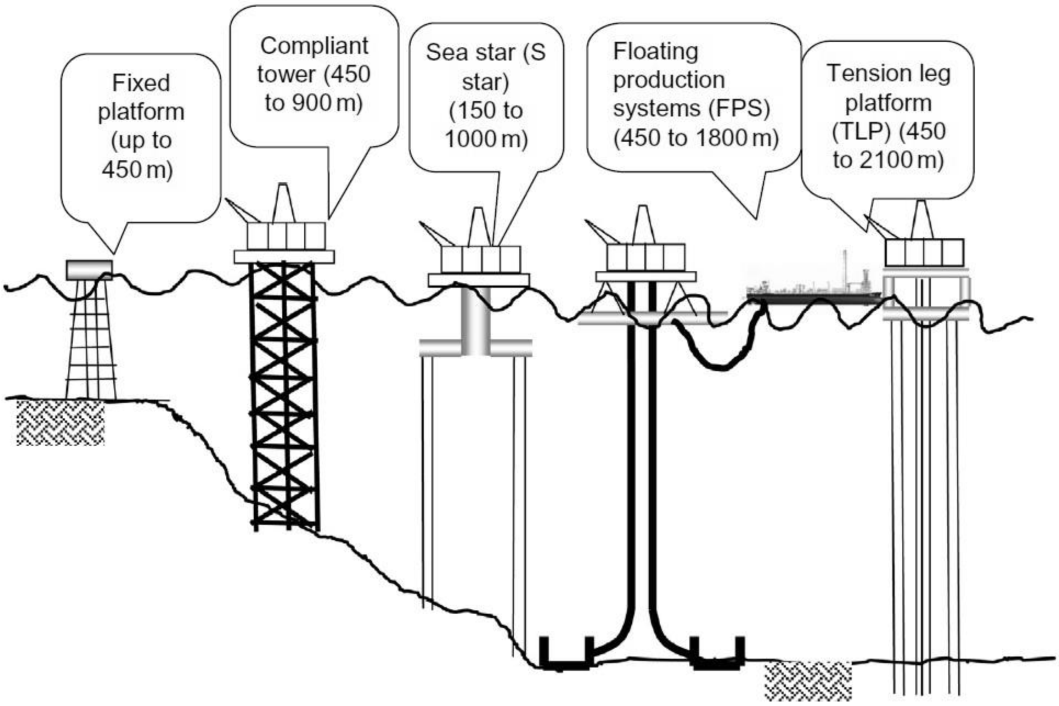

Fig. 2.1 - Various types of offshore structures and their typical locations [27].

A typical structure consists of various modules including a deck, a substructure, foundation piles, piping etc. The substructure in most cases, is a prefabricated tubular space frame, which in shallow to intermediate water depths extends from the sea floor to just above the sea surface, and is usually fabricated in one piece onshore, transported by barge, launched at sea, and upended on site by partial flooding.

Tubular pilings are driven through the main legs to fix the structure to the sea bottom, provide support for the deck, and resist the lateral loads due to wind, waves and currents. Various other structural designs exist to cater for deeper water [28].

Just as every building has a lifetime, offshore structures also have a working life. However, offshore structures have different features than classical structures due to their working conditions. In general, terms, since these structures are intertwined with petroleum raw materials, the probability of fire, explosion, and such events is much higher than the probability of occurring in a typical structure. The material to be used in offshore structures (include low to medium carbon manganese steels, high strength low alloy steels, standard and super austenitic stainless steels, duplex and super duplex stainless steels as well as nickel base, copper base, and titanium alloys) must also be of very high quality and be of higher quality than the concrete or steel used in typical structures since it is in contact with seawater. The most important feature of these materials is that they must be resistant to corrosion [7].

In fact, corrosion is one of the main causes of failure, as we can see in the following diagram:

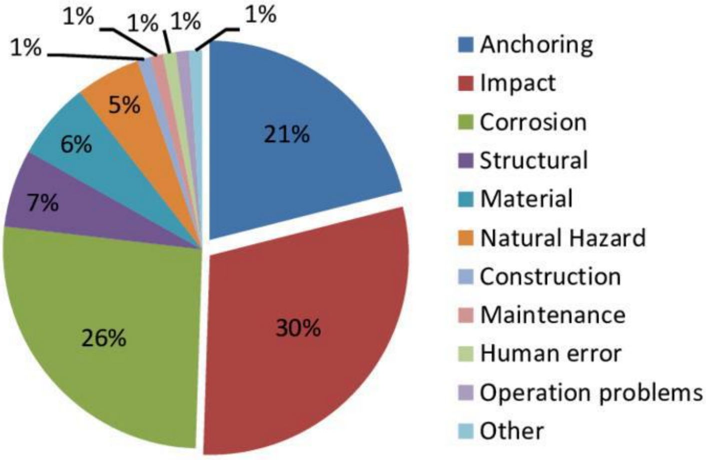

Diagram 2.1 - Causes for failure [6]

2.2 Exposure areas

Offshore platforms are exposed to five corrosion zones that include Atmospheric Zone, Splash Zone, Tidal Zone, Submerged Zone, and Subsoil Zone. Corrosion in these zones is an electrochemical process.

Studies carried out on carbon steel (CS) coupons placed in the different zones on a CS pipe pile in the Atlantic Ocean show where corrosion rates at the different zones lie within the boundaries shown in Figure 2.2.

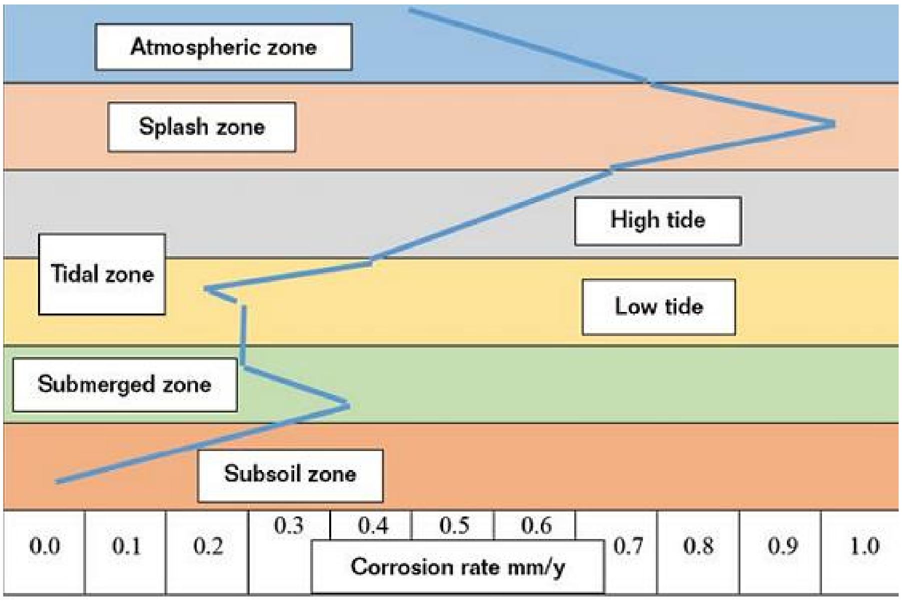

Fig. 2.2 - A depiction of corrosion rates at corrosion zones along a CS pile in the ocean [4].

Atmospheric Zone

The corrosion rate within this zone depends on the height above sea level. At ~13 m high, the rate is ~0.4 mm/y and this increases to ~0.7 mm/y as it gets closer to sea level. This is due to the sodium chloride (NaCl) entrained in air and sea sprays deposited on the metal due to the wind action. A higher chloride concentration on the metal, with time, accelerates corrosion.

Splash Zone

The highest corrosion rate occurs at this zone, at ~0.95 mm/y. This is due to the high oxygen and chloride content of the recurrent splashing of seawater, which destroys any protective film that might be formed on the steel surface.

Tidal Zone

This zone consists of both high-tide and low-tide regions. In high-tide regions, the corrosion rate ranges from 0.65 to 0.35 mm/y. Low-tide regions have a lower corrosion rate of ~0.15 mm/y, and this is due to a differential cell between the low-tide region and the peak of the adjacent submerged zone. At low tides, when the steel surfaces are exposed to the atmosphere, the corrosion products, iron oxide (FeO), are oxidized to higher oxidation states, resulting in a more noble corrosion potential. Then, when the surfaces are submerged during high tide, the noble region acts as the cathode, with the reduction of the oxides on its surfaces.

Submerged Zone

This zone has a corrosion rate of ~0.35 mm/y. Further down the steel surface, corrosion is governed by the rate of diffusion of oxygen through the water and marine growth present on the metal surface.

Subsoil Zone

At this zone, the corrosion rate is controlled by the availability of oxygen in the soil and depends on whether the soil is considered disturbed or undisturbed. It is also affected by microbial activities. In undisturbed soil the corrosion rate can go to 0.03 mm/y.

2.3 Factors that affect marine atmospheric corrosion rate

According to Ting et al. (2011), the corrosion rates of structural steel in the harsh environments of coastal areas, harbours and oceans has an impact on the economic benefit of marine structures, as steel loss and pitting can have major effects on structural protection and efficiency. With a growing focus on keeping existing structures in operation for longer time spans and thereby deferring replacement cost, there is a growing interest in predicting corrosion rates at a given location for a given duration of exposure once the protection (coatings or cathodic protections) is lost [8].

Paul (2012), stated that because of the wide range of parameters that control the corrosion rate, predicting the corrosion rates of steel structures in the universal marine environments is a difficult task. The key factors that affect the rate could include; salinity, sulfate, dissolved oxygen, pH as well as temperatures. Although the individual impacts of these factors on corrosion are well understood, the combined influence of these factors together are complicated and unknown.

Valdez et al. (2016) stated that, throughout the erosion processes, marine frameworks lose wall thickness at a rate that differs with depths. Steel corrosion rates in seawater are normally between 0.1-0.3 mm/year, but in seawater polluted with corrosive effluents, can reach 2-4 mm/year.

According to the work done by (Khodabux et al., 2020), some examples about corrosion rates from different locations are shown in Table 2.1.

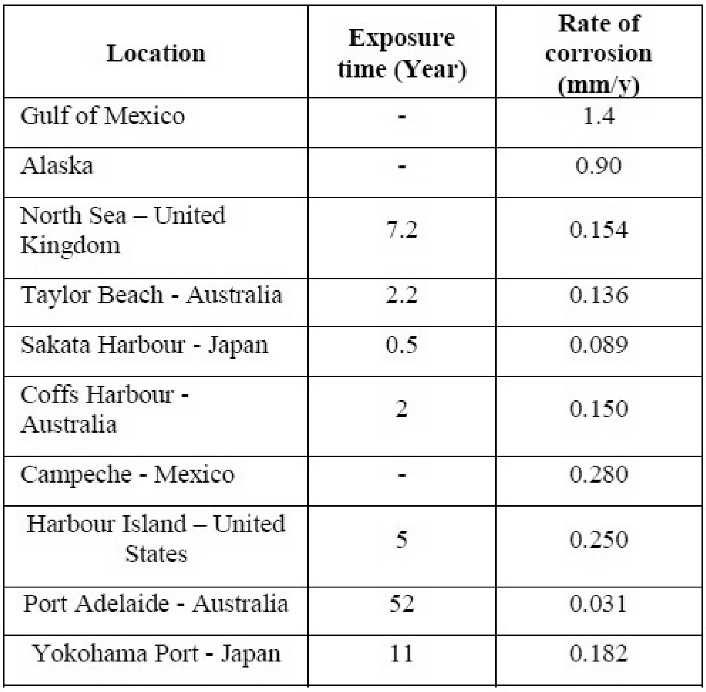

Location	Exposure time (Year)	Rate of corrosion (mm/y)
Gulf of Mexico	-	1.4
Alaska	-	0.90
North Sea – United Kingdom	7.2	0.154
Taylor Beach - Australia	2.2	0.136
Sakata Harbour - Japan	0.5	0.089
Coffs Harbour - Australia	2	0.150
Campeche - Mexico	-	0.280
Harbour Island – United States	5	0.250
Port Adelaide - Australia	52	0.031
Yokohama Port - Japan	11	0.182

Table 2.1 - Examples on corrosion rates from different locations [8]

Structural failure of offshore structures may result in loss of human life, severe environmental damage, and large economic consequences. Therefore, offshore structures must be designed with adequate safety and reliability, and their designs must be acceptable from an environmental and economic point of view. Environmental data and models represent a necessary and important input to load and response calculations of offshore structures. They should be based on the state-of-the-art met-ocean description. Related relevant uncertainties in met-ocean data and models are also a part of such input.

The design practice is moving gradually towards a more consistent probabilistic approach, for example: extremes are determined for a given return period (e.g. expected lifetime of the structure).

Typical factors that affect atmospheric corrosion rate of structures, platforms, and vessels in a marine environment include [4]:

- **Relative humidity (RH)**

Corrosion rates increase with increased RH. The typical marine atmosphere ranges between 80 and 85% RH. The moist, humid environment increases the rate of corrosion by increasing TOWs (Time Of Wetness is defined as the period of time when the relative humidity is above 80% and the temperature is over 0°C).

In most applications where relative humidity is used as an accelerating variable, the Peck accelerating model is employed, which is expressed as [9]

$$r\,(RH) = A * RH^{B} \qquad (2.1)$$

where: RH is a proportion denoting relative humidity and A , B are constants.

- **Temperature**

Increased ambient temperatures increase the atmospheric corrosion rates. The temperature during the summer day are usually in the 30s (ºC), which is a high range for atmospheric corrosion of steel in high humidity. Temperature also affects RH, TOW, and dew point, as we can see in figure 2.3:

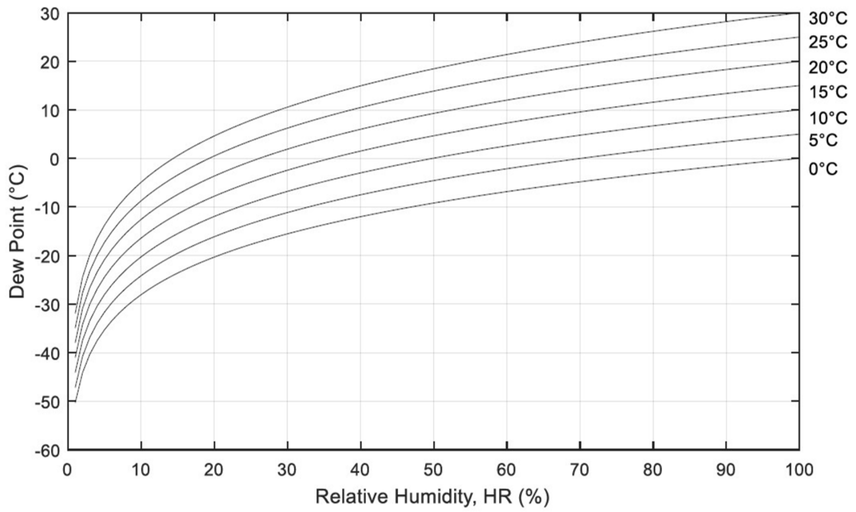

Fig. 2.3 - Relation between dew point temperature, relative humidity and metal surface temperature

Theoretically, the effect of temperature on atmospheric corrosion rate is typically described with the Arrhenius relation, which follows [9]

$$r\,(T) = D * e^{-E/T} \qquad (2.2)$$

where: r (T) is the corrosion reaction rate, D is a constant; T is the thermodynamic temperature in Kelvin; $E = E_a / K$, where E_a is the activation energy which can be estimated from experimental data, and K is the Boltzmann constant.

Sea temperature is also an important parameter in seawater corrosion because it usually accelerates corrosion by increasing the temperature. However, as the temperature rises, the solubility of oxygen decreases, which also weakens the temperature effect.

Based on the experimental evidence, a correlation factor is proposed to adjust for the effect of temperature. It is assumed that corrosion rate is a linear function of temperature for seawater temperatures below 80 °C [9]:

$$R(T) = c*T + d \qquad (2.3)$$

where: R(T) is the corrosion rate correction factor for temperature (corrosion rate at actual temperature / corrosion rate at nominal conditions), T is the temperature ratio (actual temperature / nominal temperature), c is the constant representing the slope of the R(T)-T relationship and d is the constant represents the R(T) value at zero T.

- **Wind speed**

Winds bring salt-laden moisture picked up from the ocean spray. The droplets and/or salt dust are then deposited on the metal surfaces that is in their wind path. Intense corrosion occurs on surfaces facing the prevailing winds, while little or no corrosion occurs in the sheltered areas behind.

- **Salinity**

Seawater is extremely corrosive due to its high salt content. The salinity of seawater is composed of about 90% sodium chloride (NaCl). The dissolved salt leads to a low resistivity so that the seawater acts as a good electrolyte, thereby enabling pitting corrosion. The salinity of seawater generally is 35 ppt and far higher than river water which is only 0.02 ppt. Thus, marine corrosion occurs easily and accelerates the corrosion rates. The higher the salinity of the water, the faster chloride ions succeed in penetrating the protective film. But the corrosion rates do not rise all the time with the salinity rising. Test shows that corrosion rates reach the maximum when the salinity is 32 to 35 ppt, namely the salinity of natural seawater.

This is due to the effect of salinity on the corrosion reaction. On one hand, the transfer speed of the charge is accelerated with the increase of the salinity of the seawater. On the other side, with the salt concentration increasing, the solubility of oxygen in the seawater is decreasing so that the corrosion rate will be reduced. When the salinity is less than the natural sea, the influence of electrical conductivity is dominated. When the salinity exceeds the natural sea water salinity, the increase of salinity causes the decrease of oxygen content to exceed the increase of electrical conductivity. In this case, the corrosion rate decreases with the increase of salinity.

The relation between the corrosion rate correction factors for salinity and salinity ratio, based on the results presented by Uhlig and Revie, can be modelled by a truncated log-normal function as [9]

$$\mathrm{R(S)} = \frac{\gamma}{\varepsilon\sqrt{2\pi(S+\delta)}} * e^{\left[-\frac{(ln(S+\delta)+\beta)^2}{2\varepsilon^2}\right]} \tag{2.4}$$

where: R(S) is the corrosion rate correction factor for salinity (corrosion rate at actual salinity / corrosion rate at nominal conditions), S is the salinity ratio (actual salinity / nominal salinity). γ is a constant introduced as a magnification factor to adjust the values of the corrosion rate correction factor ($\gamma \geq 0$). δ is a constant introduced to adjust the truncated portion ($\delta \geq 0$). β, and ε are constants corresponding to mean value and standard deviation of the distribution. It must be stressed that this function has been chosen just to represent the form of the curve and not as a probability density function.

- **Dissolved oxygen**

Because the corrosion of most metals in seawater is oxygen depolarization corrosion, the content of dissolved oxygen in seawater is an important factor affecting the corrosivity of seawater. The solubility of oxygen in sea water mainly depends on the salinity and temperature of the sea water. With the increase of salinity or temperature, the solubility of oxygen is reduced.

The relation between the corrosion rate correction factor for dissolved oxygen and the dissolved oxygen concentration ratio is proposed as a linear relationship [9]:

$$R(O) = a*O + b \qquad (2.5)$$

where: R(O) is the corrosion rate correction factor for dissolved oxygen concentration (corrosion rate at actual oxygen concentration / corrosion rate at nominal conditions), O is the dissolved oxygen concentration ratio (actual oxygen concentration / nominal oxygen concentration), a is a constant representing the slope of the R(O)-O relationship and b is a constant representing the corrosion rate correction factor R(O) at zero O .

- **pH**

In the range of near neutral pH, the corrosion rate of metals decreases with the increase of pH. After the reduction of pH, the corrosion rate of metals increased significantly, which is not only due to the increase of hydrogen evolution, but also the metal surface dissolved by the surface oxide film has greater affinity for oxygen and is conducive to the depolarization of oxygen. However, the pH of seawater is always stabilized at 7.6 to 8.3. That is to say, the difference of corrosion rate in this range is very small. Indeed, the pH of seawater may vary slightly depending on the photosynthetic activity. Plant matter consumes carbon dioxide and affects the pH during daylight hours. The carbon dioxide content in seawater (close to the surface) is influenced by the exchange with carbon dioxide in the atmosphere. It is reported that the usual daily fluctuations of pH has little direct effect on corrosion rate. A relation between corrosion rate and pH can be derived as [9]

$$R(pH) = k*10^{-n(pH)} \qquad (2.6)$$

where: R(pH) is corrosion rate correction factor for Ph (corrosion rate at actual Ph / corrosion rate at nominal conditions); k and n are constants.

- **Water velocity**

Flowing water can result in an increase in the amount of dissolved oxygen that reaches the material surface. Meanwhile, flowing water can remove protective films over the material surface. Higher velocity of seawater particles will lead to an increase in corrosion rate. The corrosion rate may double when water moves at 1m/s. These results suggest that the relation between the corrosion rate correction factor for velocity and velocity ratio can be modelled as an exponential relation [9]:

$$R(v) = \lambda * (1- e^{-\eta(v+\theta)}) \qquad (2.7)$$

where: $R(v)$ is the corrosion rate correction factor for velocity, v is the flow velocity ratio, λ is a magnification factor to adjust the value of the corrosion rate correction factor ($\lambda \geq 0$), θ is a constant introduced to adjust the truncated portion from the distribution ($\theta \geq 0$) and η is a factor to adjust the curvature and the slop of the curve ($\eta \geq 0$).

2.4 Main types of structural corrosion in the marine environment

A study was carried out on structures, platforms, and vessels in the offshore environment to determine the types, and prevalence, of corrosion features [4].

- **Galvanic Corrosion**

Galvanic corrosion was determined to be the most widespread corrosion mechanism observed in this study. The degradation appeared as a continuous layer of corrosion over an entire corroded surface area. This type of corrosion occurs when two dissimilar metals are electrically coupled to each other in a common electrolyte, such as a stainless steel (SS) fitting coupled with a carbon steel (CS) nut. During galvanic coupling, corrosion of the more anodic metal (CS nut) increases and the corrosion of the more cathodic metal (SS fitting) decreases. The driving force for corrosion is the difference in potentials between the dissimilar metals.

- **Crevice Corrosion**

Crevice corrosion was also prevalent in offshore environments. This corrosion develops from small volumes of stagnant chloride-rich solution present at joints between metallic surfaces (e.g., threaded pipes coupled together). Accelerated corrosion occurs at the joint resulting from a potential difference on the metal surface, due to dissimilar environments in contact with the crevice at depth, and with more oxygen near the outer surface. The crevice prevents oxygen from maintaining the passive film, which breaks down and corrosion develops.

- **Pitting Corrosion**

One of the most hazardous forms of corrosion occurs when chlorides remain within droplets formed from seawater that have been entrained in the air. The droplets settle and leave a residue of salt on the surface. This causes a breakdown in the protective film where an anodic area is established. The adjacent cathodic area causes rapid metal dissolution in the pit. As chloride concentrates in the pit, the pH decreases, leading to an increase in the rate of attack in the pit. Pits penetrate and can lead to early catastrophic failure or loss of product.

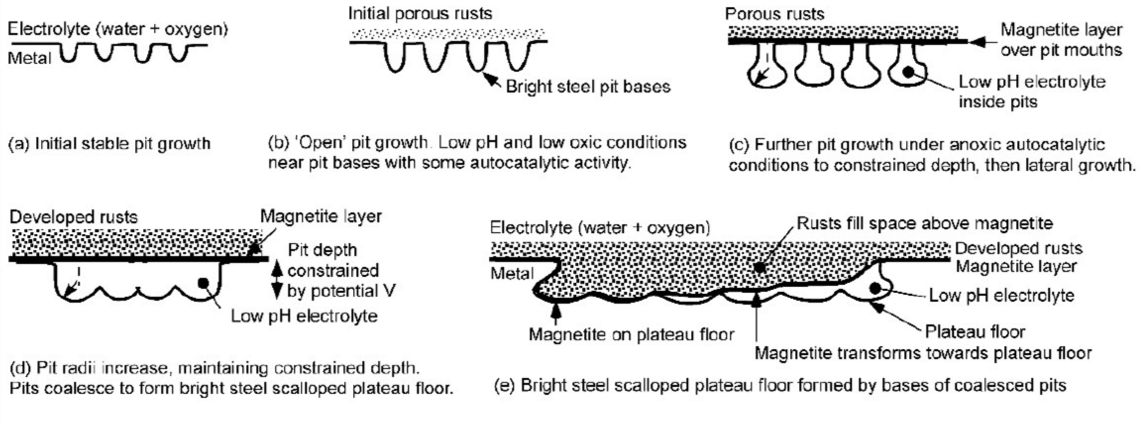

Fig. 2.4 - A schematic representation of the sequence in pit depth development [29].

Most of the theories for the initiation and development of pitting focus on the way a pit can initiate on what is close to a perfect surface, with material imperfections, inclusions and local alloy constituents producing only very small differences in local potential to drive dissolution that can lead to pit initiation. Initial pitting usually is considered to initiate at multiple sites on the surface of a metal. Only some become stable pits able to propagate with time.

Usually, it is considered that soon after a pit enters into a stable growth mode, it is necessary for the pit mouth to have a degree of cover so as to prevent the contents of the pit from interacting with the environment and thereby rendering the pit passive. For mild steels, this occurs relatively quickly, and already soon after becoming stable, the pits show localized corrosion product around and over the pit mouth; this soon develops into widespread cover by corrosion products.

As is well established, as each pit develops in size, the interior becomes sufficiently far removed from the pit mouth to render oxygen diffusion into the pit more difficult. Furthermore, the corrosion products, particularly the magnetite layer (Figure 2.4c), retard diffusion processes. The net effect is that anoxic conditions can develop inside the pits. In turn, these permit conditions suitable for autocatalytic reactions to commence. This occurs with dissociation of water and hydrogen ions replacing oxygen as the electron acceptor within the pit, with hydrogen gas evolving from the inside surfaces of the pit.

The resulting pressure then usually causes the rupture of the covering corrosion product, allowing gas effusion through the pit mouth.

As corrosion progresses, the magnitude of the exterior corrosion product will increase, and overall diffusion into and out of the pit will become more difficult.

The potential driving pitting can be the result of any imperfections. However, nit should be clear that as pit depth increases, the net potential for further pit depth development becomes, slowly, exhausted, and growth in pit depth stops.

- **Microbial-Induced Corrosion**

Seas are contaminated with microorganisms and bacteria. Aerobic bacteria, including magnesium oxidizing bacteria (MOB), and anaerobic bacteria, including sulfate-reducing bacteria (SRB), tend to colonize metal surfaces and form biofilms. The SRBs can also survive and flourish on their own in environments where there is no oxygen.

Usually, the aerobic bacteria create an environment that includes an anaerobic zone below their colonies for SRB to flourish without O dioxygen (O). As the biofilms grows, the bacteria produce a number of by-products, including organic acids, hydrogen sulfide (H S), and slime. Pitting results from acids and the modified environment of bacteria. The MOB deposits manganese dioxide (MnO_2) as corrosion product like waste, while the SRB deposits iron sulfide (FeS).

- **Sensitization in Stainless Steel Fittings**

SS fittings used in a marine environment are supposed to be in an annealed condition to relieve any internal stresses. When these fittings are welded to other components, the annealed structure around the weld becomes unstable. If left in that state, it becomes susceptible to sensitization. The weldment should be solution annealed followed by quenching to restore the original structure. Sensitization occurs when the carbon migrates to the grain boundaries and combines with the chromium in the region forming chromium carbide, thus weakening the structure. The grains become susceptible to intergranular corrosion or chloride-induced stress corrosion cracking (SCC). An example is an SS pipe welded to an SS flange that exhibited branched cracking around the weldment. The structure became sensitized and susceptible to crack propagation, caused by chloride-induced SCC initiated by pits at the surface.

2.5 Corrosion fatigue lives of offshore structures

Offshore structures are typically at the front end of service for decades. Undergoing unsymmetrical loading forces, harsh marine conditions, freezing cold temperatures and importantly corrosion. During this time, even a well-designed and optimized structure can undergo structural failure in some of the harshest and most unforgiving environments on earth.

This is particularly the case with hat of oil platforms as shown in Fig. 2.5a. These steel structures are subjected to extensive cyclical loading during their service out at sea, this can be one of the main causes structural of failure. As of 2020 there are 1470 offshore oil rigs, with the majority working in the Gulf of Mexico, the North Sea and in the Persian Gulf. Each of which is involved with the skilled work of extracting crude oil wealth from vast reserves beneath the ocean. These harsh marine environments and the presence of corrosion can also accelerate fatigue failure of a structure. This occurs due to electrochemical reactions and plastic deformation in the steel structures that accelerate anodic dissolution of metals and this results in corrosion fatigue crack initiation. The resulting effect on such structures can be a catastrophic failure [10].

It was therefore necessary to examine the corrosion fatigue durability behaviour of S355 steel, which is used in offshore structural applications. A key failure mechanism for corrosion fatigue is that cracks initiate at stress raising pits. Corrosion pits are formed at the surface of steel structures during service, and these can result in the initiation of fatigue cracks. To test the catastrophic effect of corrosion on structural steel grades, the performance was compared to parent steel structures. In the field, this was carried out by attaching sample specimens to the outer hull of an offshore structure so that they could be exposed to the elements for predetermined periods of time.

It was surprising to see the damage caused, even after a relatively short period time. As shown in Fig. 2.5b, within 50 h, hard iron oxide had formed with further deterioration and the formation of salt crystals had become extensive.

Fig. 2.5 (a) - Extensive corrosion observed on an offshore oil platform [10]

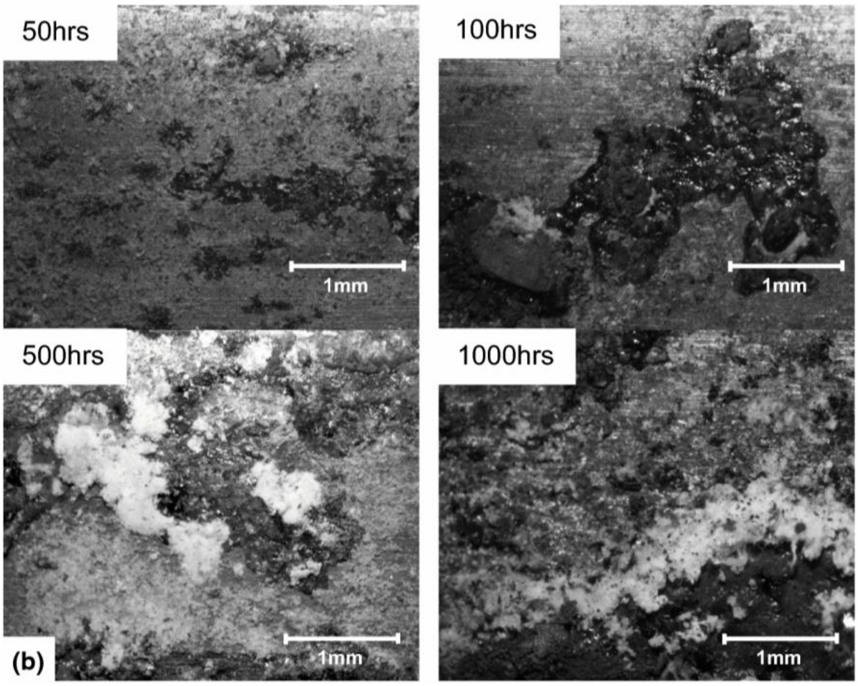

Fig. 2.5 (b) - Microscope images taken in the field of S355 steel after it was left for periods of time when exposed to the harsh marine environment. Within 500 h it was observed that excessive salt crystals and iron oxide had grown across the surface [10]

These electrochemical processes cause in the first instance cosmetic damage, but beyond this they also create microsized pits in the structure which ultimately result in localized rises in stress. Strain induced across the component, together with any formed corrosion pits promotes dissolution of the matrix and subsequently results in further pit growth. It is this that can be the starting point for the complete structural failure of an application. To test the effects of corrosion on the lives of a structure, laboratory-based tests were then carried out on retrieved test specimens. These data can then be used to understand the significant loss of fatigue lives. Since plastic strain has significant effect on the anodic activity of steels, four-point bend testing was carried out on samples as shown in Fig. 2.6.

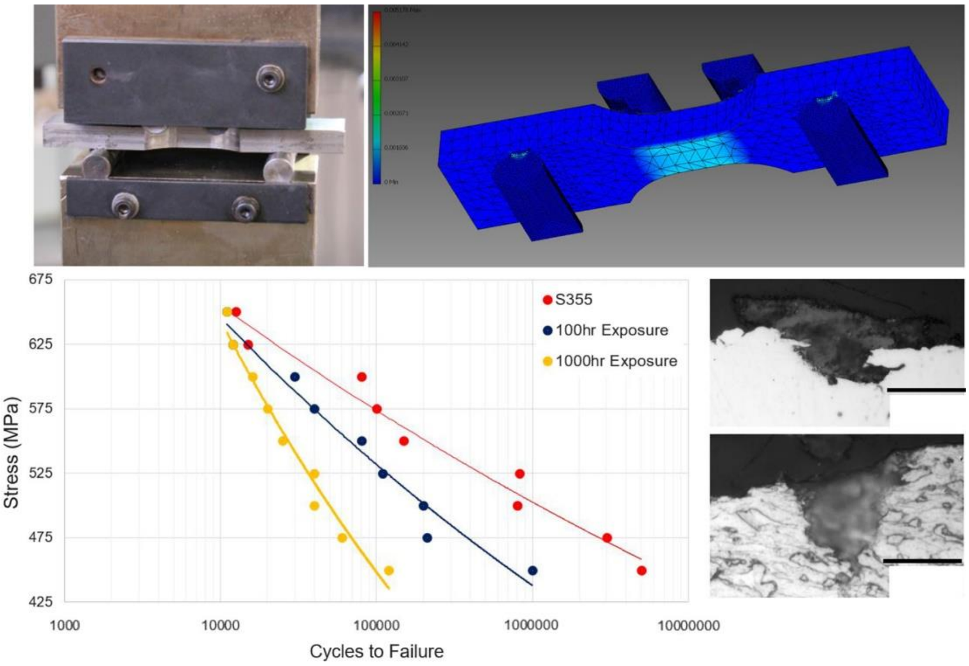

Fig. 2.6 Test samples of S355 steel under four-point laboratory fatigue testing. The resulting stress analysis and fatigue life curves to the point of specimen failure showing the significant reduction in life due to exposure to marine conditions. Micrographs of two stress raising pits generated of eth steel surface after 1000h of exposure [10]

It was staggering to observe the significant loss of fatigue life of corroded specimens, even after a relatively short period of time. During corrosion fatigue testing, pits continue to grow into the material. As a pit reaches a critical depth, then a fatigue crack will develop and propagate throughout the structure. With 1000 h of exposure to marine conditions, at the lower stress levels (high cycle fatigue), specimens lasted fifty times less than that of the fatigue life of uncorroded specimens. After later sectioning and analysis, there were observed too many hundreds of pits that were photographed transverse to the surface of the specimens.

There are two critical mechanisms that effect the behaviour of corrosion fatigue crack propagation in marine environments. These are hydrogen embrittlement and anodic dissolution at the crack tip. As the length of a crack increases as shown in Fig. 2.7, oxygen from the surface has further to diffuse to the crack tip. As a result, this leads to a reduction in the oxygen concentration at the crack tip.

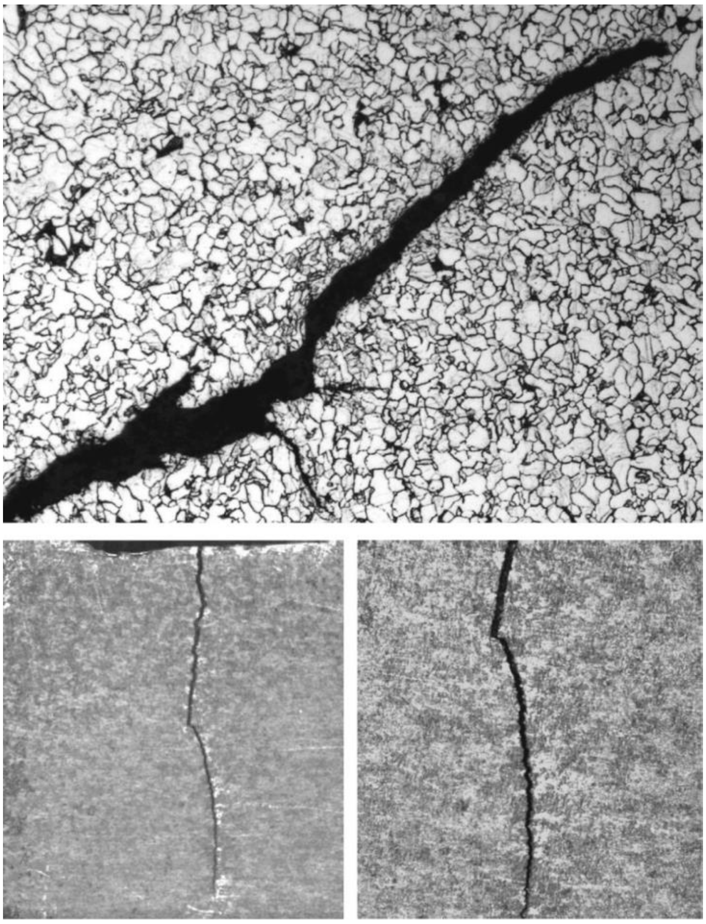

Fig. 2.7 Microstructure of a fatigue crack through S355 (etched with 2% Nital) and the change in crack orientation showing the growth of a corrosion

induced fatigue crack during the loading process and crack growth range [10]

Further to this, hydrogen embrittlement results in an acceleration in crack growth rate. This is dependent on the intensity of the stress and the induced cyclical frequency. Subsequent crack growth rate due to hydrogen embrittlement occurs when a critical stress intensity level is achieved. Under the process of sinusoidal fatigue loading, the orientation properties of the crack were observed to change. As a result, there is a transition from predominantly transgranular crack growth to that of intergranular and secondary crack growth resulting in rapid failure of the application.

It is often wise to be mindful that even the largest structures are vulnerable to the smallest defects. During subsequent testing, it was clear to observe the slow growth in the region I crack, followed by a rapid region II crack growth. It is this factor that leads to sudden and catastrophic failures of heavy industrial structures. It is the fact that exposed metal surfaces are critical towards the initiation of pits and the growth of a fatigue crack that determine the life of a structure. Therefore, it is important that offshore structures do not deteriorate to the level at which defects become observed and those structures are continuously well maintained. This preventative strategy ultimately results significantly less costly problems in the long run.

2.6 Corrosion and environment

2.6.1 Natural causes

From the perspective of environment, the corrosion activity is a natural phenomenon that is necessary for sustaining the natural balance. Corrosion is a great leveler of engineering materials in that it tries to revert the metal back to its most stable form. However, from an engineer's perspective, corrosion could be seen as a destructive attack of nature on metal. This destruction of metal is, however, brought about by nature's chemical or electrochemical reaction. It causes significant loss of material which leads to losses in terms of productivity and cost of maintenance, repair and replacements, and restoration. This does not included damage to property and the occasional loss of lives and injuries associated with failures resulting from corrosion. The impact of corrosion, and the prevention thereof, is felt economically, and affects the safety and environmental conservation of resources [3].

- Economically, it implies the loss of infrastructure by way of loss of materials used in tanks, process equipment, pipelines, platforms, bridges, and many other important structures. The economic losses could be direct or indirect. The direct losses would include, for example, the cost of replacing the corroded structures, equipment, and the cost of painting, upkeep, and monitoring of cathodic protection as well as the associated labour cost. Another cost would be the use of expensive corrosion resistance materials.

- The indirect cost of corrosion is difficult to assess accurately as more complex aspects come into play. However, activities that can be counted as contributing to the indirect cost of corrosion might include the closing of plants and facilities for repair and maintenance needed because of corrosion damages and failures. These costs add up because shut down involves reduction in production, loss of product, costs for cleaning and repair of environmental damages, and wages paid for the duration of the non-productive time. In a nutshell, it can be said that indirect losses are a chain of activities that will take place and have to be paid for even when production is not there to support those costs.

- The loss of structure materials to corrosion is not only an economic loss but it makes the structures weak and degrades their designed capabilities and reduces the structure’s designed purpose. On the extreme end of this deterioration, such structures can become a safety hazard and the loss may lead to structure failures, some of which could even be catastrophic, leading to property damage and loss of lives.

- The metal resources are primarily extracted from naturally occurring oxides of metal called ore, and if corrosion is allowed to degrade the metals, more and more resources will be required, leading to more environmental damage.

Materials, especially metals, are required to sustain the infrastructures for the development of civilization; however, care must be taken to reduce the impact of the growing demands of civilization on the environment. This should be one of the primary responsibilities of engineering. The balancing of nature and development is handled by responsible engineering and the process is a vicious cycle because the damage to the environment may itself threaten the very civilization for which the extractions are made. The human civilization has reached such a stage that, while corrosion itself is a natural recycling process, the prevention of corrosion leads to the reduction of damage to the environment. Thus, engineers have a great responsibility to balance the needs of the developing society and sustaining the environment.

2.6.2 Effects of climate changes on offshore structures

Another very important aspect that links the environment with corrosion is climate change and its consequences on structures. Unfavourable climate change is associated with rising global temperature and sea level and, consequently, with increasing frequency, intensity, extent and duration of extreme weather and climate events throughout Europe and the world.

Approaching the UK-hosted COP26, the focus on climate change and what leading countries will put in place to tackle it is at the forefront of every discussion. Often, we look at the perpetrators of climate change and denounce the wrongdoings and what should be done to remedy the situation. However, what happens to the offshore facilities damaged by changing sea levels, inclement weather, or pollution? [11]

The effects of climate change can have a significant impact especially on the service life of offshore structures.
Changing sea levels and pollution are causing further repetitive disruptions to offshore facilities. Changing sea levels, a result of global warming, are rising by about 3.1mm every year, according to the fifth annual report by the Copernicus Marine Service. Pollution from land-based activities such as farming and industry is causing ocean eutrophication – the water becomes enriched with minerals and nutrients, sometimes turning it green – which impacts delicate ecosystems.

Dr. Luke Prendergast, assistant professor at the University of Nottingham, says that climate change is leading to more adverse "weather conditions, which are more frequent and have worse magnitude".
Hurricane Ida, one of the many recent storms, which occurred from 26 August to 4 September 2021, caused many of Shell's oil and gas platforms to shut down and has slowed down oil and gas platforms with some 1.4 million barrels and 1.88 billion cubic feet of natural gas remaining offline.

When a hurricane is predicted to enter the Gulf of Mexico, oil production and transportation pipelines in the path of the storm shut down, crews are evacuated, and refineries and processing plants along the Gulf Coast close.

Drilling rigs pull pipe and move out of the expected path of the storm, if possible, or they anchor down, and supply vessels, commercial ships, and barges may be moved into a bayou where they have more protection from the storm. Shortly after the storm has passed, workers including operators and service providers regroup and return to the platforms to evaluate the damages, and facilities are repaired, if required. Production may be offline for anything from two or three days to weeks or even months [11].

Damages can vary from fatigue over time or actual physical damages – either way, all offshore facilities (whether they be platforms, vessels, or wind turbines) will require regular maintenance to ensure offshore health and safety laws are respected and followed. With up to 200 people that can be on one platform, multiplying this by the number of platforms worldwide, the risks are greater and more important.

Fatigue is one form of damage, and the most common one. It occurs over time and is commonly known as structural fatigue, resulting from temperature changes, wind strength changes, corrosion, and varying weight loads. Sufficient fatigue can lead to failures. Prendergast highlights that a structure "might be designed to withstand a very small number of really high magnitude storm events, like really bad waves, really bad wind, or millions of very low-level events. “The issue is that if you have more than expected storms occurring in the design period, it can reduce your usable design life and require more maintenance and it means more issues.”

Offshore platform and rig disasters often happen due to inclement weather and the daily threat of an unforgiving ocean, causing fires, explosions, capsizes, sinking, collisions, collapsing, and many more incidents. In the case of a storm, damages can take many forms: platforms and caissons can list, topple or be destroyed; rigs, barges, and workboats can be grounded or capsize; rigs may be torn from their moorings and set adrift. Moreover, flowlines and pipelines can be damaged by a dragged anchor or mudslides; topsides equipment such as pumps, tank batteries, and power generators may have water damage; cranes, helicopter stations, drilling rigs, and related equipment can be destroyed or severely damaged by wind.

Offshore oil and gas platforms may be able to sustain more damage than wind turbines, Prendergast adds, due to the scale of the platforms. But it isn’t a case of “the larger, the better”. In the case of platforms, the height is crucial as it is supposed to protect them from the most dangerous part of a storm – generally dealing well with wind and rainfall – but cresting waves will cause the most damage.

He goes on: “Whether a platform [or any facility] is more resilient to damage depends on the type of damage we question.”

Offshore rigs must either operate at full capacity or not at all. There is no in between as, for instance, an oil rig is not a tap with a flow that can be adjusted per needs. Although rigs have valves, they’re only used during maintenance or emergency stops.

Shutting down production for oil companies for an extended period may have three serious consequences: it may never return to their previous production rate; pumping equipment must be repaired and reinstalled at great costs; refineries and pipelines cannot be kept in operation without some minimal level of production.

In order to prevent overly frequent shutdowns, maintenance is key and, as Prendergast explains: “We build maintenance into the idea behind it, and we do it with (potential future damages) in mind.
“We can certainly optimise the design of structures to minimise the requirement for that maintenance by understanding, as best we can, the environments that we placed them into, predicting how these environments might change due to things like climate change and inclement water, and deal with that consequently”.

Prendergast highlights the phenomenon called scour erosion, which is when water washes away from around foundations of man-made structures. It is often caused by fastmoving water, so scour often occurs during floods.
While this phenomenon has become a real issue for onshore bridges or even offshore infrastructures, Prendergast insisted that it also impacts offshore structures located in waterways that have bad wave conditions or tidal conditions. Although the industry leans towards building larger infrastructures, they have their own “inbuilt issues that designers are trying to battle against”.
We need to predict the future in some respects and see how bad the weather could be, how hazardous these environments could be, and whether these structures would be safe”.

2.6.3 Indirect effects of climate changes

Not only extreme events such as heat waves, severe storms, heavy rainfall and floods can affect the safety and service life of buildings and infrastructure.
Similar effects occur with changes in different climate variables like:

- concentration of pollutants: the electrolyte film can present very high levels of contamination, due to the presence of salt or pollutants; these can accelerate the corrosion process;
- temperature: increases in average temperature can impact the corrosion rate, particularly in cold areas;
- relative humidity: longer presence of the film electrolyte means longer periods of active corrosion and, consequently, greater average corrosion rates;
- precipitation: rainfall has usually a beneficial effect by washing out the atmospheric pollutants that are deposited on exposed surfaces thus reducing the risk of corrosion; hence, in locations where projections indicate lower rainfall frequency, the cleaning effect may be reduced;
- wind patterns: the dispersion of pollutants will depend on local wind patterns for which, at this time, there are no reliable models;

Due to climate change, various models available in the literature for the estimation of the damage produced by atmospheric corrosion, are no longer adequate to describe the phenomenon. Most models describe the corrosion depth as a function of time, as expressed by (Wang et al. 2013) [12]:

$$C(t) = A \cdot t^{B} \qquad (2.8)$$

where: $C(t)$ is the corrosion depth [μm]; t is the time length of exposure [year]; A is the corrosion rate in the first year of exposure, affected mainly by the initial condition of the environment; and B is related to the corrosion development with time.

Constants A and B are determined experimentally and are dependent on the material and environment. The estimation of corrosion may be inaccurate when the environmental conditions differ from those in which the models were calibrated. This expression does not take into account the independent variation of each environmental parameter. Under climatic changes scenarios, the environmental conditions are not constant over time, and will generally differ from those of the first year of exposure. This can cause inaccuracy examining a longer time profile.

A more general model was provided by ISO 9224 (2012), in which the long-term corrosion rates of structural materials depend on the corresponding corrosivity class. In this document, five different corrosivity classes are considered, from C1, corresponding to a very low corrosive environment typical of indoor environments with insignificant pollution, or very low pollution and time of wetness, to C5, a very high corrosive environment, present in temperate and subtropical regions with very high pollution or significant presence of chlorides. ISO 9224 (2012) also considers an additional category CX, correspondent to extreme corrosivity, associated with very high pollution or chloride content in tropical or subtropical regions and very high time of wetness. It is recommended that one-year corrosion losses are used to predict future corrosion. The standard (ISO 9223, 2012) provides guidelines to decide about the corrosivity categories depending on the measurable environmental parameters, such as:

- Time of Wetness (TOW),
- SO2 concentration,
- Cl- deposition rate.

The general model provided by ISO 9224 indicates that the average corrosion rate follows a bi-linear law. According to this model, for the first 10 years, the corrosion depth is dependent on the average corrosion rate; while, after 10 years of exposure, the corrosion rate is assumed to be constant with time. Taking into account the rates of corrosion provided by the standard for carbon steel and weathering steel, the corrosion depths for both types of steels are indicated in Figure 2.8.

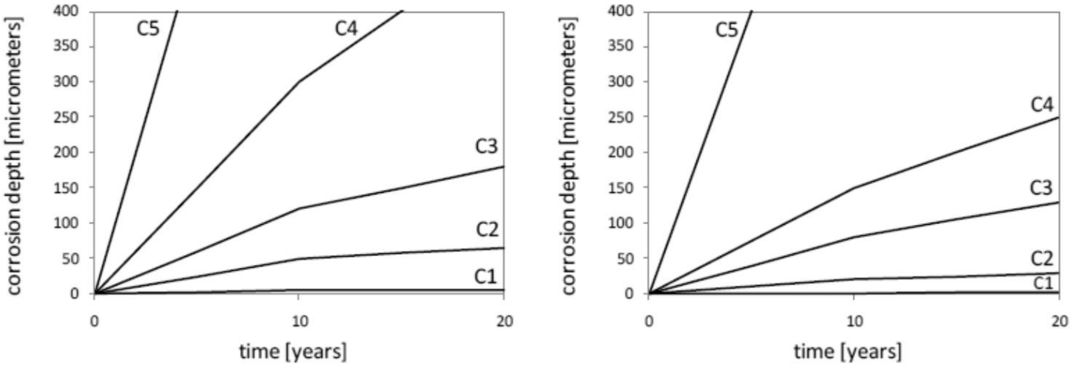

Fig. 2.8 - Thickness loss as a function of time according to ISO 9224 and different corrosiveness classes: for carbon steel (left) and weathering steel (right) [12]

The Safety and Security of Buildings Unit of the European Commission Joint Research Centre (JRC) conducts pre-normative research towards European standards for safety and security of the built environment, also addressing sustainability and efficiency issues. In the framework of Administrative Arrangements between the JRC and the Directorate-General for Internal Market, Industry, Entrepreneurship and SMEs (DG GROW), that JRC Unit is working on establishing the needs for research, guidelines and standards to better address the adaptation of the design of buildings and infrastructure to a changing climate.

In this regard, the JRC has established a scientific network to promote an interdisciplinary collaboration between experts in the fields of climate change, structural design, standard writers and policy makers. The network is participated by experts on climatology, structural design, structural corrosion and economic assessment of climate adaptation from the Euro-

Mediterranean Centre on Climate Change (CCMC) in Italy, Delft University of Technology in the Netherlands, Coimbra University in Portugal, University of Nottingham in the United Kingdom and University of Nantes in France.

As regards the existing structures, it is therefore necessary to study the faster progress of corrosion due to climate change and apply adequate control and maintenance measures.

3. Corrosion protection and degradation modelling

3.1 Corrosion control

Steel alloys are used in numerous and diverse applications in marine and offshore industries. Stainless steel grade 316 alloys are commonly used in offshore applications because of their corrosion resistant nature. It is regarded as safe for design life when choosing a material in an aggressive environment. Nevertheless, even though these alloys offer a better resistance to general corrosion, they are still susceptible to pitting corrosion. The most common causes of failure of stainless steel in marine environments is pitting corrosion because the material can quickly be penetrated despite that its general corrosion rate is very low.

For the sake of this discussion, offshore structures can be divided into structures that are above the water level and those that are below water. The above-water structures and equipment are often protected from external corrosion by suitable coating, selection of CRA (corrosion-resistant alloy), or a combination of both methods. The below-water group is divided into structures that are in the splash zone and structures that are fully submerged in water. These two areas are generally coated with a high-efficiency coating system. In addition, submerged structures are protected from corrosion by making them cathodes in relation to a set of sacrificial anodes placed in the sea water, which is the electrolyte in the corrosion cell [3].

Despite their similarities, all other types of offshore structures have designs that are specifically tailored to their intended purposes, and the nature and use of the structures determine which exposed surfaces may be coated or painted and which need to be safeguarded via cathodic protection.

The design of a corrosion control system starts with the design of structure itself. This approach reduces the possibility of including design features that may become detrimental to a structure's life and performance. By their very nature, some design features may be prone to promote corrosion or may lead to corrosion failure. For example, certain weld-designs that could be the cause of corrosion are listed below.

- Stitch welding
- Weld-designs that include backing strips
- Weld ends that aren't rounded to create a seal
- Rough surface welds that are not dressed to remove the possibility of stress points
- A possible crevice in a weld that could become a node for corrosion and possible failure

The design of the offshore structure itself could present unique issues that increase the likelihood of corrosion. Potentially corrosion-prone design features include T-K-Y-type joints, joint location, member materials, joint fitups that overstress adjacent materials, weld designs that lead to overwelding, welds with improper high-low positioning and poor transitions, pipe-ends with or without a dead leg, and the absence of seals for the ends of members to be flooded during the installation process. The very location of a structural member could present corrosion challenges.

- The atmospheric zone is the section of the structure that is above the splash zone, and by its very definition, this zone is not wetted or affected by the rise of tidal waves; hence, it is not in the electrolyte. The corrosion control of this zone is achieved through the application of a suitable coating system. Given that this zone is not in contact with the electrolyte (seawater), the coating does not need to be complimented by cathodic protection, the structure design essentially tries to minimize the exposed steel surface area in this zone. Minimizing the exposed surface area is primarily done through the use of tubular members. Clean welds with good profiles that blend into the parent metal then prevent any crevices that might promote corrosion, and the boxing in of the steel structures can accomplish the same goal. Substituting steel with corrosion resistant materials and nonmetals wherever possible is another example of designing a structure with a reduced tendency to corrode. Planners should avoid designs in which dissimilar metals are joined, however, or they should provide insulation between dissimilar metal joints.

- The splash zone is the section of the structure that is intermittently in or out of seawater during the structure's service life. Tides and wind are often the responsible for wetting this section. The range of the zone varies with the height of the sea's rise and fall due to daily tide cycles in the specific geographic area. The corrosion protection of material in this zone requires a different approach than the conventional approach discussed for the submerged zone.
- The submerged zone is the section of the structure that is below the lowest end of the splash zone and is always below the sea level. From the cathodic protection point of view, this portion of the structure is always in the electrolyte. The corrosion protection of this zone is achieved through a well-designed program that includes the application of a high-performance coating system supplemented by an equally well designed cathodic protection system. To reduce corrosion risk, the structural design preferably uses tubular

construction, as tight or recessed corners and crevices are difficult to protect in this zone. A stress-reduction design is also encouraged to minimize fatigue stress, and where required, the design should also relieve the stress placed on welded members.

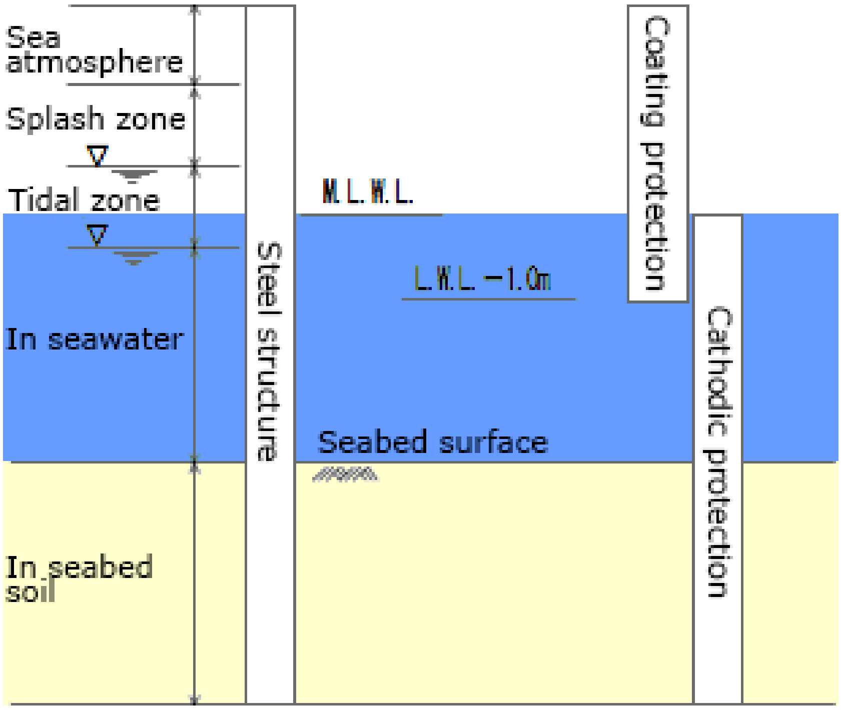

Fig. 3.1 – Schematic view of the corrosion protection as a function of the exposure areas[18]

3.1.1 Cathodic Protection

To ensure adequate protection, the surface areas of all exposed structural members are calculated during the design of the Cathodic Protection (CP) system.

The aim of this technique is to transform the metallic structure into a cathode of an electrochemical cell, to conduct electrons for cathodic reactions.

The general objective of a cathodic protection system is to polarize the steel structure to an electrical potential generally between -800 mV and -1100 mV, as measured against a Silver/Silver chloride/Seawater (Ag/AgCl/Seawater) reference electrode. This polarization is maintained throughout the designed life of the structure. The bare (noncoated) material should not be polarized to a more negative potential than -1.05 mV in reference to the Ag/AgCl/seawater reference electrode.

External corrosion control can be achieved through various levels of cathodic polarization. These variations are a function of the environment in which the structure is located.

CP can be accomplished in two ways; the first one is the impressed current cathodic protection (ICCP) systems while the second is the sacrificial anodes cathodic protection (SACP) systems [8]:

- In ICCP system, an external DC power source is used to generate electrons. The system is made up of; rectifier, anodes, reference electrodes and control unit. The rectifier provides the requisite positive current, that is then connected to the structure to be secured by the anodes. During this operation, the reference electrodes keep track of the protections level while the control unit adjusts the output current consequently. Ultimately, the metal structure become passively charged, that eventually causes the potential to fall below a predetermined level.
- In SACP system, reactive metals are utilized like anodes which are electrically attached to the metals to be protected. The difference in natural potentials between the anodes and the metals, as shown by their relative positions in the galvanic series, generates a positive current that flows in the electrolyte, from the anodes to the metal. As a result, the metal's entire surface becomes more negatively charged and serves as the cathode.

Anode Materials

Anodes are made out of alloys that are more electrochemically active than the material they are intended to protect from corrosion. As a result of interactions with surrounding structures and fluids, the anode depletes during the lifetime of the designed structure. The anodes that are used to prevent corrosion in cathodic design systems are called sacrificial anodes.

The principle of the sacrificial anode is the same as the principle of cathodic protection, wherein metal surfaces come into contact with electrolytes, leading to an electrochemical reaction called corrosion. Metal in seawater is an example of this principle, as exemplified by a steel structure coming into contact with electrolytes in the ocean. Under normal circumstances, the steel will react with the electrolytes and begin to corrode, growing structurally weaker and disintegrating over time. However, if the electrolyte contains another metal that is more active than the steel, then the more active metal will corrode preferentially, thus protecting the steel from corrosion.

The sacrificial anodes that are used in offshore cathodic protection are intended to be consumed over the lifetime of the protected structure.

In relation to standard carbon steel, which is used for the construction of structures and piping components placed in the seawater, materials such as aluminum, zinc, magnesium, and their purpose-designed alloys are more active, and hence, they corrode preferentially to the steel structure, protecting it.

The current capacity and operating voltage of the sacrificial material are the two most important properties to be considered in selection of anode material. The current capacity of an anode is its ampere hour per unit output. The anodes are tested to give consistent output in densities from as low as 860 mA/M2 to 15,100 mA/m2. If an anode is well cast, the current capacity values should not be significantly affected by changes in environment and operational variables.

The operating potential of an anode material is another factor that gives the driving voltage for the current to flow and protect the structure. This property must balance the high potential to drive the current, but it must not be so high that it depletes the life of the anode (Figure 3.2).

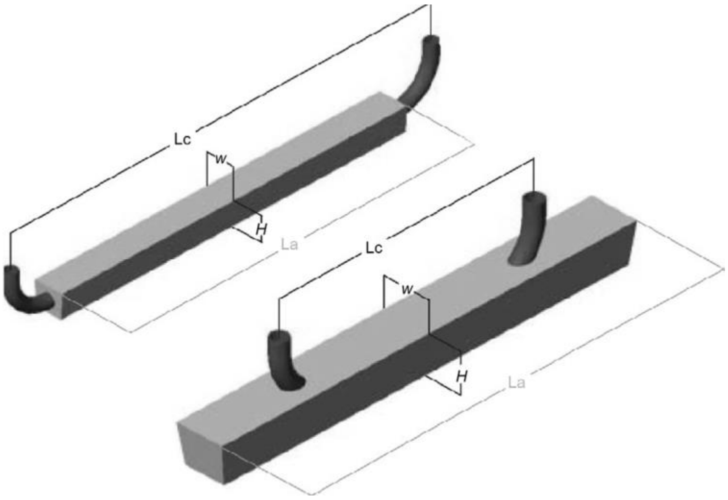

Fig. 3.2 - Typical anode type shows the steel core and various dimensions of an anode [3]

Metals with the described properties are used as anode materials, but they are often alloyed to improve their performance in terms of current output.

For example, the standard reduction potential of zinc is about -0.76 V. The standard reduction potential of iron is about -0.44 V. This potential difference between two metals is the key to cathodic protection using sacrificial anodes, and it creates the driving voltage of a zinc anode if used in this form. The driving voltage should not adversely affect the output current densities, should be constant throughout the life of the installed anode, and it should not polarize.

The consistency of both the current capacity output and the potential behaviour are key to a good anode material. The above discussion about using pure metals and alloys as anodes suggests that anodes must be tested to ensure that they meet the desired current output.

3.1.2 Coating for corrosion prevention

Coating systems is a simple way to prevent corrosion. During this method, a barrier is built between the steel and the sea water, thus the surface is isolated. Different types of coatings are applied to achieve different objectives. For example, specialized coatings are applied to protect pipes from abrasion damages during the pipe-laying process or from the surface conditions of the lay. Coatings are also developed to protect metal structures in different temperature ranges or to enhance the flow efficiency of the pipe's internal surfaces. In the latter case, the flow efficiency is increased by reducing the coefficient of friction between the pipe's surface and the fluid being transported.

Corrosion protection coatings are also designed to address various conditions. Some of these coatings are simple single-layer coatings applied to the steel substrate, while multilayered coatings provide more robust protection in different service conditions. As shown in Figure 3.3, the components of such a system can include a surface pretreatment, primer, undercoat, and topcoat.

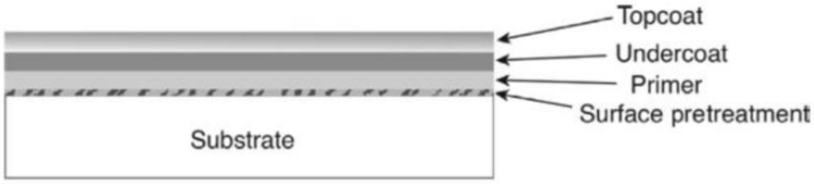

Fig. 3.3 – Typical arrangement of a coating system with multiple layers [3]

However, different layers of protection can exist within a coating group. Such a combination of different coating layers results in a very effective system that provides protection from a wide range of corrosion mechanisms.

For example, a combined layer system could provide protection from mechanical damages and electrochemical reactions causing corrosion damage.

The term coating points to a chemical compound, and a coating is essentially composed of synthetic resins or inorganic silicate polymers. When applied to a prepared surface, these chemicals will form a coating that resists the harsher environments of industry and sea. In terms of adhesion, toughness, and resistance to weather and seawater, these applications perform far better than a paint system.

In spite of very efficient coating application systems, no coating system can be treated as defect-free. The coating industry often claims to have a 100% efficient system, and they are correct regarding the efficiency of their product. However, in practical terms, efficiency is not always so high, mainly due to construction and transportation stresses that damage the applied coatings. This leaves possibility of defects in the coating called holidays. Holidays may be small pores, and they become anodic in the corrosion process. Due to the relatively small size of these holidays, a small anode to a large cathode ratio is created, and the metal around the holidays tends to corrode rapidly and fail the structure. Cathodic protection provides additional protection at holiday locations. Figure 3.4 graphically illustrates the general reaction that takes place on coated steel, including the permeation, holiday, coating disbonding, and electrochemical cell formation.

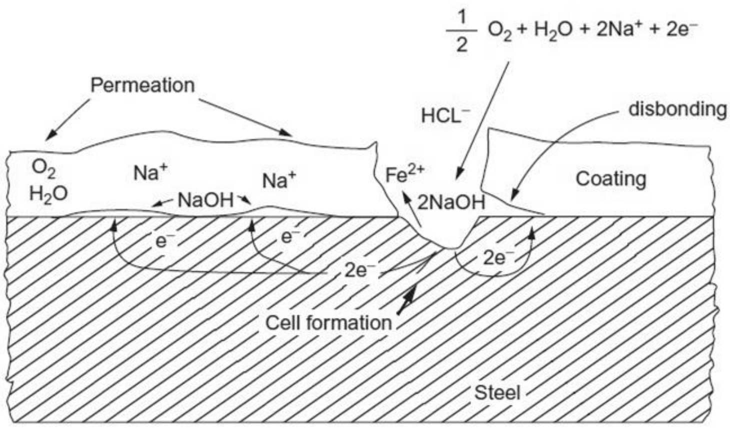

Fig. 3.4 - Typical corrosion reaction at failed coating [3]

There are various types of coating that have been developed to address specific environment and service conditions. In a very broad sense, they can be classified into the following groups according to how they are made.

- Organic coating
- Enamel
- Metallic coating
- Cement mortar

These coatings have different properties, and they are suitable for application to specific environments. Matching the coating properties to the environment is the right way to select suitable coating. In fact, a coating's specific properties are the reason for selecting it for a specific application, and coating properties should remain stable and not change in the given environment for a significantly long period, often exceeding the designed life of the structure they are applied to as protection.

In general, pipelines and structures are coated with high-efficiency coating systems composed of fusion-bonded epoxy, two layers of extruded polyethylene, and three heavy layers or multilayers of (polyolefin) polyethylene or polyurethane coatings. These systems have performed very well, but their success depends on correct application and quality control in terms of surface preparations, surface temperature, coating application procedure, etc.

Fig. 3.5 shows the factors that affect the durability of an anticorrosive coating system. The protective coating should have a high resistance to ultraviolet radiation as well as adequate resistance to altering weather conditions and impact from objects. Environmental degradation caused by moisture, temperature and ultraviolet radiation will reduce the lifetime of the coating.

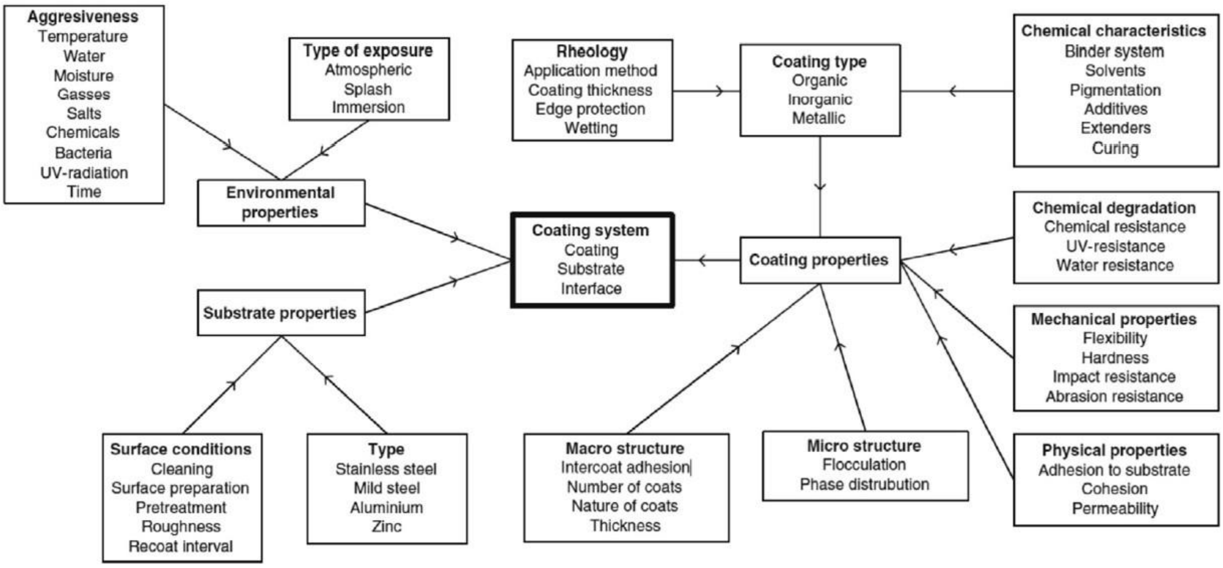

Fig. 3.5 - Factors affecting the durability of an anticorrosive coating system [13]

Can be identified six primary causes of the majority of paint and coating-related failures:

1 - Improper surface preparation,

2 - Improper coating selection,

3 - Improper application,

4 - Improper drying, curing and over-coating times,

5 - Lack of protection against water and aqueous systems

6 - Mechanical damage.

3.1.3 Corrosion allowance

The meaning of corrosion allowance is the use of thicker steel as necessary for the constructions. If conventional protection systems fail, or if coating damage occurs, this can be used as a backup solution. In addition, a corrosion allowance is required to cover the time durations up to the ICCP installation and steel polarization. This can extend the structure's life in the event of technical issues with impressed current cathodic protection system or galvanic anodes (such as passivation).

The thickness is determined based on the estimated erosion rate of the steel in the marine environments. Corrosion allowances of 0.2 to 1.20 centimetre are recommended. The steel is mostly made of iron, and also includes traces ranging from 0.01 to 1.65 percent of C, Si, Mn, S, P, Al, Ni, Mo, Cr, V, Co, and Cu [8].

3.2 Methods of identification of pitting corrosion

History shows that pitting corrosion is a dominant cause of structural failure in marine and offshore sectors. The reason for this is due to the well-known fact that seawater is an aggressive corrosive environment and the structures are generally fabricated with alloy steel which favours pitting corrosion.

The first stage in understanding pitting corrosion of steel is to correctly identify the phenomenon.

There are many techniques that can identify the presence of pitting [13].

3.2.1 Visual inspection

To identify pitting corrosion, visual inspection can be done in ambient light to determine location and severity of pitting. Photographic imaging is often used to document the difference in appearance of pits before and after removal of corrosion products. This technique is easiest to employ as it does not require specialized equipment and is relatively economical. Recently, the use of remotely operated vehicles (ROV)(figure 3.6) and autonomous underwater vehicles (AUV)(figure 3.7) replaces dangerous human effort for deep water inspection and underwater work. They increase safety, reduce costs and increase efficiency. These technologies utilize visual imaging and produce high resolution photographs of the corrosion susceptibility in structures.

Fig. 3.6 - The Mohawk ROV in Flower Garden Banks National Marine Sanctuary. Photo provided by NOAA [19].

Fig. 3.7 – An AUV being lowered into the water [20].

3.2.2 Metallographic examination

Metallographic examination is an investigative technique that can be used to determine the size, shape and density of corrosion pits. Metallographic examination is typically a destructive analysis technique as the specimen must be cut from the component and examined with a microscope.

Power and Shirokoff (2012) studied the simultaneous electrochemical analysis and in situ optical microscopy for 316L stainless steel samples submerged in sulphuric acid based solutions. They reported that this technique provides both a detailed visual account of the corrosion process as well as a standard electrochemical analysis of the pitting potentials and corrosion rate.

Fig. 3.8 - Metallographic examination performed by using state of the art optical microscope equipped with a PAXcam™ III digital camera and image analysis software [21].

3.2.3 Non-destructive testing (NDT)

Non-destructive testing (NDT) is a key technique used in industry to evaluate the current state of component and equipment in service and to aid in maintenance planning. It plays an important role in the continued safe operation of physical assets. American Society for Nondestructive Testing (ASNT) defines NDT as "the determination of the physical condition of an object without affecting the object's ability to fulfil its intended function.

NDT techniques typically use a probing energy form to determine material properties or to indicate the presence of material discontinuities". ASTM G46-96 stated that NDT technique is applicable to identify pitting corrosion however, it is not effective at characterizing pitting as a destructive method.

An NDT method is classified according to its underlying physical principle and common methods are:

- Visual and optical Testing (VT)
- Radiographic Testing (RT)
- Electrochemical and Electromagnetic Testing (EC, ET)
- Ultrasonic Testing (UT)
- Liquid Penetrant Testing (PT)
- Magnetic particle Testing (MT)
- Acoustic Emission Testing (AET)
- Infrared and thermal Testing (IRT)

Fig. 3.9 - Acoustic Emission Testing which relies on detecting the short bursts of ultrasound emitted by active cracks under a load. Sensors dispersed over the surface the structure detect the AE [22].

3.2.4 Surface analysis technique

Methods of surface analysis are increasingly being used to detect and quantify elements present inside the passive layer. Auger electrons spectroscopy (AES) is a common analytical technique used in the study of the composition of the outer 1e5 atomic layer of the surfaces of solids.
During AES, the sample is attacked with 1e10 KeV electrons and the instrument analyses the emitted auger electrons. The sensitivity to individual elements is about 0.1%, however the accuracy of the result is fairly poor.

X-ray photo-electron spectroscopy (XPS) consists of subjecting a specimen to X-ray photons and analysing the ejected electrons. The main advantage of this technique is that the energy of these electrons varies with the chemical state of the sample element. The depth sampled, and the sensitivity, is approximately the same as for AES. The main disadvantage of

XPS is the poor lateral resolution obtained due to the absence of focus by the incoming energy.

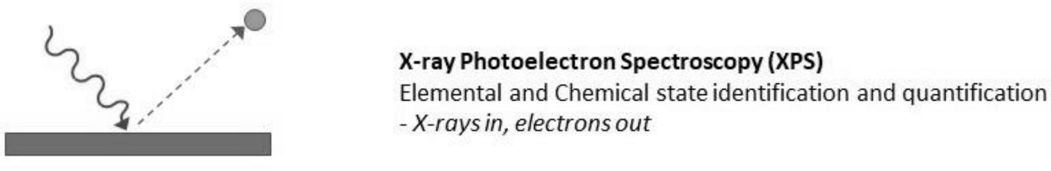
X-ray Photoelectron Spectroscopy (XPS)
Elemental and Chemical state identification and quantification
- X-rays in, electrons out

Secondary ion mass spectrometry (SIMS) is a technique for surface and thin-film analysis. SIMS has been extensively reviewed from various instrumental aspects such as analytical applications, comparison with other surface analytical techniques, application of surface studies and fundamental aspects of ion emission.

Usually, these techniques are associated with ion sputtering (ejecting the atom from a solid) to allow for in-depth analysis of the sample. However, sputtering has various disadvantages because it destroys the chemical bonding which may have been present on the surface, as well as at the original find topography. It may also form a cavity when sputtering is uneven, and some elements may sputter more slowly than others creating a new distribution in the removed sample.

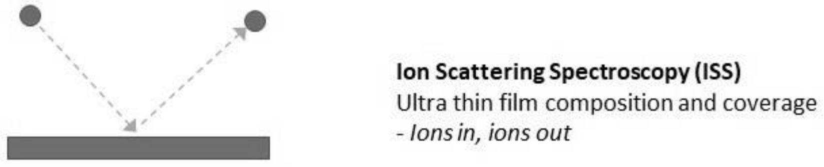
Ion Scattering Spectroscopy (ISS)
Ultra thin film composition and coverage
- Ions in, ions out

3.2.5 Probabilistic Approach for Pit Identification

Pitting corrosion has long been known to be a particularly inconsistent and unpredictable process. More precisely, it is challenging to forecast when a pit will initiate and where this is going to take place, therefore researchers have tried to extract data from the distributions during times of pit nucleation events.

Shibata et al. were the first to postulate that the critical potential necessary to induce pitting, and the induction time elapsed before pits become observable, are both statistically distributed quantities. They asserted that the nucleation of a pit is a statistical process similar to the development of a crack in brittle material. They conjectured that the pit generation process has the Markov property, i.e. that the future probability of pit nucleation is uniquely determined once the state of the system at the present stage is known.

Henshall et al. found that the stochastic model of pitting corrosion was useful in predicting corrosion damage of high-level radioactive waste containers. They stated that the model includes simple phenomenological relationships describing environmental dependence of stochastic parameters, and that it can simulate pit initiation and growth under various environments, including those that change during exposure.

Similarly, Valor et al. used a new stochastic model for pit initiation and pit growth. Spatial distribution models are commonly used in locational analysis, including spatial location of activities among the zones of a region and measure of interaction between zones. In the case of pitting corrosion models, spatial distributions is used when the pits on the sample do not exactly follow a poisson distribution. Several researchers have modified the spatial distributions to model pitting corrosion.

In addition, Aziz et al. introduced exponential distribution of the pit depth to calculate the maximum depth by the statistic of extreme values.

3.3 Modelling and prediction of long-term corrosion

So-called whole-of-life assessments increasingly are being used for decision processes. Such algorithms require models of sufficient rigor and robustness to represent (a) the demands or loadings expected to be placed on the system; (b) the ways in which the system may respond; and (c) prediction of likely future response, including deterioration and effectiveness of repairs [14].

Consistent with modern decision theory, the models required for (a) and (b) are probabilistic (Melchers, 1998). Until recently, models for (c) were largely ignored.

Most infrastructure has expected lives of several decades. The only way such predictions can be made is to invoke a combination of scientific understanding of deterioration processes. The quantitative understanding (i.e. a model) of how the corrosion process operates as a function of exposure time and under various environmental influences is necessary. It is also required to predict the likely amount of corrosion in the future for defined conditions. Thus, it is necessary to deal with the development of corrosion models, particularly for longer-term exposures. Despite good maintenance regimes, and the availability of protective coatings and of various forms of cathodic protection, field evidence shows that existing infrastructure often shows signs of corrosion, particularly in severe environments, such as for offshore facilities.

Prediction and identification of pitting corrosion in marine and offshore structures is a difficult problem for a number of reasons. Firstly, the events take place on a very small scale, with passive film nanometres in thickness and with initiation sites of similar sizes. Immediately after initiation, the rate of pit growth can be extremely high, even tens of A/cm2. Frankel and Sridhar

(2008) considered the pitting location as an extremely dynamic one with rapidly moving boundaries and rapidly changing chemistries.

The modelling of pitting corrosion in marine and offshore conditions has been study of interest for some time. The effect of the main factors in pitting corrosion modelling, such as temperature, bacterial community, oxygen concentration, pH, and velocity, has been considered in the past by several researchers (Melchers, 2001a; Moayed et al., 2003; Böhni, 2000; Melchers, 2002; Younis et al., 2012; Malik et al., 1992a; Pardo et al., 2000; Scheers, 1992).

Researchers proposed a widely accepted multiphase phenomenological model for corrosion loss as a function of exposure period.

3.3.1 A simplified model

Models may be considered as mathematical constructs that, at some level of abstraction, represent the phenomenon of interest. Typically models are tailored to their application and used for specific purposes. They also need to provide meaningful answers. A statement such as obtained from electrochemical potentials, “Corrosion is highly likely,” may be of some general interest but is of limited technical value for estimating the rate of corrosion.

Various approaches to model development exist. For some, a model is the outcome of an attempt to establish correlation between available data for corrosion loss or pit depth and data for the various factors believed to be of influence. Typically it provides a best fit curve (or surface) through data points. However, any objective evaluation repeatedly shows high levels of uncertainty, low confidence levels or poor correlation coefficients (e.g. Dean and Reiser, 2002). The reason is that these models are empirical and lack reference to fundamental understanding of the processes involved. Also, extrapolation is questionable since there is no theoretical basis for it.

Potentially more powerful and therefore more interesting are models based on fundamental principles and the calibrating of these models to actual (particularly field) data.

Calibrating a theory-based model implies that each set of data is treated as a sample set of all possible observations. In essence this approach asks: Can the data be interpreted as consistent with the model? It is implicit that some degree of uncertainty always is associated with each data point. (It is also possible for some data points to be called wrong owing to errors in observation or data processing.) As in science generally, the test is whether it is possible to disprove the model; if so, model refinement (or abandonment) is required.

An appropriate probabilistic formulation for corrosion loss c(t) as a function of exposure period t is expressed by equation (3.1):

$$c(t) = b(t) * f(t) + \varepsilon(t) \tag{3.1}$$

where f(t) is the mean-value function for corrosion loss, $\varepsilon(t)$ is a zero-mean error function, and b(t) is a bias function with unit mean, all as functions of t. If the mean value function f (t) is a poor choice, the relationship to real data will be poor, and there will be a large error term $\varepsilon(t)$. Conversely, a high-quality model should produce a good fit to data and leave only a small error term. It follows that model development should focus primarily on a sufficiently good-quality mean value function.

The problem may be illustrated using the hypothetical but distinctly nonlinear corrosion loss curve shown in Fig. 3.10.

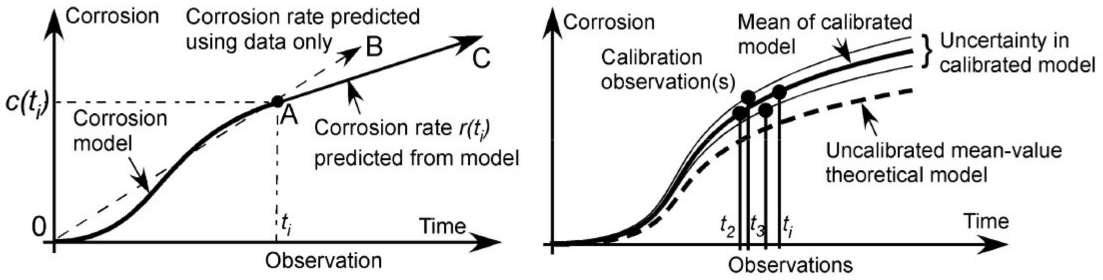

Fig. 3.10 - Corrosion model 0AC and prediction of corrosion rates (b) showing estimation of uncertainty in model from various data [14]

At time ti , the estimated corrosion loss is c(ti) shown at A. Of interest is the likely rate of corrosion r(ti) for t > ti , i.e. projection AC. Simple linear extrapolation from the origin O through the current observation A (i.e. the line OAB) usually will overestimate the rate. Knowledge of the underlying model for the corrosion process, i.e. OAC, allows the likely future corrosion loss rate r(ti) (i.e. AC) to be estimated. For this, knowledge of the model (OA) is essential.

From Fig. 3.10a and from Eq. 1, it is clear that in developing a (probabilistic) corrosion or pit depth model (see also Fig. 3.10b) the first priority should be the mean value function f(t). The existing applied corrosion literature, reflected in many well-known texts, suggests various corrosion rates, apparently constant in time (Jones, 1996). In engineering and naval architecture this is still the common understanding although various other models have been proposed. A review of these is available (Melchers 2008a). However, for most of these the actual corrosion loss measurements have very high uncertainties (Guedes Soares et al., 2006). In the atmospheric corrosion literature, the almost universally accepted model is the so-called power-law model, which has corrosion loss c(t) as a function of exposure time t represented by equation (3.2) of Feliu et al. (1993):

$$c(t) = A\,t^{B} \qquad (3.2)$$

where A and B are constants obtained from fitting Eq. 2 to the available data. (It might be noted that the special case B = 1 yields a linear function in which A is the corrosion rate.) Despite its long history, it has been shown only recently that the derivation of this model from diffusion principles involves a number of major assumptions (Melchers, 2003c).

Good-quality atmospheric corrosion data deviate from Eq. 2 in a consistent manner, and A and B are functions of the length of the data record (Melchers, 2009). This is inconsistent with a good-quality model.

For longer term corrosion loss, Equation (32) can be approximated by a linear function (Eq. 3.3):

$$c(t) = a + b\,t \qquad (3.3)$$

where a and b are constants obtained by fitting to data. It should be noted that although Equation (3) is linear for $t > 0$, it does not pass through the origin like the conventional corrosion 'rate' [23].

3.3.2 A more robust model

Analyzing the corrosion process over time it can be seen that within hours of first exposure, very small pits initiate on a steel surface. These pits grow quickly in depth to some 100 microns within days of exposure and later they grow in width. Many early pits stop growing soon after formation and are essentially overtaken by others. It follows that microscopic examination of a corroded steel surface invariably reveals a complex mix of larger and smaller pits as well as unaffected regions (cathodes), at least for some time. Fig. 3.11 shows a schematic view of the development of pitting with increased exposure time.

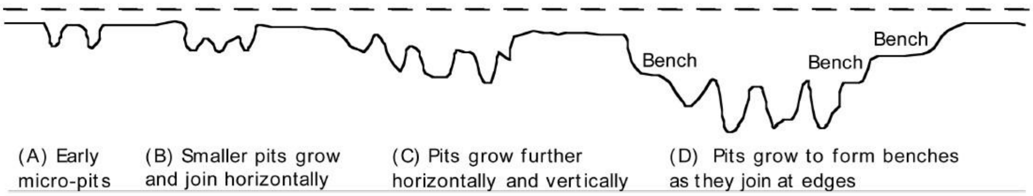

Fig. 3.11 - Development of pitting as a function of time, showing initial pitting broadening out to form a rough plateau on which new pits then form [14]

In particular it shows that the initial major pits stop growing in depth but amalgamate to form shallow depressions, and that later new pitting develops on the depression surfaces. The result is the formation of a series of depressions and a range of pit depths and sizes. This shows that the growth of pit depth is not a continuous process, at least for longer exposures.

This pattern of behavior for pit growth and development contrasts with the conventional wisdom, which assumes a continuous single functional process for pit depth development.

It follows immediately from these longer-term field observations that so-called uniform or general corrosion is an erroneous but still convenient practical concept. In practice it usually is obtained from the changes in mass loss of nominally identical coupons exposed for different periods.

Because of its practical importance for structural strength loss and because of its central position in conventional corrosion research and testing, the uniform corrosion model is used here for model development.

The environmental factors E that influence even the apparently simplest case and the corrosion of fully immersed steel in seawater are summarized in Table 1, together with their importance (Schumacher, 1979). Also of potential importance are: (a) steel composition, (b) size and orientation of the steel item, (c) surface roughness of the steel, and (d) shielding of the object by adjacent structures.

Factor	Importance	Factor	Importance
bacteria	high	pollutants	varies
biomass	low	temperature	high
oxygen supply	short term	pressure	no
carbon dioxide	little	suspended solids	no
salinity	not by itself	wave action	high
pH	high	water velocity	high
carbonate solubility	low		

Table 3.1 - Selection of factors E known to influence corrosion [14]

The model development described below does not consider all these factors but the most influential variables, like (a) water temperature and (b) microbiological influences. In fact, in real seawater invariably there also will be a colonization of the steel surface by biofilms. Usually these provide environments suitable for colonization by microorganisms such as bacteria present in seawater.

The former is simplified to the annual average seawater temperature, and the latter is considered only in terms of nutrients necessary for microbiological activity; if these are absent or severely limited, microbiological activity cannot be important. The principal features of the model are summarized in Fig. 3.12.

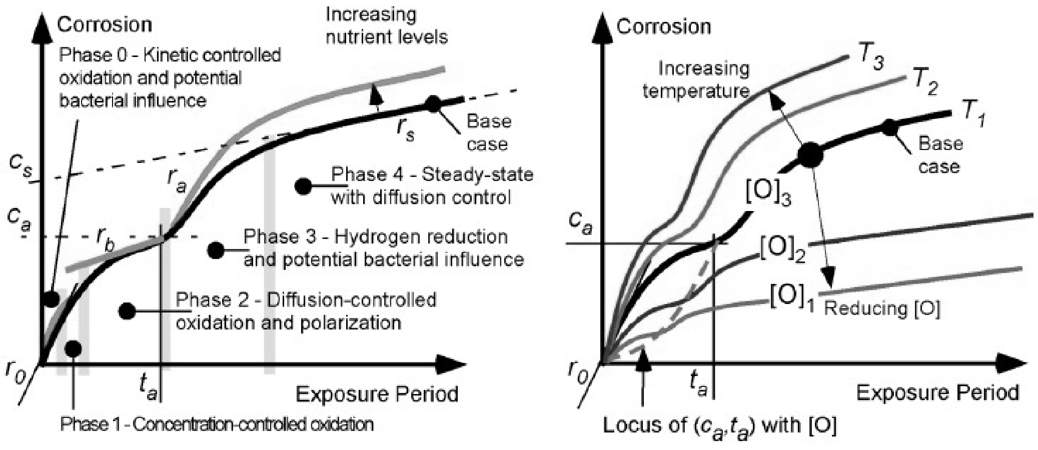

Fig. 3.12 - Model for corrosion showing (a) sequential phases, model parameters (r0, ca, ta, cs , rs) and early and later influence of nutrient availability levels; and (b) effect of increasing water temperature and reducing dissolved oxygen concentration [14]

The underlying model (base model) is based on the idealization that the corrosion process changes as rust layers build up on the metal surface, and that these are not removed to any major extent.

Thus, the model has several phases, including kinetic, diffusion, transition, and anaerobic, and each of these phases is believed to control the corrosion process. From Fig. 3.12a, the number of sequential phases which correspond to the different processes controlling the rate of corrosion for 'at sea' conditions is summarised as below:

- The first phase (0) is quite short (days) and includes both bacterial and electrochemical processes. Scientifically of great interest, it is of limited engineering importance as it has little influence over longer-term corrosion.
- In phase 1, the (instantaneous or tangent) rate of corrosion is limited by so-called concentration control, in which the rate of transport of oxygen from the surrounding (sea)water or moisture layers is controlled by the rate at which it diffuses under the concentration gradient established next to the metal surface.
- In phase 2, the rate of corrosion is controlled by the slowly decreasing rate of diffusion of oxygen through the increasing thickness of the rust layers (under wet corrosion conditions the anodic reaction is the dissociation of ferrous metal from ferrous ions in which metallic iron oxidizes).
- Provided the data sets available are sufficiently rich, eventually the corrosion loss (and maximum pit depth) trends show an upswing in the instantaneous corrosion rate. This is the early part of phase 3 in Fig 3.12a.

- The latter part of phase 3 has a declining corrosion rate, eventually leading to an almost constant corrosion rate, represented by phase 4.

Phases 3 and 4 have been associated with biologically influenced corrosion. This arises from the development of anoxic conditions within micro-niches in the rust layers, particularly those close to the corroding metal. These provide conditions suitable for colonization, for example, by the obligatory anaerobic sulfate-reducing bacteria (SRB). In field conditions, as distinct from laboratory studies, bacterial colonization and activity invariably involve broad communities of microorganisms. This cohabitation provides mutual support for energy transfer and nutrient availability, although typically the community requires nutrients and energy inputs from the external environment. It follows that the rate of nutrient supply may play a rate-controlling role in corrosion resulting from bacteria such as SRB. Bacteria also may play a role in corrosion during phases 0 and 1 in the anoxic niches that can develop adjacent to the corroding steel surface. This is a transient phenomenon, as indicated in Fig. 3.12a. During these early phases there is little to impede the diffusion of nutrients to the bacteria from the (supposedly nutrient-rich) external environment. This is not the case in phases 3 and 4, when a considerable rust layer is present between the bacteria and the external environment.

Anoxic conditions also may permit wet corrosion under the cathodic hydrogen evolution reaction. Under these conditions the corrosion rate is controlled, initially at least, by the rate of (outward) diffusion of molecular hydrogen. For a given thickness and diffusivity of the rust layers present at the end of phase 2, this is much faster than the inward diffusion of oxygen because of the much smaller size of molecular hydrogen. The relative rates are shown schematically as ra and rb respectively in Fig 3.12a.

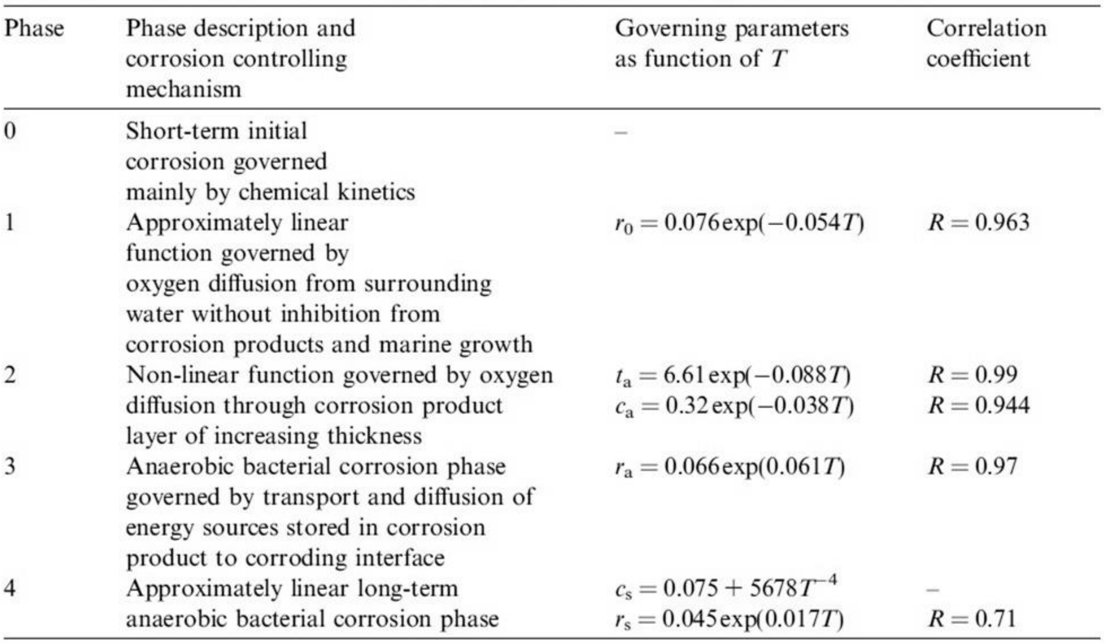

Phase	Phase description and corrosion controlling mechanism	Governing parameters as function of T	Correlation coefficient
0	Short-term initial corrosion governed mainly by chemical kinetics	–	
1	Approximately linear function governed by oxygen diffusion from surrounding water without inhibition from corrosion products and marine growth	$r_0 = 0.076\exp(-0.054T)$	$R = 0.963$
2	Non-linear function governed by oxygen diffusion through corrosion product layer of increasing thickness	$t_a = 6.61\exp(-0.088T)$ $c_a = 0.32\exp(-0.038T)$	$R = 0.99$ $R = 0.944$
3	Anaerobic bacterial corrosion phase governed by transport and diffusion of energy sources stored in corrosion product to corroding interface	$r_a = 0.066\exp(0.061T)$	$R = 0.97$
4	Approximately linear long-term anaerobic bacterial corrosion phase	$c_s = 0.075 + 5678T^{-4}$ $r_s = 0.045\exp(0.017T)$	– $R = 0.71$

Table 3.2 – Phases and calibrated parameters for $f_n(t,T)$ as a function of T [25]

Since each phase of the model describes a different principal corrosion mechanism, each may be expected to respond differently to steel composition (Fig. 3.13) and to various environmental conditions, including water temperature, dissolved oxygen, salinity, carbonate and sulfate contents. Indeed this has been observed in careful data analyses. This also has facilitated extension of the model to conditions other than natural, unpolluted seawater.

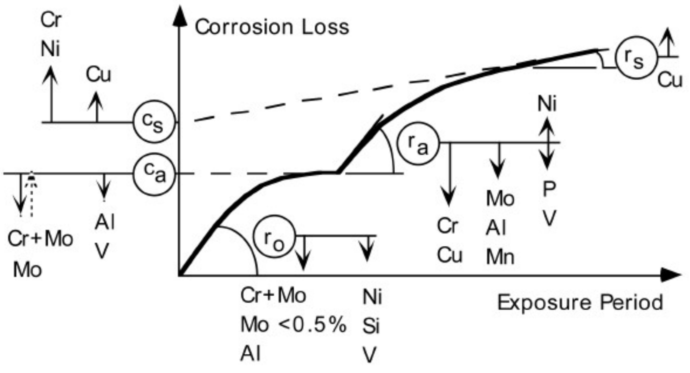

Fig. 3.13 - Schematic representation of effects of small amounts of alloying materials on corrosion loss; effects are different for various parts (phases) of model. Also, higher carbon content appears to increase both cs and rs [14]

3.3.3 Maximum pit depths

Measurement of maximum pit depths on multiple mild-steel coupons exposed for various periods of immersion seawater has shown, repeatedly, a distinctly nonlinear, bimodal trend (e.g. Fig. 3.14). The trend curve depends on the exposure conditions, a little on steel composition, but mainly on water temperature. The bimodal pit depth trend curve shown in Fig. 3.14 is similar to the model for corrosion loss. This is not surprising as pitting underlies also the uniform corrosion process.

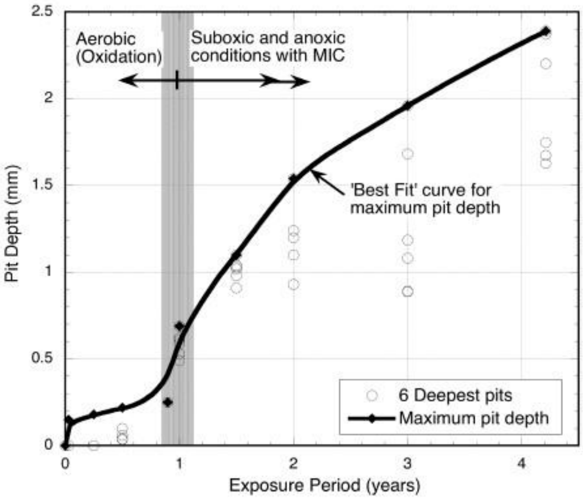

Fig. 3.14 - Maximum pit depths as a function of exposure period for natural coastal seawater (Taylors Beach, Australia) [14]

In applications, interest lies mainly in the maximum pit depth that may occur for larger steel surfaces, or equivalently, over longer exposure periods. The conventional approach is to assume that the statistics of maximum observed pit depths may be represented in terms of Extreme Value (EV) statistics (Galambos,1987). In fact, pitting corrosion usually is considered one of the prime applications of EV analysis.

In brief, the maximum of independent maxima may be considered distributed according to the well-known Gumbel Extreme Value distribution (for maxima). Fig. 3.15 shows an example of a so-called Gumbel plot. It is a special probability paper in which the cumulative probability distribution, shown on the left axis, is distorted in such a way that data that are truly Gumbel distributed plot as a straight line. (This is similar in concept to the so-called Normal probability plot). The left axis conventionally is labeled using the standardized variable w, defined below. The equivalent cumulative probability (i.e. the probability that the variable of interest is less than the value on the horizontal axis) is shown on the right vertical axis.

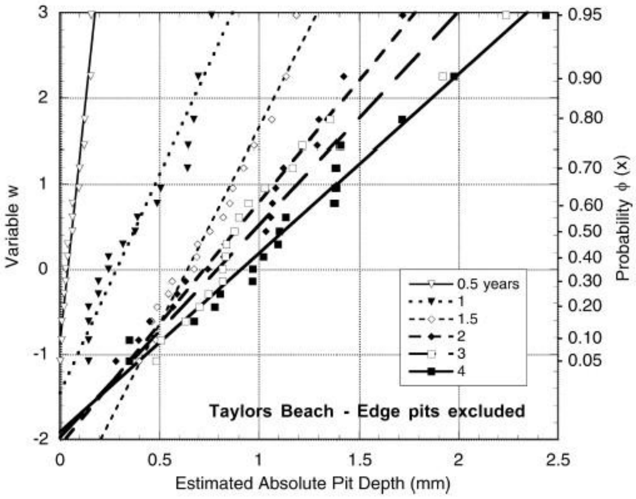

Fig. 3.15 - Gumbel plot with maximum pit depth data at various exposure periods for 18 surfaces of mild-steel plate coupons continuously immersed in Pacific Ocean seawater

For pitting, each pit depth is assumed to be an independent maximum (or, can be so assumed in the limit as the number of pits becomes large). Then, on the standard Gumbel plot, Fig. 3.15, the standardized variable for the maxima is given by:

$$w = (y - u)\alpha \tag{3.4}$$

which is defined through the cumulative distribution function (CDF) for y, i.e. by $F_Y(y)$ and its probability density function (PDF) $f_Y(y)$ as:

$$F_Y(y) = F_W[(y - u)\alpha] \qquad \text{with } F_W(\omega) = \exp(-e^{-\omega}) \tag{3.5}$$

$$f_Y(y) = \alpha\, f_W[(y - u)\alpha] \tag{3.6}$$

Here u and α respectively are the mode and slope of the Gumbel distribution and are related to the mean μ_Y and standard deviation σ_Y through:

$$\mu_Y = u + 1.1396/\alpha \tag{3.7}$$

$$\sigma_Y = 0.40825\pi/\alpha \tag{3.8}$$

A number of standard techniques exist to plot the data from a data set on a Gumbel plot.

Fig. 3.15 shows 6 sets of data, each one for a different period of exposure. It is seen that straight lines can be fitted through each data set, indicating the conventional Gumbel trend. It is seen also that the slopes of the lines (α) increase with longer exposure, indicating greater variability in pit depth with increasing exposure period. Closer examination of maximum pit depth data for longer periods of exposure has shown that the data are not particularly closely linear, but that they have a distinctive characteristic trend, also seen for other data sets. Fig. 3.16 shows the modified trends.

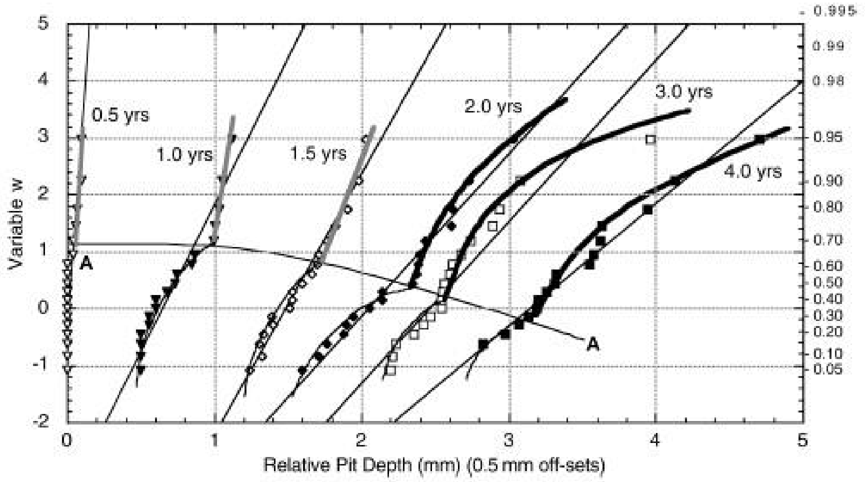

Fig. 3.16 - Gumbel plot of Fig. 12 with each data set is off-set by 0.5 mm for clarity; straight light lines through data are Gumbel trends and comparison to data shows that data trends are not linear as assumed in Fig. 3.15 [14]

The most important observation in Fig. 3.16 is that for exposures > 105 years and for the deeper pits (i.e. those above and to the right of the line AA), the extreme value distribution that best fits those data is the Frechet EV distribution. It is evident that there can be very large differences between Gumbel and Frechet in the probabilities associated with a given depth of pitting. This may have important practical implications.

A review of data and influencing factors for the corrosion of steels in marine environments has shown that corrosion loss as a process is best represented by the bi-model model that represents the changes that occur as corrosion develops, including microbiological effects, both on mass loss and for pitting. The representation of maximum pit depth statistics requires consideration of these changes. The conventional Gumbel extreme value distribution ignores these changes and may not be adequate for prediction.

The above principles and models have been applied to the corrosion inside water ballast tanks for ships (Gudze and Melchers, 2008), the corrosion of steel piles in harbors by so-called accelerated low water corrosion (Melchers and Jeffrey, 2009), the corrosion of mooring chains for offshore floating production and storage platforms (Fontaine et al., 2012), and for the internal corrosion of water injection pipelines used in the oil industry (Comãnescu et al., 2012).

4. Reference standards

4.1 International bodies that address corrosion

The science of corrosion has had two periods of rapid advancement. One, in the first half of the nineteenth century, was a result of intense and sustained scientific interest and activity aroused by the invention of the galvanic battery, and the controversy over the nature and source of the galvanic current. The other, in the first half of the twentieth century, was stimulated by growing realization of the immense economic cost of corrosion in a rapidly developing industrial age. In the latter period, a number of theories and facts established in the earlier one were rediscovered or elaborated, or both. These include the electrochemical theory of corrosion, proposed by Wollaston in 1801, developed by de La Rive in 1830, confirmed by Ericson-Auren and Palmaer in 1901, and rediscovered by Whitney in 1903. As early as 1819, Hall demonstrated the necessity of dissolved oxygen for appreciable corrosion of iron in water at ordinary temperatures and Sir Humphrey Davy published results of his work on cathodic protection of copper bottoms for British naval vessels in 1824.

These early experiments established a practical base for the application of cathodic protection, which led to the development of galvanized iron. In 1906, Committee U of the American Society for Testing Materials (ASTM) was formed to promote the development of corrosion tests.

Shortly afterward, other organizations began to pay attention to corrosion and its control. Among pioneers in studying the effects of corrosion was the American Committee on Electrolysis, which noted in 1921 that its preliminary report had been published in October, 1916. This committee concerned itself with the then serious problem of stray current damage to underground metal structures, especially the protection of communication cable from electrified street and interurban railways. In England, the Corrosion Committee of the Iron and Steel Institute issued its first report in 1931 and sixth in 1959. An American Coordinating Committee on Corrosion was organized with representatives from 17 technical societies in 1938.

This group, which aimed at coordinating the activities of societies to prevent duplicated work was absorbed by the National Association of Corrosion Engineers (NACE) in 1948 and was renamed the Inter-Society Committee on Corrosion Control. It functioned in a semiautonomous manner until it was finally disbanded about 10 years later. This was largely because the growth of abstract publications and numerous other periodicals permitted easy interchange of most information.

Although Germany had a corrosion journal, Korrosion and Metallschutz, prior to World War II, which was interrupted during the war and reissued after its end under a new title, Werkstoffe und Korrosion, it was not until after NACE began publishing the magazine Corrosion in 1945 that journals on corrosion control were started in other countries. Since then, one or more magazines about corrosion control have been started in most industrialized countries of the world. In addition to the present NACE International association, many other scientific engineering, governmental, and trade organizations are active in corrosion control work. Leaders among the scientific and engineering groups in North America are the American Society for Metals (ASM), American Society for Testing and Materials (ASTM), American Chemical Society (ASC), and The Electrochemical Society (ECS).

There are many other notable groups and associations dealing with some aspects of corrosion prevention and control in the Americas and in the rest of the world.

Several international bodies address various aspects of corrosion and corrosion control measures. These bodies may adopt different approaches to tackling the same issue, and they may prescribe different standards for acceptance criteria, tests, and testing methods. But, regardless of an organization's approach, the main principles and definitions of corrosion and corrosion prevention and mitigation remain basically the same [3].

Some national specifications put more emphasis on local factors considered to be more likely to contribute to corrosion. Such elements and local conditions may also find more emphasis in local standards. This chapter focuses on the specifications of international bodies, however, as those guidelines are more or less universally accepted as code or may be the basis for local codes regarding the engineering, design, prevention, and control issues involved with corrosion control. From time to time, the specifications generated by the bodies are amended, merged, removed, or changed, so the most recently updated version of their specifications must always be used and referenced.

4.2 National Association of Corrosion Engineers International (NACE)

The National Association of Corrosion Engineers International (NACE International) was established in 1943 by 11 corrosion engineers from the pipeline industry. The founding engineers were originally part of a regional group formed in the 1930s when the study of cathodic protection (CP) was introduced.

Since then, NACE International has become the global leader in developing corrosion prevention and control standards, certification, and education. The members of NACE International still include engineers, as well as numerous other professionals working in a range of areas related to corrosion control.

NACE International, The Corrosion Society, serves nearly 30,000 members in 116 countries, and it is recognized globally as the premier authority for corrosion control solutions. The organization offers technical training and certification programs, conferences, industry standards, reports, publications, technical journals, government relations activities, and more.

NACE International is headquartered in Houston, Texas, with offices in San Diego, Kuala Lumpur, and Shanghai. NACE International issues documents and publications relevant to various aspects of corrosion control methods. Not all of those documents can be listed or referenced, but some typical NACE specifications and publications used in CP and coating are listed below.

- NACE Standard RP 0169 - Control of External Corrosion on Underground or Submerged Metallic Piping Systems:

  This standard practice (SP) presents procedures and practices for achieving effective control of external corrosion on buried or submerged metallic piping systems. These recommendations are also applicable to many other buried or submerged metallic structures, and they are intended for use by corrosion control personnel concerned with the corrosion of buried or submerged piping systems, including pipes for oil, gas, and water, as well as similar structures. This standard describes the use of electrically insulating coatings, electrical isolation, and CP as external corrosion control methods.

  It contains specific provisions for the application of CP to existing bare metal and coated piping systems, as well as new structures. Also included are procedures for the control of interference currents on pipelines. For accurate and correct application of this standard, the standard must be used in its entirety. Using or citing only specific paragraphs or sections can lead to misinterpretation and misapplication of the recommendations and practices contained in this standard. This standard does not designate practices for every specific situation because of the complexity of conditions to which buried or submerged piping systems are exposed.

- NACE Standard RP 0176 - Corrosion of Fixed Offshore Structures Associated with Petroleum Production:

  This NACE standard provides guidelines for establishing minimum requirements for the control of corrosion on fixed offshore steel structures associated with petroleum production, and on the external portions of associated oil- and gas-handling equipment. Fixed structures include platforms, tension leg platforms, and subsea templates. The guidelines for the control of corrosion on temporarily moored mobile vessels used in petroleum production are not covered by this standard. This standard, divides fixed structures into three zones requiring different approaches to corrosion control. These zones are listed below as:

  - The submerged zone
  - The splash zone
  - The atmospheric zone

  As we have discussed in earlier sections, the submerged zone requires sacrificial

  anodic CP, and this standard addresses that part of the structure.

  The corrosion control of atmospheric and splash zones are addressed differently,

  and they are not part of this standard.

- NACE RP 0675 - Control of External Corrosion on Offshore Steel Pipelines: This standard is intended to serve aa a guide for establishing minimum requirements for control of external corrosion on offshore steel pipelines, when the need for corrosion control has been determined by physical, environmental, economic, and other factors. Particular reference is made to:
    - New piping system
    - Existing coated piping systems
    - Existing bare piping systems.

- NACE RP 0387 - Metallurgical and Inspection Requirements for Cast Sacrificial Anodes for Offshore Applications:
  This recommended practice (RP) defines minimum physical quality and inspection standards for cast sacrificial anodes for offshore applications. The two main objectives of the standard are listed below.
    - To standardize an industry-wide practice that can be used by consultants, manufacturers, and users to define the physical requirements of anodes
    - To be specific enough to assist the inspection authority in its task of confirming that anodes comply with the physical requirements

- NACE RP 0287 - Field Measurement of Surface Profile of Abrasive Blast Cleaned Steel Surface Using a Replica Tape:
  This standard describes a procedure for the on-site measurement of the surface profile of abrasive blast-cleaned steel surfaces that have a surface profile ranging from 38 to 114 mm (1.5 and 4.5 mils). The procedure correlates with the measurements obtained by the defined

laboratory procedure on nonrusted panels prepared in accordance with the NACE No. 1/SSPC-SP 5, NACE No. 2/SSPC-SP 10, or NACE No. 3/SSPC-SP 6. The specification also gives suggestions regarding the implementation and use of this procedure.

- NACE RP 0188 - Discontinuity (Holiday) Testing of Protective Coatings:
  In 2006, this RP was converted to SP, and it is now available as NACE SP 0188. The specification provides a procedure for the electrical detection of minute discontinuities called "holidays" in coating systems that are liquid applied to conductive substrates other than pipelines. Procedures are also described for determining discontinuities using two types of test equipment:
    - Low-voltage wet sponge
    - High-voltage spark testers.

- NACE TM0 190 - Impressed Current Laboratory Testing of Aluminum Alloy:
  This standard details the quality assurance procedure for determining the potential and current capacity characteristics under laboratory conditions for aluminum alloy anodes used for CP. The procedure screens various heats or lots of anodes to determine performance consistency on a regular basis from lot to lot. One method for anode potential evaluation and two methods (mass loss and hydrogen evolution) for current capacity evaluations are described. Performance criteria and sampling frequency are left to the discretion of the users of the standard.

- NACE Publication 7L198 - Design of Galvanic Anode Cathodic Protection Systems for Offshore Structures:

This publication is similar to several published by NACE on specific subjects. It describes a new design method based on first principles derivations, summarizes laboratory and field experimental data related to the new design approach, gives examples of how existing design criteria are incorporated into the new design equation, and presents two example designs using the new equation. The new design approach allows for the more precise design of CP systems, particularly in deep water or new geographic areas.

NACE and SSPC (The Coating Society: SSPC.Org) have issued joint standards for surface preparation in advance of coating and painting applications, and these standards contain the numbers described below. As the names indicate, the level of cleanliness is described by numbering systems. For example, the NACE No. 1, which is equal to SSPC-SP 5, is described as white metal blast cleaning.

- NACE No. 1, SSPC-SP 5 - White Metal Blast Cleaning:

  This joint standard covers the requirements for white metal blast cleaning of unpainted or painted steel surfaces through the use of abrasives. These requirements include the end condition of the surface and materials and procedures necessary to achieve and verify the end condition. A white-metalblast-

  cleaned surface, when viewed without magnification, shall be free of all visible oil, grease, dust, dirt, mill scale, rust, coating, oxides, corrosion products, and other foreign matter.

- NACE 2/ SSPC-SP 10 - Near-White Metal Blast Cleaning:

  This joint standard covers the requirements for near-white blast cleaning of unpainted or painted steel surfaces through the use of abrasives. These requirements define the end condition of the surface and materials and the procedures necessary to achieve and verify the end condition. A nearwhite-metal-blast-cleaned surface, when viewed without magnification, shall be free of all visible oil, grease, dust, dirt, mill scale, rust, coating, oxides, corrosion products, and other foreign matter, except for staining, as noted.

Random staining shall be limited to no more than 5% of each unit area of surface, as defined, and may consist of light shadows, slight streaks, or minor discolorations caused by stains of rust, mill scale, or previously applied coating.

- NACE 3/ SSPC-SP 6 - Commercial Blast Cleaning:

  This joint standard covers the requirements for commercial blast cleaning of unpainted or painted steel surfaces through the use of abrasives. These requirements include the end condition of the surface and materials and procedures necessary to achieve and verify the end condition. A commercial-blast-cleaned surface, when viewed without magnification, shall be free of all visible oil, grease, dust, dirt, mill scale, rust, coating, oxides, corrosion products, and other foreign matter, except for staining, as noted.

  Random staining shall be limited to no more than 33% of each unit area of surface, as defined, and may consist of light shadows, slight streaks, or minor discolorations caused by stains of rust, mill scale, or previously applied coating.

- NACE 4 /SSPC-SP 7 - Brush-Off Blast Cleaning:

  This joint standard covers the requirements for brush-off blast cleaning of unpainted or painted steel surfaces by the use of abrasives. These requirements include the end condition of the surface and materials and procedures necessary to achieve and verify the end condition. A brush-off-blast-cleaned surface, when viewed without magnification, shall be free of all visible oil, grease, dirt, dust, loose mill scale, loose rust, and loose coating. Tightly adherent mill scale, rust, and coating may remain on the surface. Mill scale, rust, and coating are considered tightly adherent if they cannot be removed by lifting with a dull putty knife after abrasive blast cleaning has been performed.

4.3 International Organization for Standardization (ISO)

The International Organization for Standardization (ISO) started with a meeting of delegates from 25 countries in 1946, at the Institute of Civil Engineers in London. Theses delegates agreed to create a new international organization "to facilitate the international coordination and unification of industrial standards."

The name "International Organization for Standardization" should logically have acronym IOS. However, the word order would not be correct in other languages. For example, in French, the name would be Organisation internationale de normalization, leading to the acronym OIN. So, to avoid such conflicts, the originators of the organization agreed on a more acceptable acronym, ISO, which is derived from the Greek word isos, meaning equal. The acronym's connection to isos reflects that, in whichever country and whatever the language, the short name is always ISO.

Since its founding, ISO has added several members, correspondents, and participants, and as of this writing, ISO has members from 164 countries and functions through 3368 technical bodies that participate in the standard development process. The office of ISO is called the Central Secretariat, and it is located in Geneva, Switzerland. ISO is possibly the world's largest organization engaged in developing voluntary international standards, and it forms a network of national standards bodies. These national standards bodies make up the ISO membership and they represent ISO in their country.

International Standards provide state-of-the-art specifications for products, services, and good practice, helping to make industry more efficient and effective. There are ~19,500 different standards developed by ISO. These standards are developed through global consensus, and as a result, they are acceptable internationally for various products ranging from food safety to computers. Typical ISO specifications applicable to corrosion prevention and CP follow.

- ISO 8501-1: Preparation of Steel Substrate Before Application of Paints and Related Products – Visual Assessment of Surface Cleanliness
- ISO 1461: Hot-Dip Galvanized Coating on Fabricated Iron and Steel Articles – Specification and Test Methods
- ISO 8044: Corrosion of Metals and Alloys – Basic Terms and Definitions
- ISO 4628: Paints and varnishes — Evaluation of degradation of coatings — Designation of quantity and size of defects, and of intensity of uniform changes in appearance
- ISO 3506-1: Mechanical properties of corrosion-resistant stainless steel fasteners – Part 1: Bolts, screws and studs
- ISO 3651: Determination of resistance to intergranular corrosion of stainless steels
- ISO 9227: Corrosion tests in artificial atmospheres – Salt spray tests
- ISO 10683: Fasteners – Non-electrolytically applied zinc flake coating systems
- ISO 12944-2: Paints and varnishes – Corrosion protection of steel structures by protective paint systems – Part 2: Classification of environments

- ISO 14713-1: Zinc coatings – Guidelines and recommendations for the protection against corrosion of iron and steel in structures – Part 1: General principles of design and corrosion resistance
- ISO 15589-2: Petroleum and Natural Gas Industries – Cathodic Protection of Pipeline Transportation Systems – Offshore Pipelines
- ISO 21809-1: Petroleum and Natural Gas Industries – External Coating for Buried or Submerged Pipelines Used in Pipeline Transportation Systems (Polyolefin Coatings – 3 Layers of PE and 3 Layers of PP)
- ISO 21809-2: Petroleum and Natural Gas Industries – External Coating for Buried or Submerged Pipelines Used in Pipeline Transportation Systems (Fusion Bonded Epoxy Coatings)
- ISO 21809-3: Petroleum and Natural Gas Industries – External Coating for Buried or Submerged Pipelines Used in Pipeline Transportation Systems (Field Joint Coatings)
- ISO 21809-4: Petroleum and Natural Gas Industries – External Coating for Buried or Submerged Pipelines Used in Pipeline Transportation Systems (Polyethylene Coatings – 2 Layers of PE)
- ISO 21809-5: Petroleum and Natural Gas Industries – External Coating for Buried or Submerged Pipelines Used in Pipeline Transportation Systems (External Concrete Coatings)

4.4 Det Norske Veritas (DNV)

Det Norske Veritas (DNV) literally translates to “the Norwegian truth,” and it is the name of an independent foundation charged with safeguarding life, property, and the environment. DNV was founded in Norway in 1864 for the purpose of inspecting and evaluating the technical condition of Norwegian merchant vessels. Since then, DNV has concentrated on identifying and assessing risk in different fields, while advising corporations on ways to manage that risk. Such DNV efforts include:

- Classification of ships
- Certification of an automotive company's management system
- Advice how to best maintain an aging oil platform

DNV mainly focuses on the safety and responsible improvement of business, and it uses a unique risk management approach to offer innovative services that meet customers' needs across industries and countries. As a result, DNV enjoys a singular position as a trusted partner in the improvement of quality, safety, and efficiency in high-risk global industries. DNV specifications provide an excellent reference and guide for meeting the basic requirements of CP system design. Typical relevant DNV specifications are listed below.

- DNV RPF103: Cathodic Protection of Submarine Pipelines by Galvanic Anodes
- DNV RPB401: Cathodic Protection Design
- DNV RPF106: Factory Applied External Pipeline Coatings for Corrosion Control
- DNV RPF102: Pipeline Field Joint Coating and Field Repair of Linepipe External Coating

4.5 Norsk Sokkels Konkuranseposisjon (NORSOK)

The Norsk Sokkels Konkuranseposisjon (NORSOK) standards are developed by the Norwegian petroleum industry to ensure adequate safety, value-adding, and cost effectiveness for industry developments and operations.

Furthermore, the NORSOK standards are intended to replace oil company specifications to the greatest extent possible, while serving as references in the authority's regulations.

- NORSOK M 501: Standard for Surface Preparation and Protective Coating
- NORSOK M 503: Cathodic Protection, (This Specification Addresses the Cathodic Protection of Submerged Installations and Seawater Containing Compartments and Manufacturing and Installation of Sacrificial Anodes)

4.6 American Society for Testing Materials (ASTM)

The American Society for Testing Materials (ASTM) offers specifications that complement most construction specifications, and these specifications and codes address several material and testing procedures and requirements, while offering related guidance.

The ASTM specifications (www.astm.org) are organized according to material type, and the letters prefixed to the specification number are indicative of the material type. For example, the letter A is for all ferrous materials; the letter B is for all nonferrous materials; and the letter C is for cementations, ceramic, concrete, and masonry. The letter D is used to indicate specifications-related miscellaneous material, such as chemicals, polymers, paints, coatings, and their test methods, and similarly, the letter E is used to denote specifications that address miscellaneous subjects, including subjects related to the examination and testing of material. The following is a short list of some groups included in the specifications.

- ASTM G 8: Test Method for Cathodic Disbonding of Pipeline Coating
- ASTM D 1141: Specification for Substitute Ocean Seawater

- ASTM D 4060: Standard Guide to Standard Test Methods for Unsintered Polytetrafluoroethylene (PTFE) Extruded Film or Tape
- ASTM D 2583: Standard Practice for Fusion of Poly(Vinyl Chloride) (PVC) Compounds Using a Torque Rheometer
- ASTM D 185: Test Methods for Coarse Particles in Pigments, Pastes, and Paints
- ASTM D 1640: Test Methods for Drying, Curing, or Film Formation of Organic Coating at Room Temperature
- ASTM G 6: Test Method for Abrasion Resistance of Pipeline Coatings
- ASTM G 9: Standard Test Method for Water Penetration into Pipeline Coatings
- ASTM D 10: Standard Test Method for Specific Bendability of Pipeline Coatings
- ASTM G 14: Standard Test Method for Impact Resistance of Pipeline Coatings (Falling Weight Test)
- ASTM D 2240: Standard Test Method for rubber Propery-Durometer Hardness
- ASTM G 11: Test Method for Effects of Outdoor Weathering on Pipeline Coatings
- ASTM G 12: Standard Test Method for Nondestructive Measurement of Film Thickness of Pipeline Coating on Steel
- ASTM G 48: Standard Test Methods for Pitting and Crevice Corrosion Resistance of Stainless Steels and Related Alloys by Use of Ferric Chloride Solution
- ASTM D 792: Standard Test Methods for Density and Specific Gravity (Relative Density) of Plastics by Displacement
- ASTM D 1505: Standard Test Method for Density of Plastics by the Density-Gradient Technique

- ASTM D 1693: Standard Test Method for Environmental Stress-Cracking of Ethylene Plastics
- ASTM D 4138: Standard Practice for Measurement of Dry Film Thickness of Protective Coating Systems by Destructive, Cross-Section Means
- ASTM D 4940: Standard Method for Conductimetric Analysis of Water Soluble Ionic Contamination of Blasting Abrasives

4.7 Canadian Standards Association (CSA)

The Canadian Standards Association (CSA) is an organization that develops industrial standards spanning over 57 different industrial areas. This not-for-profit organization has representatives from industry, government, and consumer groups and publishes standards CSA is accredited by the Standards Council of Canada, which is a crown corporation that develops and issues standards to promote standardization and efficiency in industrial production processes in Canada. The CSA standards are available in print and electronic form.

Starting as the Canadian Engineering Standards Association (CESA) in the early 1900s, the CSA was created as a result of Sir John Kennedy’s efforts to emphasize the need for such an organization. Initially, the organization addressed the needs of industries involved in the production of aircraft parts, the design and construction of bridges, the construction of buildings, and electrical work, among other endeavors. The first standards issued by CESA were for steel railway bridges, in 1920. CESA was renamed the CSA in 1944, and its certification mark was introduced in 1946. The organization now operates in 57 different areas of specialization, including climate change, business management, and safety and performance standards for electrical and electronic equipment, industrial equipment, boilers and pressure vessels, compressed gas-handling appliances, environmental protection, and construction materials. The following list presents some of the widely adopted CSA standards that relate to corrosion protection by way of coating quality control.

- CSA Z 245.20 - External Fusion Bond Epoxy Coating for Steel Pipe:

  The CSA Z 245.20 specification covers the qualification, application, inspection, testing, handling, and storage of coating materials. This specification is applicable to fusion-bonded epoxy (FBE) coating applied in the plant. The pipes coated with FBE are intended for use in submerged offshore applications or for pipelines buried underground. The specification covers different types of coating systems and classifies them with alpha-numeric identifiers, as listed below.

  1A: Single-layer FBE with glass transition temperature of <110 °C
  1B: Single-layer FBE with glass transition temperature of <110 °C
  2A: Two-layer FBE with a corrosion coating and protective overcoat
  2B: Two-layer FBE with a corrosion coating and an abrasion-resistant overcoat
  2C: Two-layer FBE with a corrosion coating and an antislip overcoat
  3: Three-layer FBE with an antislip overcoat applied over a corrosion coating and protective overcoat.

- CAS Z 245.21 - External Polyethylene Coating for Steel Pipe:

  The CSA Z 245.20 specification covers the qualification, application, inspection, testing, handling, and storage of coating materials. This specification is applicable to the external coating of pipes with polyethylene. The pipes with this coating system are primarily intended for use in submerged offshore applications.

4.8 European standards (EN)

European Standards (abbreviated EN, from the German name Europäische Norm ("European Norm")) are technical standards which have been ratified by one of the three European standards organizations: European Committee for Standardization (CEN), European Committee for Electrotechnical Standardization (CENELEC), or European Telecommunications Standards Institute (ETSI). All ENs are designed and created by all interested parties through a transparent, open, and consensual process [30].

The Eurocodes are the ten European standards (EN; harmonised technical rules) specifying how structural design should be conducted within the European Union (EU). These were developed by the European Committee for Standardization upon the request of the European Commission.

The purpose of the Eurocodes is to provide:

- a means to prove compliance with the requirements for mechanical strength and stability and safety in case of fire established by European Union law.
- a basis for construction and engineering contract specifications.
- a framework for creating harmonized technical specifications for building products (CE mark).

By March 2010, the Eurocodes are mandatory for the specification of European public works and are intended to become the de facto standard for the private sector. The Eurocodes therefore replace the existing national building codes published by national standard bodies (e.g. BS 5950), although many countries had a period of co-existence. Additionally, each country is expected to issue a National Annex to the Eurocodes which will need referencing for a particular country (e.g. The UK National Annex). At present, take-up of Eurocodes is slow on private sector projects and existing national codes are still widely used by engineers.

In 1975, the Commission of the European Community (presently the European Commission), decided on an action programme in the field of construction, based on article 95 of the Treaty. The objective of the programme was to eliminate technical obstacles to trade and the harmonisation of technical specifications. Within this action programme, the Commission took the initiative to establish a set of harmonised technical rules for the design of construction works which, in a first would serve as an alternative to the national rules in force in the member states of the European Union (EU) and, ultimately, would replace them. For fifteen years, the Commission, with the help of a steering committee with representatives of the member states, conducted the development of the Eurocodes programme, which led to the first generation of European codes in the 1980s.

In 1989, the Commission and the member states of the EU and the European Free Trade Association (EFTA) decided, on the basis of an agreement between the Commission and to transfer the preparation and the publication of the Eurocodes to the European Committee for Standardization (CEN) through a series of mandates, in order to provide them with a future status of European Standard (EN). This links de facto the Eurocodes with the provisions of all the Council's Directives and/or Commission's Decisions dealing with European standards (e.g. Regulation (EU) No. 305/2011 on the marketing of construction products and Directive 2014/24/EU on government procurement in the European Union).

The Eurocodes are published as a separate European Standards, each having a number of parts. In particular one deals with corrosion in stainless steels:

- EN 1993-1-4:2015-10, Eurocode 3: Design of steel structures – Part 1-4: General rules – Supplementary rules for stainless steels

4.9 Other standards

There are several other bodies that issue specifications, RPs, and test methods, and their guidelines are often widely referenced and used internationally.

Among them are documents from Deutsches Institut fu¨ r Normung, which is commonly referred as DIN:

- DIN 50018: Testing in a saturated atmosphere in the presence of sulfur dioxide

As the previous lists suggest, all these specifications, RPs, and test methods address a specific area of the subject, and they are to be used accordingly. Use of the most recent issue of a specification document is always recommended, unless the situation demands the use of a previously issued version.

5. Corrosion monitoring and residual safety assessment

5.1 Pitting degradation modeling of ocean steel structures

Modeling depth of long-term pitting corrosion is of interest for engineers in predicting the structural longevity of ocean infrastructures. Conventional models demonstrate poor quality in predicting the long-term pitting corrosion depth. Recently developed phenomenological models provide a strong understanding of the pitting process; however, they have limited engineering applications. In this study, a novel probabilistic model is developed for predicting the long-term pitting corrosion depth of steel structures in marine environment using Bayesian network (BN). The proposed BN model combines an understanding of corrosion phenomenological model and empirical model calibrated using real-world data.

A case study, which exemplifies the application of methodology to predict the pit depth of structural steel in long-term marine environment, is presented. The result shows that the proposed methodology succeeds in predicting the time-dependent, long-term anaerobic pitting corrosion depth of structural steel in different environmental and operational conditions [15].

5.1.1 Bayesian Network

Bayesian network (BN) is a probabilistic graphical method which uses Bayes' theorem for updating the prior occurrence probability of failures. It indicates a set of random variables and associated conditional dependencies in form of a directed acyclic graph (DAG), containing a set of nodes to represent variables and edges to denote probabilistic causal dependence. It involves independent and dependent variables known as causes and consequences respectively, which are connected via direct arrows pointing from the causes to the consequences. BN signifies the joint probability distribution and it is flexible to perform predictive (forward) as well as diagnostic (backward) analysis. In recent years, BNs have been extensively used for modelling of corrosion in marine structures as well as optimising the RBI (Risk-Based Inspection) plans [16].

The BN offers a formal method for encoding joint probability distributions using a set of statistical variables in which the information about independencies is explicitly separated from numerical quantities. Figure 5.1(a) represents a schematic structure of BN; the arrow in the figure represents causal relationship between the variables (A and B) through the probability distributions function illustrated in Fig. 5.1(b). BN allows estimating likelihood of rare failure events of complex structures in an efficient way. It also assists in updating the prediction by using new information obtained through measurements, monitoring, and inspection.

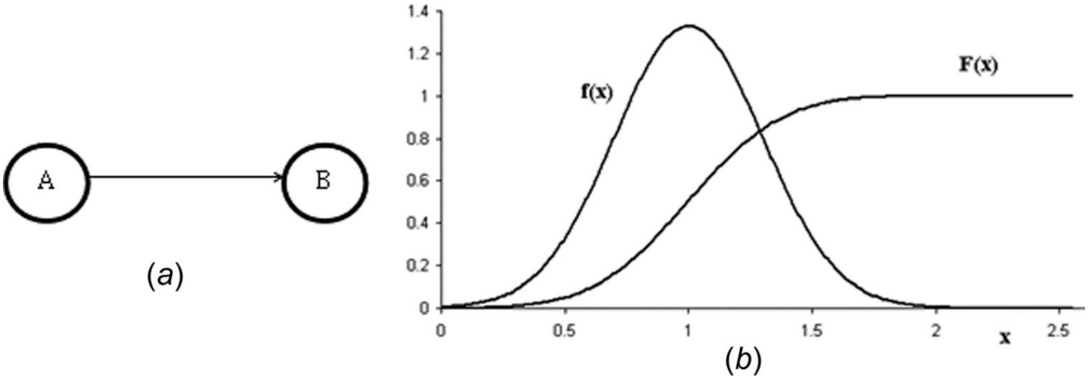

Fig. 5.1 - Structure of BN model (the arrow in the network represents the relationship between the nodes through the probability distributions function) [15]

In BN, “probability inference of an event is conditional on the observed evidence.” BN not only implements forward or predictive analysis, but it also performs backward or diagnostic analysis. Considering the conditional dependencies of variables, BN represents the joint probability distribution P(U) of variables U = [A_1 ...... A_n] as

$$P(U) = \prod_{i=1}^{n} P(A_1|Pa(A_i)) \tag{5.1}$$

where Pa(A_i) is the parent set of A_i in the BN, and P(U) reflects the properties of the BN. BN takes advantages of Bayes’ theorem to update the prior occurrence (or failure) given that the observation of another set of variables evidence E. The posterior probability distribution of a particular variable can be computed using different classes of inference algorithms, such as the junction tree or variable elimination, based on Bayes’ theorem:

$$P(U|E) = \frac{P(U,E)}{P(E)} = \frac{P(U,E)}{\sum_U P(U,E)} \tag{5.2}$$

The denominator is called the probability of observation and is the sum of all the conditional probabilities of E given events, and U multiplied by the probabilities of U. The prior and posterior probabilities can also be considered as “causes” and “consequences” of a process. The term consequences is a relationship between two events in a process - one leading to the other. An example would be the presence of sulfate-reducing bacteria and other environmental factors leading to pitting corrosion of steel structures in a marine environment.

5.1.2 Statistical data analysis using Gaussian Kernel Density Estimator

The application of probability density estimation is the informal investigation of the properties of a given set of data. A Kernel density estimator (KDE) is a nonparametric technique used to estimate the PDF of the random variable. Nonparametric density estimation is particularly valuable for exploratory data analysis and in situations where available information is insufficient to specify a parametric model. These methods are "hypersensitive" and no assumptions are needed beyond the smoothing of the functions to be estimated. Hence, the advantage of using Kernel distributions is that it produces a nonparametric PDF that adapts itself to the data rather than selecting a density with a particular parametric form and estimating the parameters. It must also be noted that the PDF, estimated using the nonparametric approach such as KDE, requires less assumptions to be made about the distributions of the observed data.

Lehmann stated that KDE is an alternative to the parametric approach in which one specifies a model up to a small number of parameters and then estimates the parameters via the likelihood principle. The advantage of the nonparametric approach is that it offers a far greater flexibility in modeling a given data set and, unlike the classical approach, it is not affected by specification bias. A nonparametric density estimator such as KDE can also be used for the summarization of Bayesian posteriors, classification, and discriminant analysis.

In this study, the Gaussian kernel density estimator was used to estimate the PDF for one-dimensional data. Given N independent realizations $X_N = (X_1, X_2, \ldots, X_N)$ from an unknown continuous PDF f on X, the Gaussian kernel density estimator is defined as

$$\hat{f}(x;\, t) = \frac{1}{N}\sum_{i=1}^{N} \Phi(x, X_i;\, t) \tag{5.3}$$

where $\Phi(x, X_i;\, t) = (1/\sqrt{2\pi t})e^{-(x-X_i)^2/2t}$ is a Gaussian PDF with location X_i and scale $\sqrt{t}$. The scale is usually referred to as bandwidth.

The performance of the Gaussian KDE depends significantly on the value of smoothing parameters, which is known as bandwidth. The Gaussian kernel is assumed, and the smoothing parameters' "bandwidth" is assumed using asymptotic approximation of mean integrated squared error (AMISE). It is performed by applying the asymptotic approximation to the random sample. The computational software MATLAB is used in converting the onedirectional data to nonparametric Gaussian Kernel PDF. To validate that Gaussian KDE is the better approach to develop PDF for the obtained data set, Normality test was also conducted using Anderson– Darling test considering Gaussian KDE.

Figure 5.2 is the illustrative comparison of different PDFs with parametric and nonparametric density functions for the data adapted from the ASTM world-wide corrosion test. The Gaussian KDE is tested between normal and logistic PDF. The X axis represents the calibrated data for power law constant B. As illustrated in Fig. 5.2, the nonparametric KDE function best fits the data.

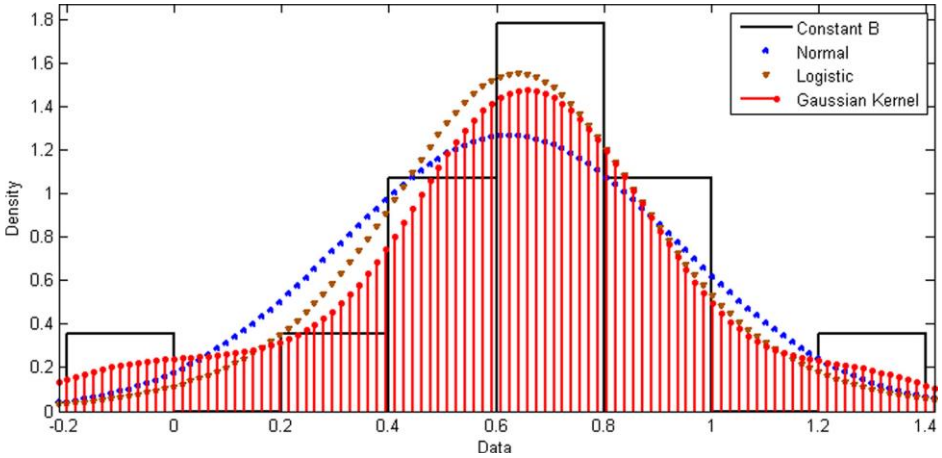

Fig. 5.2 - Comparison of different available probability distributions [15]

Figure 5.3 shows the normality test conducted using Anderson–Darling test considering normal distributions for environmental parameter "salinity." Based on this analysis, it is clear that the data do not follow normal distributions, and the p-value is less than or equal to the significance level;

hence, the decision is to reject the null hypothesis and conclude that the salinity data do not follow normal distribution. Also, it is visually clear from the normality test that the data points do not follow the fitted distribution line and the data are skewed from a curved line.

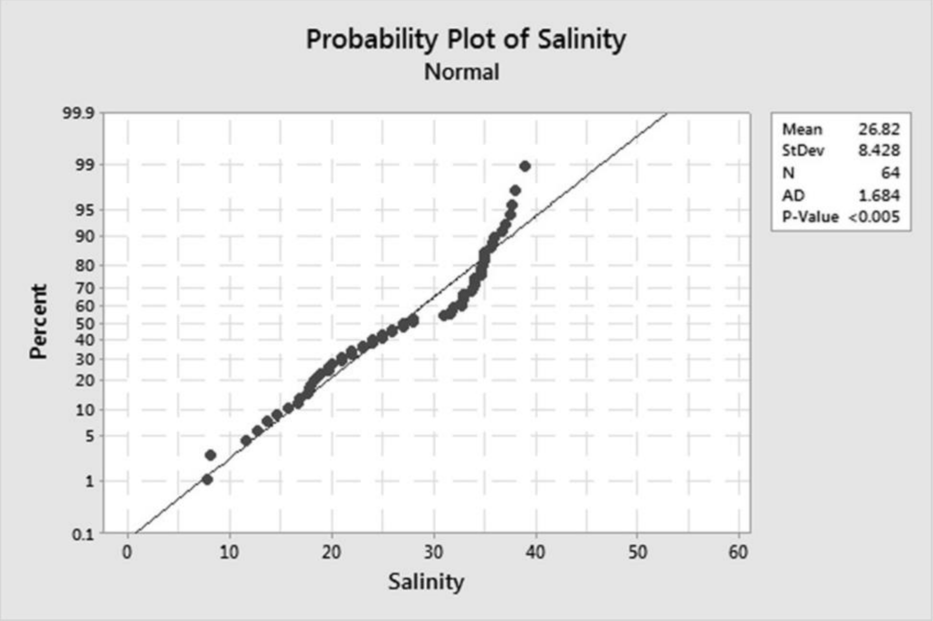

Fig. 5.3 - A probability plot based on Anderson–Darling approach to identify the best fit distributions for the environmental parameters such as salinity [15]

5.1.3 Development of methodology - pit depth modeling

Long-term pitting corrosion depth prediction and identification in marine and offshore structures is a complex problem for a number of reasons. The pit takes place on a very small scale with passive film in nanometers of thickness and with initiation sites of similar sizes. Immediately after initiation, the pit growth rate can be extremely high. Due to the complex nature of pitting corrosion, no specific methodology exists for predicting the precise pitting depth under long-term anaerobic conditions. Researchers have performed several lab and field experiments in order to identify pitting corrosion loss; however, most of these attempts were in order to find the relationship between pitting depth and the environmental factors. These assessments have not been successful in developing a model that predicts the future pitting depth in long-term anaerobic conditions.

In this study, an advanced methodology that integrates a probabilistic approach with the phenomenological and empirical models is presented to predict the pitting depth. The BN is used as a probabilistic data-modeling tool to model complex statistical relationships between inputs such as environmental factors and materials properties and pitting depth. The overall steps of the proposed methodology, as presented in Fig. 5.4, are divided into two main parts: experimental analysis and probabilistic modeling. These two parts are then combined together to predict the time-dependent pitting corrosion depth of a structural steel in long-term marine environment.

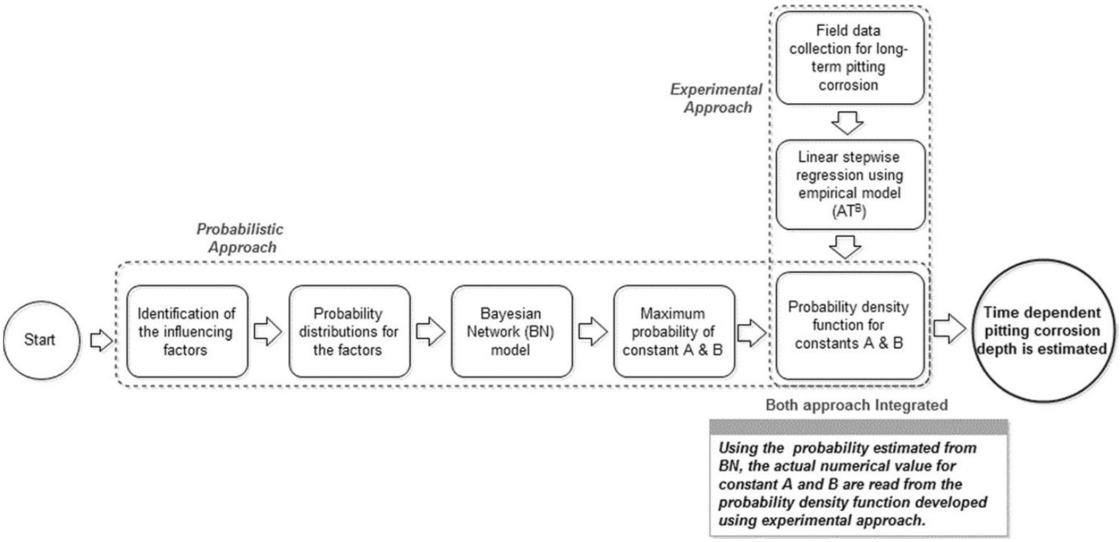

Fig. 5.4 - Development of a methodology for predicting the long-term time-dependent pitting corrosion depth [15]

In pitting corrosion depth modeling, it is crucial to grasp the significance of the phenomenological model because it provides a strong understanding of the corrosion process and the contributing factors that control the pit growth.

Likewise, an empirical corrosion model that represents the pit depth growth should be carefully considered. In the corrosion-related literature, there is a strong history of empirical model development for long-term exposure. Apart from the correlation studies conducted by several researchers, the most frequent models are based on a power law (as seen in the chapter 3.3.1) which is applied for atmospheric corrosion loss/pitting depth.

The development of the proposed pit depth prediction methodology starts with the probabilistic approach, which is then integrated with the experimental approach as demonstrated in Fig. 5.4.

In the first step of the probabilistic approach, the influencing factors that control the long-term pitting corrosion in marine environment are identified. The most influencing factors are selected based on the technical review conducted by Bhandari et al. and by studying theoretical corrosion phenomenon model. Temperature, salinity, pH, bacterial activity, velocity, exposure period, and alloy effects are considered to be the most influencing factors governing the long-term anaerobic conditions. Among these factors, temperature and bacterial activities play an important role for pit growth in both short- and long-term corrosion. Melchers reported that seawater temperature is considered to be the major influencing factor in pitting corrosion loss. He also nominated microbiological activity as another very important factor that controls long-term pitting corrosion loss in marine environmental conditions. Microbiological growth is a function of available energy sources and available nutrients, which enables microbiological metabolism.

In the next step, the probability distributions are developed to ascertain the influencing factors that control the pitting corrosion. These probability distributions are also called the priors because they assign a basic probability to the factors that lead to the particular consequences. The prior probabilities are crucial in modelling the causes-consequences relationship using BN. The prior probabilities of the influencing factors are estimated from their corresponding probability distributions, which are developed based on available observational data. For example, Fig. 5.5 illustrates the prior probability distribution for temperature.

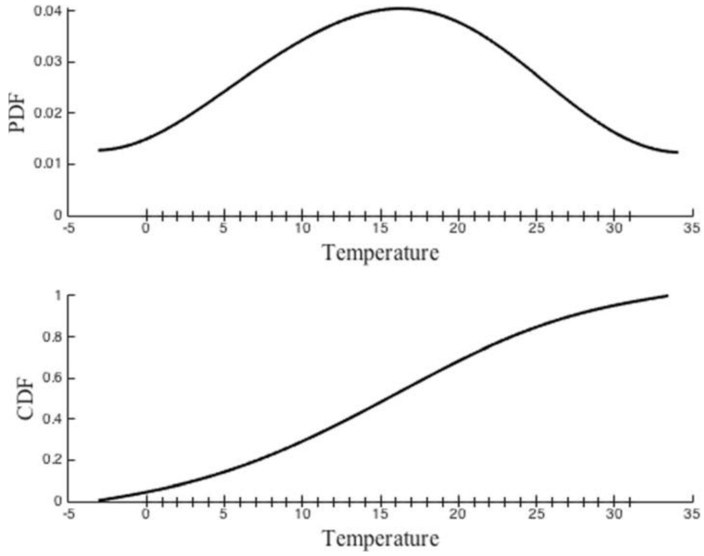

Fig. 5.5 - Prior probability distribution of a influencing factor "temperature" [15]

Subsequently, a BN model is developed to estimate the maximum occurrence probability of constants A and B. In the BN model, inputs such as the environmental factors and the material properties are required in order to exercise the model.

A conditional probability table (CPT) is developed to estimate the probabilities of each state of the variables and considers each combination of the parent states. The conditional probabilities for the child nodes were created by studying the relationship between different factors that control pitting corrosion depth in long-term exposure. Most of the information was derived from the field data. In addition to field data, the theoretical corrosion loss model and additional expert knowledge were used to develop the conditional probability table.

To exercise the experimental analysis, the first step requires the collection of long-term exposure pitting corrosion data (>2.5 years) along with the specific operating conditions. The power law model is then applied to represent the pit depth as the function of time.

The model is then calibrated using a thorough re-examination of literature data and the extensive use of specially commissioned field tests. The parameters of the power law model (A&B) for each site are derived using linear stepwise regression. First, the hypothetical value is assigned to empirical constants A and B to calculate the pitting corrosion depth c(t). Later, the predicted pitting corrosion depth c(t) was compared with the experimental pitting corrosion depth. The standard deviation was calculated to find the amount of variation in a power law constant values.

Following this, the PDF for constants A and B is developed based on the numerical value obtained from fitting the model to the observed data. The PDFs are determined empirically (that is, based entirely on available observational data). Furthermore, the assumed probability distributions are verified in the light of available data, using the normality test as explained in Sec. 5.1.2. This test is implemented by considering several PDFs, and by carefully selecting the one that best fits the calibrated data. This approach is generally used to eliminate the uncertainty associated with the estimation of the probability of occurrence of undesirable events and their consequences. As discussed in Sec. 5.1.2, quantitative data analysis is also preferred as a part of the methodology in order to access generic data, to statistically evaluate data, and to develop incident distributions using the data.

Finally, the BN result and experimental results are integrated by PDFs of constants A and B. Using the maximum probability from BN, the actual numerical value of constants A and B is obtained from their posterior PDFs developed using experimental analysis. The obtained numerical value for constants A and B is then applied to the power law model to predict the time-dependent pitting corrosion depth.

5.1.4 Application of the methodology: a case study

A case study is used to illustrate the application of the proposed methodology to predict the time-dependent pit depth of structural steel in long-term marine exposure.

The data were obtained from the world-wide test program undertaken by ASTM Task Group, which assessed the relative corrosivity of seawater at 14 various test sites. These field tests were accomplished by exposing aluminum alloy, copper–nickel alloy, and mild steel specimens at 14 distinctive test sites. However, this study is only focused on the pitting corrosion observations of mild steel specimen exposed for 0.5, 1, 3, and 5 years in marine environments. Regrettably, suitable data sources for the calibration of this model are very limited and relatively few data sources provide sufficient information about operating (environmental) conditions. Therefore, in this case study, the ASTM worldwide corrosion tests provide the sole data observed for pitting corrosion depth as well as the operating conditions. Their data were exclusively adopted to conduct this study and to test the applicability of the proposed methodology.

Pitting corrosion depth data adapted from ASTM are shown below:

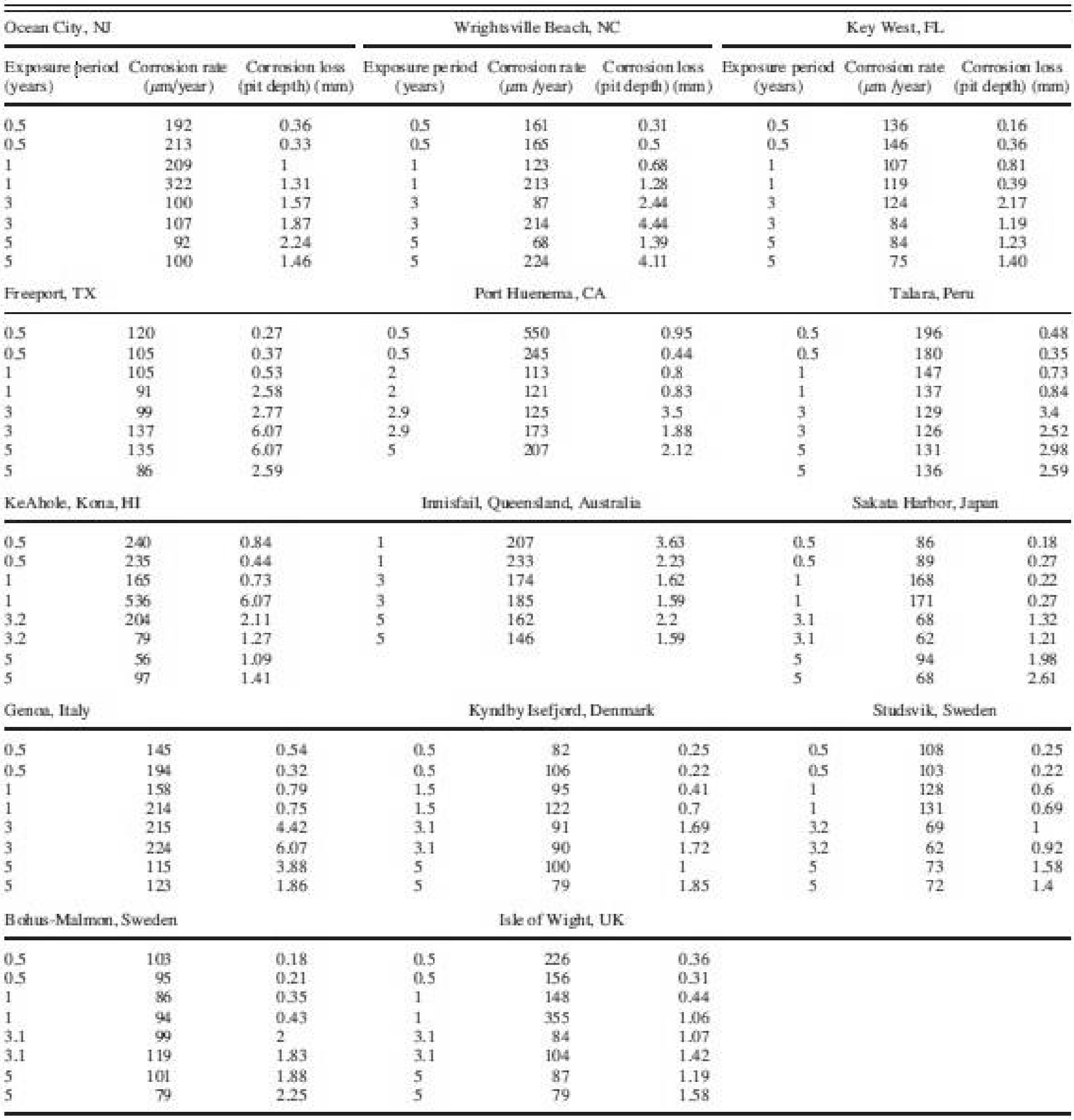

Ocean City, NJ			Wrightsville Beach, NC			Key West, FL		
Exposure period (years)	Corrosion rate (μm/year)	Corrosion loss (pit depth) (mm)	Exposure period (years)	Corrosion rate (μm /year)	Corrosion loss (pit depth) (mm)	Exposure period (years)	Corrosion rate (μm /year)	Corrosion loss (pit depth) (mm)
0.5	192	0.36	0.5	161	0.31	0.5	136	0.16
0.5	213	0.33	0.5	165	0.5	0.5	146	0.36
1	209	1	1	123	0.68	1	107	0.81
1	322	1.31	1	213	1.28	1	119	0.39
3	100	1.57	3	87	2.44	3	124	2.17
3	107	1.87	3	214	4.44	3	84	1.19
5	92	2.24	5	68	1.39	5	84	1.23
5	100	1.46	5	224	4.11	5	75	1.40
Freeport, TX			Port Huenema, CA			Talara, Peru		
0.5	120	0.27	0.5	550	0.95	0.5	196	0.48
0.5	105	0.37	0.5	245	0.44	0.5	180	0.35
1	105	0.53	2	113	0.8	1	147	0.73
1	91	2.58	2	121	0.83	1	137	0.84
3	99	2.77	2.9	125	3.5	3	129	3.4
3	137	6.07	2.9	173	1.88	3	126	2.52
5	135	6.07	5	207	2.12	5	131	2.98
5	86	2.59				5	136	2.59
KeAhole, Kona, HI			Innisfail, Queensland, Australia			Sakata Harbor, Japan		
0.5	240	0.84	1	207	3.63	0.5	86	0.18
0.5	235	0.44	1	233	2.23	0.5	89	0.27
1	165	0.73	3	174	1.62	1	168	0.22
1	536	6.07	3	185	1.59	1	171	0.27
3.2	204	2.11	5	162	2.2	3.1	68	1.32
3.2	79	1.27	5	146	1.59	3.1	62	1.21
5	56	1.09				5	94	1.98
5	97	1.41				5	68	2.61
Genoa, Italy			Kyndby Isefjord, Denmark			Studsvik, Sweden		
0.5	145	0.54	0.5	82	0.25	0.5	108	0.25
0.5	194	0.32	0.5	106	0.22	0.5	103	0.22
1	158	0.79	1.5	95	0.41	1	128	0.6
1	214	0.75	1.5	122	0.7	1	131	0.69
3	215	4.42	3.1	91	1.69	3.2	69	1
3	224	6.07	3.1	90	1.72	3.2	62	0.92
5	115	3.88	5	100	1	5	73	1.58
5	123	1.86	5	79	1.85	5	72	1.4
Bohus-Malmon, Sweden			Isle of Wight, UK					
0.5	103	0.18	0.5	226	0.36			
0.5	95	0.21	0.5	156	0.31			
1	86	0.35	1	148	0.44			
1	94	0.43	1	355	1.06			
3.1	99	2	3.1	84	1.07			
3.1	119	1.83	3.1	104	1.42			
5	101	1.88	5	87	1.19			
5	79	2.25	5	79	1.58			

Tab. 5.1 - Pitting Corrosion Depth Data Adapted From ASTM [15]

The operating conditions adapted from the ASTM worldwide test are shown below:

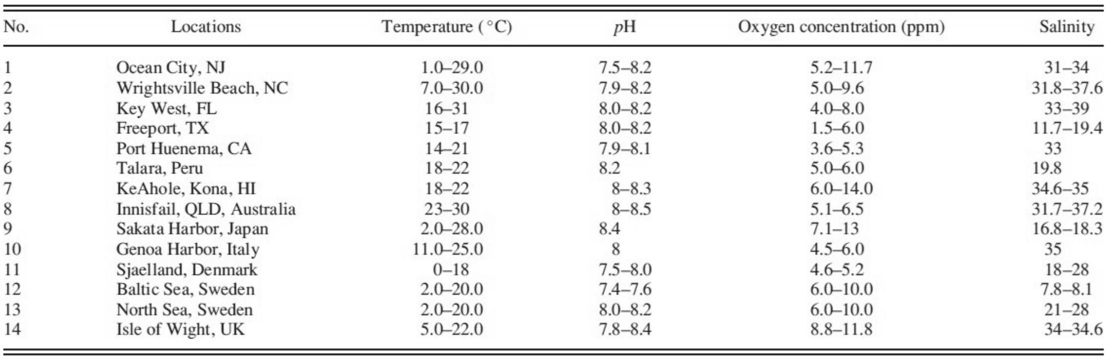

No.	Locations	Temperature (°C)	*p*H	Oxygen concentration (ppm)	Salinity
1	Ocean City, NJ	1.0–29.0	7.5–8.2	5.2–11.7	31–34
2	Wrightsville Beach, NC	7.0–30.0	7.9–8.2	5.0–9.6	31.8–37.6
3	Key West, FL	16–31	8.0–8.2	4.0–8.0	33–39
4	Freeport, TX	15–17	8.0–8.2	1.5–6.0	11.7–19.4
5	Port Huenema, CA	14–21	7.9–8.1	3.6–5.3	33
6	Talara, Peru	18–22	8.2	5.0–6.0	19.8
7	KeAhole, Kona, HI	18–22	8–8.3	6.0–14.0	34.6–35
8	Innisfail, QLD, Australia	23–30	8–8.5	5.1–6.5	31.7–37.2
9	Sakata Harbor, Japan	2.0–28.0	8.4	7.1–13	16.8–18.3
10	Genoa Harbor, Italy	11.0–25.0	8	4.5–6.0	35
11	Sjaelland, Denmark	0–18	7.5–8.0	4.6–5.2	18–28
12	Baltic Sea, Sweden	2.0–20.0	7.4–7.6	6.0–10.0	7.8–8.1
13	North Sea, Sweden	2.0–20.0	8.0–8.2	6.0–10.0	21–28
14	Isle of Wight, UK	5.0–22.0	7.8–8.4	8.8–11.8	34–34.6

Tab. 5.2 - Parameters for Predicting the Long-Term Pitting Corrosion Depth Adapted From ASTM [15]

Based on the ASTM field tests, the contributing factors of long-term pitting corrosion in marine environment are identified as temperature, salinity, pH, oxygen concentration, exposure period, and velocity. Some of these factors, such as the existence of SRB (Sulfate-Reducing Bacteria) and the alloying effect, were not calibrated when ASTM tests were conducted. For this study, the authors have included the effects of SRB and alloy composition based on the phenomenological model and from several published works including the recent review by Bhandari et al. SRB is the most active contributor to pitting in long-time exposure of carbon steel materials in marine environment because the metabolic activities result in sulfate ion reduction to hydrogen and sulfide. The sulfide ion attacks the steel electrochemically causing more pitting corrosion due to an increase in anodic/cathodic reactions caused by sulfate reduction. The effect of oxygen concentration was omitted in this study because it does not affect the long-term pitting corrosion process.

The prior probabilities for environmental parameters and material properties are obtained through the distribution developed for individual factors. The distribution for each particular factor is established by considering the operating conditions of all 14 test sites. When considering a PDF, the prior probability of different states (such as high, average, and low value) is estimated for each factor as demonstrated in Table 5.3. The high and low states represent the higher and lower bound in the PDFs.

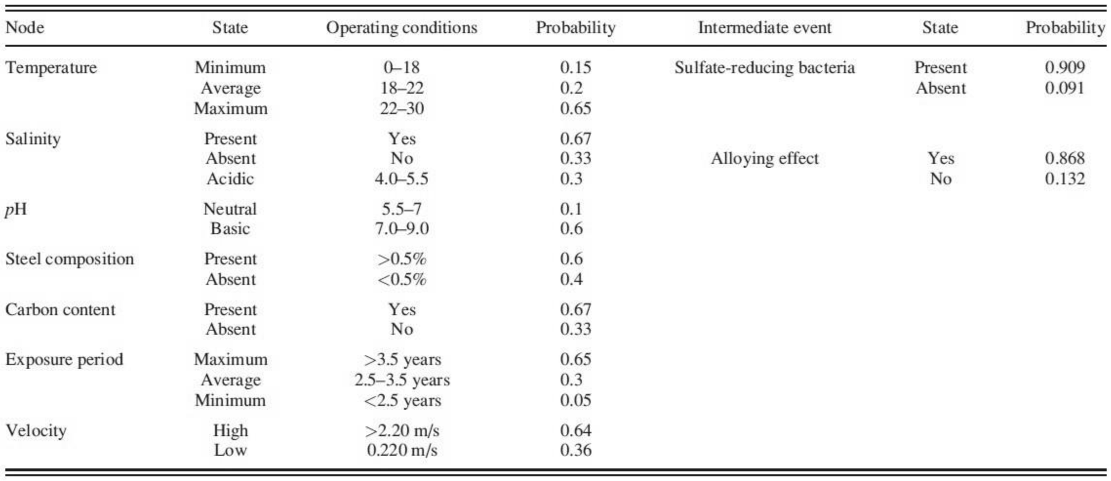

Node	State	Operating conditions	Probability	Intermediate event	State	Probability
Temperature	Minimum	0–18	0.15	Sulfate-reducing bacteria	Present	0.909
	Average	18–22	0.2		Absent	0.091
	Maximum	22–30	0.65			
Salinity	Present	Yes	0.67			
	Absent	No	0.33	Alloying effect	Yes	0.868
	Acidic	4.0–5.5	0.3		No	0.132
*p*H	Neutral	5.5–7	0.1			
	Basic	7.0–9.0	0.6			
Steel composition	Present	>0.5%	0.6			
	Absent	<0.5%	0.4			
Carbon content	Present	Yes	0.67			
	Absent	No	0.33			
Exposure period	Maximum	>3.5 years	0.65			
	Average	2.5–3.5 years	0.3			
	Minimum	<2.5 years	0.05			
Velocity	High	>2.20 m/s	0.64			
	Low	0.220 m/s	0.36			

Tab. 5.3 - Parameter for predicting long-term pitting corrosion depth [15]

After establishing the prior probabilities for the environmental factors and material properties, a causes-consequences relationship model is developed using BN. To predict the probability of the constants (A and B), the contributing factors and their assigned prior probabilities are applied to BN as listed in Table 5.3.

Figure 5.6 demonstrates the developed BN model, which estimates the maximum probability of constants A and B, respectively. The probability of these constants is a complex function of environmental variables, such as temperature, exposure period, and bacterial activities, as shown in Table 5.1. These variables influence the occurrences probability of constants A and B, which indirectly controls the growth of the pitting corrosion depth.

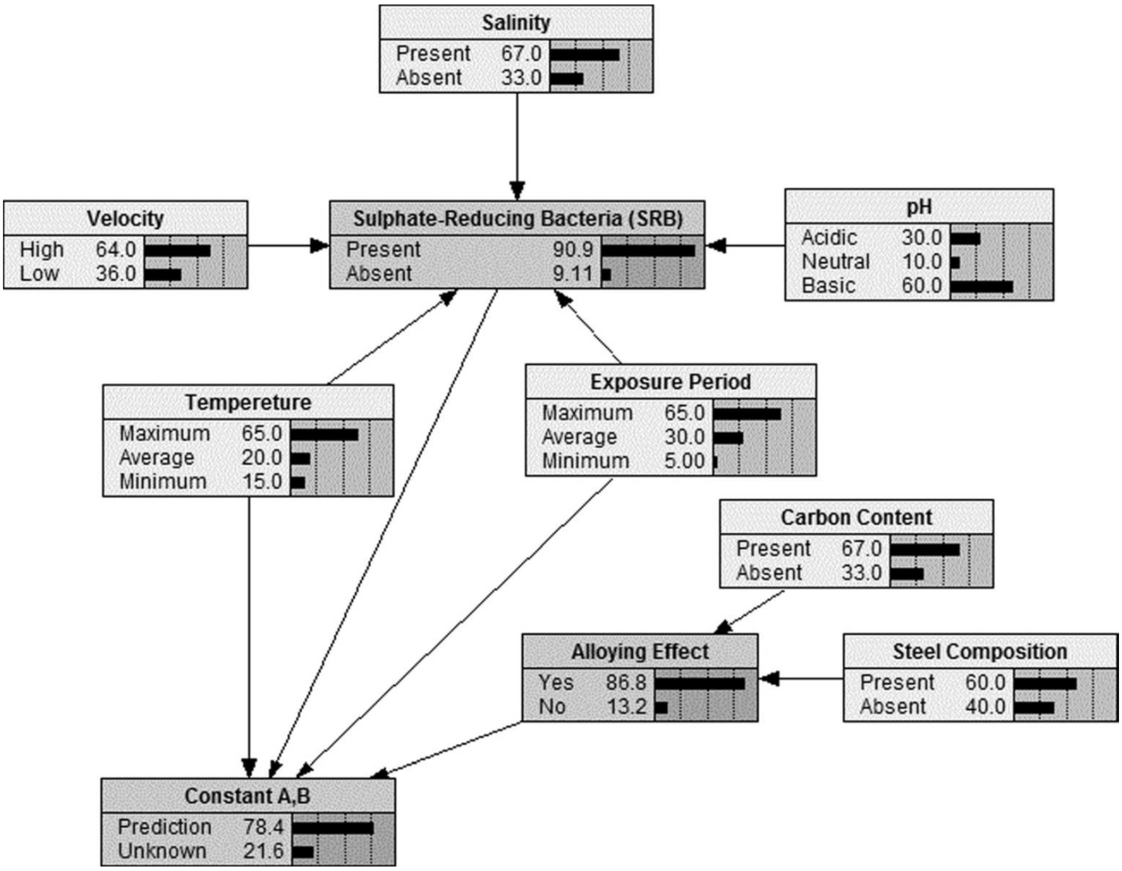

Fig. 5.6 - Developed BN model to predict pitting depth constants (A&B) [15]

Therefore, the developed model should take into account the relationship between these variables to predict the maximum probability of the constants. The final probability of constants A and B depends on the conditional probability matrix. As previously stated, the conditional probabilities table in this study is developed based on the perception of theoretical corrosion model, from the field test data, and through expert judgments.

In the BN model, inputs such as environmental factors and materials properties are used to exercise the model. As mentioned earlier, the effect of temperature has long been recognized as an important influencing factor. This is confirmed in the BN model based on both theoretical corrosion principles and field observations. In this study, the operating temperature is considered to be within the range of 0–30 °C. The highest temperature was reported at Wrightsville Beach, NC and the lowest temperature was reported in Sjaelland, Denmark. For the short-term exposure, the pH of seawater is found to be consistent for all sites; however, the effect of carbon dioxide can affect the range of pH during long-term corrosion exposure. The pH is used in three different states in this study and, as presented in Table 1, the acidic, neutral, and basic states are found to be within the range of 4–9. The exposure period is crucial for predicting long-term pitting depth. Only long-term corrosion (more than 0.5 years) is considered in this study. Melchers and Jeffrey also considered the data for 0.5 to more than 4 years of exposure in their study. However, they stated that there is usually a considerable increase in the instantaneous corrosion rates for both weight loss and for pitting depth after 2 years exposure.

The effect of seawater salinity is conventionally considered to be a very important factor with regard to pitting corrosion. It was found that the amount of salinity present in the seawater was relatively inconsistent for all the considered exposure sites. However, it should be noted that the variations of salinity for different sites were fairly minimal. Two binary states of "present or absent" are considered for the occurrences of seawater salinity in this study. Similarly, the effect of alloy composition acts on the tendency for an alloy to initiate pit and also affects the rate of corrosion. The effect of the alloy composition may have a favorable effect in corrosion resistance ability of the materials under certain exposure conditions such as seawater immersion and atmospheric conditions. In this study, the significant effect of alloy composition in predicting the probability of constants (A and B) is observed as demonstrated in the BN. The effect of water velocity on long-term pitting corrosion is also found to be significant. This was found to be in line with Melchers' report, which states that the water velocity increases the rate of pitting corrosion nonlinearly. Melchers indicated that when corrosive products and/or marine growth is disrupted or removed (as through erosion or abrasive action), the effect of water velocity on pitting corrosion can become more severe. This study indicates that the effect of microbiological activities is significant in predicting pitting corrosion depth. From the developed BN, it can be seen that the sulfate-reducing bacteria increase the maximum values of constants A and B which, in turn, increases the depth of pit as a function of time consistently. Southwell et al. and Melchers and Jeffrey have also discussed the influence of the microbiological activities on both the short- and long-term corrosion of steels.

The BN model illustrated in Fig. 5.6 estimates the maximum possible probability of constants A and B. The value estimated represents the occurrence probability of constants A and B to a maximum probability when all the operating conditions and their conditional probabilities are satisfied. The final probability of constants A and B is calculated as 0.784 (refer Fig. 5.5). It can be seen that the probability of A and B is remarkably similar; however, the relationship between the variables and the conditional probability table is different. This will lead to a separate numerical value for the individual constants (A and B) when considering the similar probability received from the BN.

In the experimental analysis, the corrosion loss/pitting depth versus the exposure time observation (for each of 14 sites) is plotted to examine whether the data agree with the phenomenological corrosion model trends. As illustrated in Fig. 5.7, the data are considerably at variance with the pit depth growth law considered in this study. It clearly shows that the idealized bimodal model of the type shown in Fig. 3.12 of 3.3.2 is suitable for pitting corrosion. Indeed, there is a need of model calibration to extensive data derived new field observations. Data for four different sites are plotted in Fig.

5.7, where the line represents the power function regression curves and the dot represents the actual data.

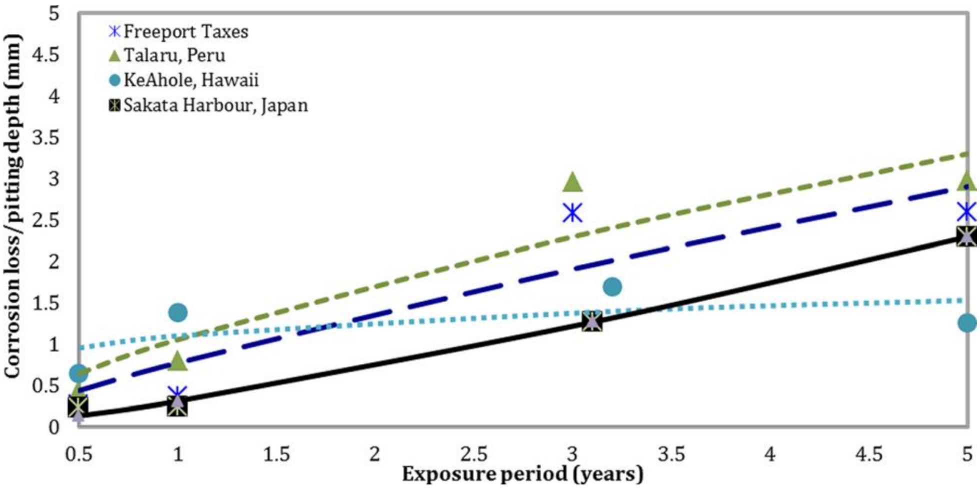

Fig. 5.7 - Localized corrosion data for mild steel exposed to surface seawater conditions at four different sites (the solid lines represent power law model and dotted line represents actual data) [15]

This graph shows fairly acceptable agreements between the experimental corrosion data and the power function regression curves obtained using power law model ($c(t) = A\ t^{B}$). In Fig. 5.7, some of the graph does not appear to have a perfect fit; this could be due to the lack of enough observed data points from the field test.

The parameters of the power law model (A&B) for each site are derived using linear stepwise regression. Then the PDF for constants A and B is developed based on the numerical value obtained from fitting the model to the observed data. Figure 5.8 shows the posterior PDF for constants A and B developed from the value obtained by fitting power law model to the calibrated data from all the test sites.

In order to estimate the depth of the pit as a function of time, the result obtained from BN is used to read the corresponding numerical value of A and B when considering PDFs. Considering the maximum probability of 78.4%

(obtained from BN), the numerical value of A and B is found to be 1.5 and 0.8, respectively.

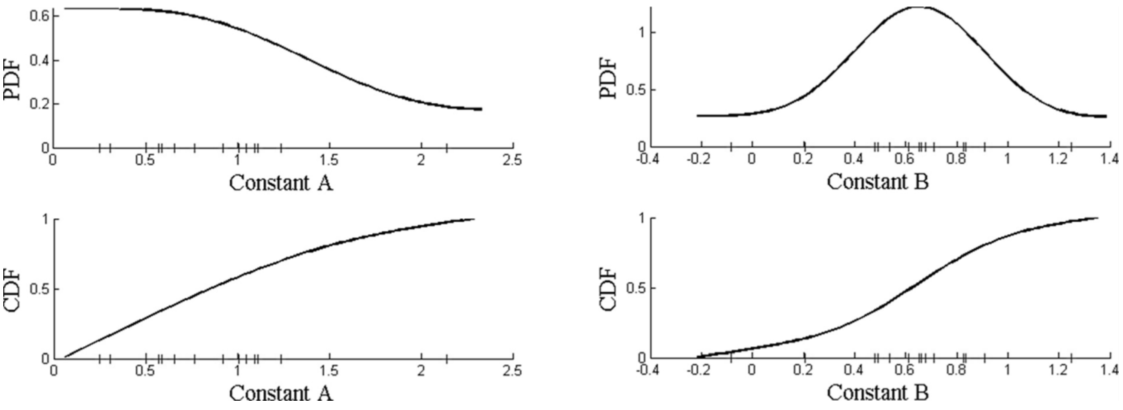

Fig. 5.8 - Posterior probability distribution for constants (A and B) [15]

In predicting the value of constants A and B from the empirical pit depth model, comparable outcomes are reported in several previously published studies. Sowinski and Sprowls considered the power law model for various alloys exposed to the marine environment for up to 30 years in U.S.; they found the value of B to range between 0.33 to more than 1. Melchers considered the power law in his previous studies and indicated that B should be 0.5 for pure Fickian diffusion and homogenous rusts; however, his calibration to field data invariably showed that B varies between 0.3 and 0.8. For short-term laboratory studies of the pit depth, this value may differ. Aziz and Godard reported that for short-term laboratory tests on pitting depth, the value of B is in the range of 0.33 and 0.55. Based on the previous literature, the value for A has not been reported as comparable to B. However, Hou and Liang established the multi-correlation coefficient value of A and B as 0.82 and 0.9 after analyzing 16 years exposure data of steel. Their value of A shows a slight discrepancy from the value reported in this study. The reason could be attributed to the uncertainty associated with each data point, or to errors in their experimental data and/or data processing.

Southwell et al. reported a data of 8-years exposure tests of structural steel exposed to seashore and inland environments in the Panama Canal Zone. Their data were applied to the proposed methodology to estimate the corrosion loss model using power law considering the operational conditions.

Figure 5.9 shows the comparison of power law model calibrated to the actual data for a variety of metals in the Panama Canal Zone. The compassion shows the remarkable agreement between actual data (lines) and the power law model calibrated to the field data (dots).

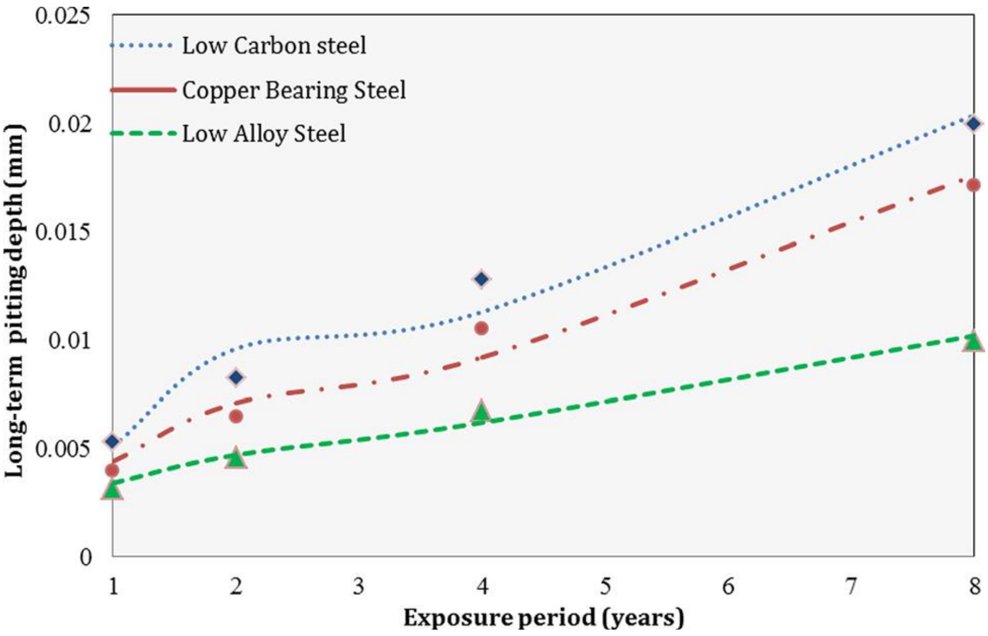

Fig. 5.9 - The pitting corrosion loss model developed from Panama Canal Zone data, which is applied to proposed methodology [15]

Furthermore, Hou and Liang used the regression analysis approach that does not take account of the conditional dependency among variables, whereas the BN is a powerful technique, which predicts the probabilities of constants.

This study used the prior knowledge of pitting corrosion phenomena, together with the observed data. BN is also capable of establishing the probabilistic relationship between variables to deal with the uncertainty associated with the data set.

This analysis confirms that the proposed methodology is successful in predicting the long-term anaerobic pitting corrosion depth of structural steel as a function of time in different environmental and operational conditions. The developed methodology in this study has advantages for estimating the pitting depth as compared to the previously used conventional techniques.

This BN-based methodology can be practiced to predict the future deterioration of newly built or older offshore infrastructures using their specific operating conditions. This novel concept for modeling pit depth focuses on interpreting data in terms of a priori model using Bayesian statistics rather than using data alone to indicate a model, such as typical correlation studies do. Using this methodology, the result illustrates that this approach is successful in providing new interpretations and better understanding of empirical “field” observations.

Furthermore, the sensitivity analysis is performed to investigate the most influencing factors as well as their contributions to the pitting depth. It is conducted by assigning a zero probability to the individual factors affecting the pitting depth. The BN model calculates the percentage contributions by comparing each case with the base case when all factors are active. The result shows that the temperature and the exposure period are the most influencing factors affecting the pitting depth.

Comparable investigations are reported by several researchers. Melchers reported that the pitting corrosion rate should be doubled for every 10 °C increase in temperature. He further stated that the microbiological reaction process for corrosion becomes faster with increase in temperature after the initial stage; this suggests that the corrosion rate increases with the rise in seawater temperature. Melchers also confirmed that both temperature and the exposure time play a vital role toward increasing the biological activities in seawater.

5.2 Residual safety assessment

5.2.1 Expected lifetime

Aging steel structures may be subjected to strength and stiffness changes beyond their baseline condition for design. These changes may impair the safety and serviceability of the structure and should be considered as part of the process by which a structure is evaluated for continue future service. Over the structure's lifetimes, the result of the interactions between metallic structures of offshore platforms with the maritime environment, corrosion occurs [26].

Occurrence of the local or overall corrosion should be considered in determining the residual strength of corroded tubular members. However, there is no sufficient information on how to model the corrosion damage for strength assessment in the International Standards [39].

It is noted that in many cases steel structures are protected either by protective coatings (such as paints) or cathodic protection, at least when first constructed. In actual practice these protective measures are not always maintained and, with time, the question arises what the safety might be of the remaining, partly or wholly corroded structure. In some applications, such as for the holds inside bulk carrier ships, and the mooring chains for offshore oil and gas facilities, protective coatings or cathodic protection are not practical. During the design of the marine structures, a corrosion thickness allowance is added to compensate the potential thickness reduction due to corrosion along the service life. For these types of applications, prediction of the rate and manner of material deterioration with time is required to assist with assessment of structural safety [23].

Because the risks and the costs, including those of potential failure and of premature repairs or replacement, are high, good quality mathematical models for corrosion are required. As mentioned above, building such models requires good understanding of the (changing) underlying physical and chemical processes.

The mathematical models allow to estimate the expected structural lifetime. Consider a simple structure with capacity $R = R(t = 0)$ (strictly a random variable) at time of design ($t = 0$) given by a design value R_k the characteristic value, for which, ideally, the probability density function is known, or at least the mean μ_R and standard deviation σ_R are known or can be inferred. Similarly, let the applied loading be considered translated to one or more stress resultants through structural analysis. Each of these will have a characteristic value of S_k with, ideally, a known or inferred probability density function or, at least, with known or inferred mean μ_S and standard deviation σ_S. Usually S is a random process given more generally by $S(t)$. As always, failure at any time t is defined as:

$$R(t) < S(t) \tag{5.4}$$

and the probability of failure as:

$$f(t) = \mathrm{Prob}[R(t) < S(t)] \tag{5.5}$$

Further, the probability of failure in the interval 0-t is bounded from above by the well-known expression:

$$p_f(t) \leq p_f(0) + [1 - p_f(0)]\, \nu\, t \tag{5.6}$$

where $p_f(t)$ is the probability of failure in the time period [0-t]. Of most interest is the period $[0 – t_L]$ with t_L denoting, as usual, the structural life span of interest. In addition, $p_f(0)$ is the probability of failure at $t = 0$, that is, at the time of first load application, and ν is the so-called 'up-' (or 'out-) crossing' rate. It denotes the rate at which the load process (or processes) crosses-up (or -out) of the safe domain into the unsafe domain. For a continuous process ν is given by Rice's formula or generalisations thereof. Various approximate solutions are available, also for non-continuous formulations. The precise details need not be considered here save to note that in some situations ν will be constant in time (such as if R(t) = constant and S(t) is a stationary process) but more generally it will be a function of t.

The above shows the close relationship between the estimate of the probability of failure $pf(t_L)$ in a given life time t_L, the mean outcrossing rate ν and the changing (usually declining) capacity R(t) of the structure. The challenge for deteriorating (corroding) structural systems is how to determine a reasonable function for R(t) given that at design time only R(0) is known (probabilistically anyway).

Figure 5.10 shows that, the strength function (R) deteriorates with time (t1, t2, t3 are different time points) due to corrosion, fatigue, etc., while the overlap with load density function (Q) get bigger. This overlapping is the failure criterion for the structure. It can be seen that the resistance probability density function flattens by time as well as the mean value decreases while the standard deviation increases. This explains the effect of corrosion on strength and reliability of offshore structures.

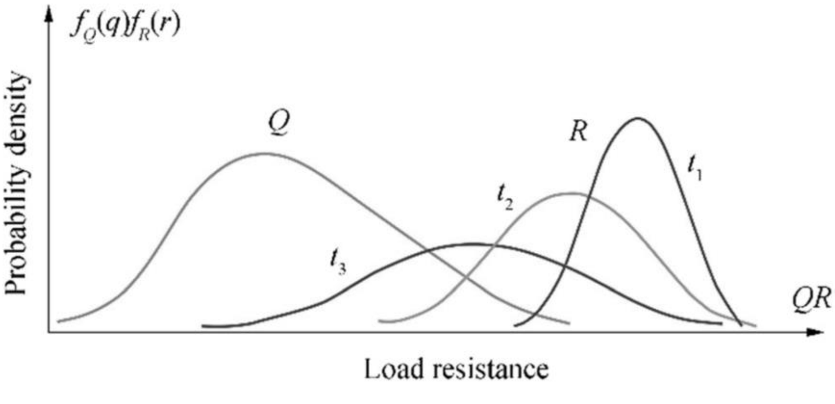

Fig. 5.10 - Resistance distribution decay by time [32]

A slightly different aspect is the estimated structural reliability at some point in time, t_1 say, and the reliability expected in the future (i.e. for $t > t_1$). In this case instead of p_f (t=0) in the previous equation the probability of interest is p_f (t = t1). Further, for relatively short forecasting (or prediction) periods Δt at $t > t_1$, the up- or out-crossing rate ν is likely to change little and thus the rate ν(t = t1) will be applicable. Again, these estimates require the capacity $R(t \geq t_1)$ to be available.

The sensitivity of the expected lifetime of a structure to the rate and pattern of deterioration of structural resistance is illustrated, schematically, in Figure 5.11. It shows that even for small changes in the rate of loss of resistance, there are quite significant changes in expected lifetime. The sensitivity is greater for much longer expected lifetimes. Although shown for a given peak load level, a similar result applies for random process loadings. It follows directly from these introductory remarks that the estimation of the expected life time or the prediction of the remaining reliability at some point in time, perhaps set within a life-cycle costing framework, requires high quality modelling of the deterioration process.

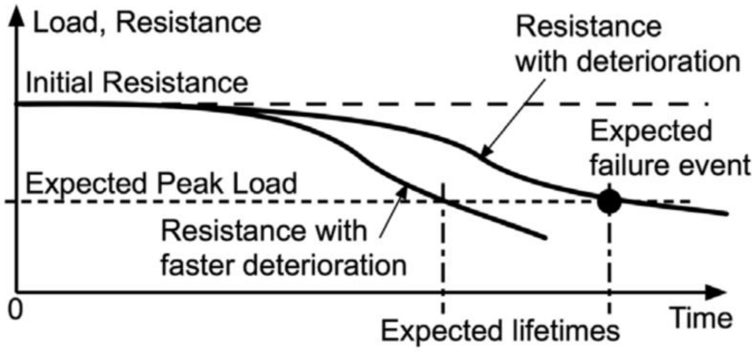

Fig. 5.11 - Sensitivity of the expected structural lifetime on the rate of deterioration of structural resistance for a given (expected) loading (schematic) [23]

5.2.2 Corrosion effect on ultimate strength

Corrosion is one of the most important factors reducing the structural capacity during structures service life. In order to ensure the safety of offshore structures, it is necessary to understand the effect of pitting corrosion of welding material and steel structural members on the local strength capacity [24].

As we have seen previously, corrosion can lead to structural material degradation, this material degradation results in loss of mechanical properties of the structure such as strength, ductility and impact strength. This is further aggravated with poor and less emphasised maintenance scheme by the operators. Limitation of resources, time and cost are to be blamed for the improper platform maintenance [32].

Material degradation also leads to loss of material and, at times, to ultimate failure. Hence the assessment of the ultimate strength of corroded structures is crucial, since realistic safety margins for a structural system cannot be determined unless the ultimate strength is precisely estimated [26].

There are usually two critical design criteria that are strength capacity and integrity for structural system such as offshore platform and ships. As stated by Melchers the first one is basically a function of material loss due to pitting corrosion. As for the second one it is quite localized and in particular due to pitting corrosion and both of them are considered as structural capacity perspective [17].

For structural capacity it is usually depends on the cross-sectional dimensions of the structural member. In figure 5.12a, the axial member of cross-sectional area A are under axial stress σ and surrounded by sea water.

$$R\ (t) = \sigma * [A - P * c\ (t)] \qquad (5.7)$$

Where corrosion loss $c\ (t)$ is a function of time and P is the perimeter area exposed to seawater.

For plate bending with a possible corrosion on both side of the plate, the bending resistance become:

$$R\ (t) = k\ {*}\sigma_b{*}\ [d\ (t)]^{2} = k\ {*}\sigma_b{*}\ [d_0 - 2\ {*}c\ (t)]^{2} \tag{5.8}$$

Where d_0 is the initial thickness of the plate, $d\ (t)$ is the remaining thickness, σ_b is the maximum stress imposed by bending fracture, k = 0.25 for elastic-plastic material response and 0.167 for elastic response (Fig. 5.12b).

When considering the strength in ductile (plastic) structure, it is acceptable to obtain $c(t)$ from weight-loss measurements or estimation of the corrosion depth, averaged over a local surface area. Local maximum of $c(t)$ at the point of maximum local stress is required when local stress is intensity and cause local rupture, as in brittle material.

As for pitting (Fig. 5.12c), remaining thickness $d\ (t)$ of a plate of initial thickness d_0 is given by:

$$d\ (t) = d_0 - d_p\ (t) \tag{5.9}$$

Where $d_p\ (t)$ is the maximum depth at time t. Since the first pit will cause perforation, the maximum probable pit depth is required. Occurs when $d(t) \rightarrow 0$.

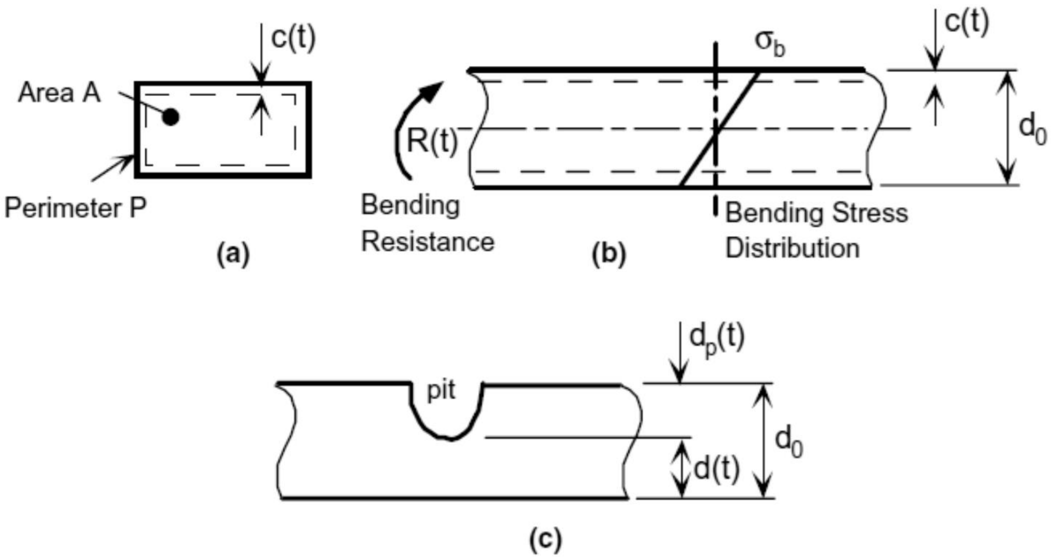

Fig. 5.12 - (a) Cross-section of a bar under axial stress showing corrosion loss, (b) cross-section of a plate under bending stress showing effect of corrosion and (c) cross-section of a plate subject to pitting from one side [17].

In practice the dimensions such as d_0 will vary somewhat from location to location over the surface of a steel plate or member, and in addition the actual dimension may differ appreciably from the nominal dimensions. This gives rise to variability and to bias respectively for the dimensions. The locally relevant applied stress (σ or σ_b) depends directly on the loadings applied to the structure and hence also have random properties (expressed either as random variables or random processes).

That there is considerable variability in corrosion losses such as c(t) and $d_p(t)$ is evident from the wide disparity in average corrosion rates (c(t)/t and $d_p(t)/t$) quoted in the literature. It has been suggested previously that a more appropriate approach is to consider these parameters as random variables with properties that change with time [25].

5.2.3 Strength loss of tubular members with localized pitting damage

Pitting corrosion often produces pits on a member as widely scattered pitting that occurs over the entire surface of a member (widespread pitting), or localized region of pitting (localized pitting). Corrosion pits result in an irregular surface on the member [39].

A large number of experimental and numerical studies have been conducted to investigate the effect of widespread pitting on pitted structures including plates and stiffened panels under compression, plates under shear, and tubular members under compression. To model the uneven surface of a pitted member, corrosion pits were commonly dealt with the circular cavities of the same size and depth, and with a specified regular or irregular distribution. It was shown that widespread pitting causes a significant reduction in ultimate strength, mainly depended on the volume loss of corroded material. In contrast to general (uniform) corrosion, pitting corrosion causes a larger strength reduction under the same level of corrosion damage, despite no consideration in its random nature. In addition, it leads to great variation in the ultimate strength of tubular members, which may follow a normal distribution. Apart from causing the variation and the reduction of ultimate strength, the random pitting damage has a significant influence on the failure modes of pitted structures.

The effect of localized pitting on ultimate strength and structural behavior has also been widely concerned. Localized pitting was usually simplified into the form of patch corrosion. The patch had an equivalent section with a locally and uniformly thinned wall thickness in lieu of the irregular one of pitting corrosion. Based on the equivalent method, a lot of experiments and numerical studies have been carried out to investigate the ultimate strength and structural behavior of various sections including H-shaped short piles, pipelines and tubular members. It was found that the simplified uniform corrosion leads to an overestimation on ultimate strength under the same level of corrosion damage. This is due to no consideration to the uncertainties of corrosion features (pit size and depth) that can only be described statistically. In fact, they can cause great variation in the ultimate strength of pitted structures with widespread pitting. Similarly, the localized pitting causes a reduction of ultimate strength by inducing the volume loss of corroded material. Whereas the localized pitting has extra uncertainties in the location, size and shape of the corrosion patch, as shown in Figure 5.13.

Fig. 5.13 - Locally pitted tubular steel columns under marine environment [39]

These influential factors significantly influence the ultimate strength and the compressive behavior of tubular members with localized pitting damage. However, their effects were not correlated with the reduction of ultimate strength quantitatively, due to insufficiency that random nature of localized pitting cannot be reflected fully in the limited experimental study.

Corrosion data derived from normal inspection is generally statistical but not specific, leading to an inaccurate corrosion mapping. The random nature of pitting corrosion can be reflected by random variables relevant to the sizes (radiuses or diameters), depths and distribution locations of corrosion pits. The distribution location of corrosion pits was thought to comply with a uniform distribution that is typical for the pitting distribution on ship and marine structures.

More specifically, the localized pitting was described using two vectors that were named as a shape vector and a location vector. The radiuses, r, and depths, d, of corrosion pits formed the shape vector S, while the pit locations composed the location vector P. Each element of two vectors was determined through performing stochastic simulation. In order to reflect the random nature in pitting distribution, the surface of a tubular member was unfolded into a rectangular plate. The plate had a length of L being the member length, and a width of π D being the member perimeter. It was then split into a series of grids with a uniform size. Every corner point of the grids was a possible location to hold a pit, and all the corner points were stored in a vector U. To simulate the random pitting distribution, the pits in the vector S were randomly assigned onto some of corner points in the vector U. The assigned location of each pit was stored in the location vector P ($P \in U$).

With respect to localized pitting, apart from random nature in the corrosion pits, the corrosion patches with these pits have an extra random nature. It lies in the variation of corrosion features due to the uncertainties in the distribution location (along the length and hoop of a member), the size (length and width) and the shape of a corrosion patch. Therefore, the possible location to hold a pit was limited within the patch. The determination to the locations of pits can be implemented by randomly selecting elements from a limited range of the vector U, in line with the size and location of the patch, as equation:

$$x_i = random(x_{min}, x_{max}) \tag{5.10}$$

$$z_i = random(z_{min}, z_{max}) \tag{5.11}$$

where x_{min} and x_{max} denote the start and end columns in the hoop of a member, respectively, while z_{min} and z_{max} represent the start and end rows in the length of the member.

Conventionally, the degree of pitting intensity (DOP) and the degree of corroded volume loss (DOV) are used to describe the extent of corrosion damage of the member with widespread pitting. The two damage indexes are all defined in terms of the entire surface of a member. As for localized pitting, the DOP was supposed to be defined according to locally corroded area (corrosion patch) rather than the entire surface, as follows:

$$DOP = (A_c / A) \times 100(\%) = (1 / \mu_L \mu_P D L) \times \sum_{i=1}^{k} r_i^2 \times 100(\%) \tag{5.12}$$

Correspondingly, the DOV within the corrosion patch can be defined as:

$$DOV = (V_C / V) \times 100(\%) = (1 / 2 \mu_L \mu_P R L t) \times \sum_{i=1}^{k} d_i r_i^2 \times 100(\%) \tag{5.13}$$

Where:

- A_c and V_c denote the lost area and volume due to corrosion pits within the corrosion patch, respectively;
- A and V are the original area and volume without corrosion pits in the corrosion patch;
- t is the virgin wall thickness of the member;
- R is the radius of intermediate surface of the member, equal to (D-t)/2;
- K is the number of the corrosion pits in the corrosion patch;
- r_i and d_i are the radius and depth of i^{th} pit, respectively;

- μ_L equals to $(z_{min} - z_{max})/L$ being the ratio of the patch length to member length;
- μ_P equals to $(x_{min} - x_{max})/\pi D$ being the ratio of the patch width to member perimeter.

Moreover, an additional parameter, which is named as shape ratio (SR) being the ratio of the length to width of the patch, is useful to describe the localized pitting complementally, as equation:

$$SR = \mu_L L / (\mu_P \pi D) = S_r (L / (\pi D)) \qquad (5.14)$$

where S_r is the relative shape ratio that is normalized as μ_L / μ_P and independent of the dimensions of members.

It investigates the influence of the DOP on the variation of the compressive strength as a function of the thickness of the tubular element.

Figure 5.14 shows different pitting distribution patterns in a tubular member with DOP equal to 10%, 20%, 30% and 50%:

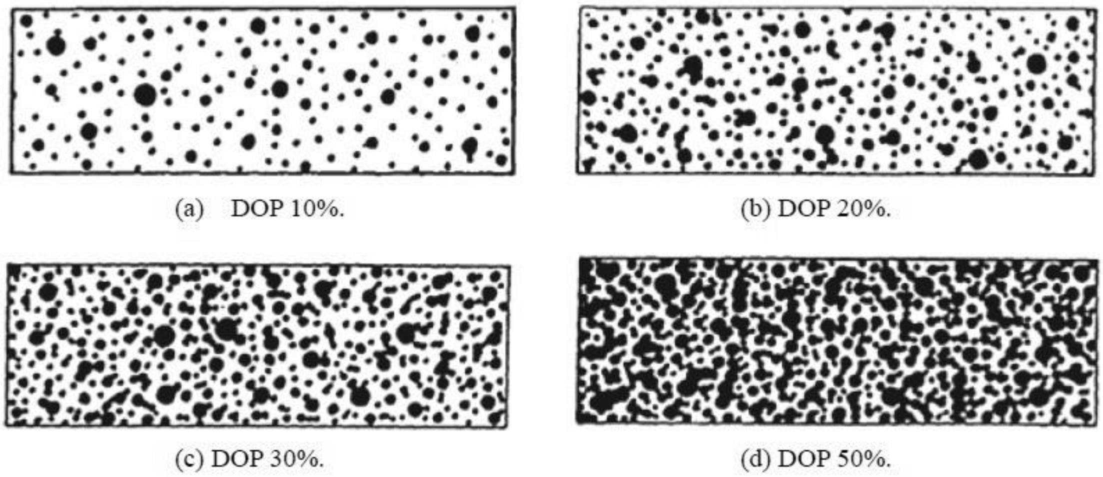

(a) DOP 10%.

(b) DOP 20%.

(c) DOP 30%.

(d) DOP 50%.

Fig. 5.14 - Pitting distribution patterns

The resisting normal stress of the compressed tubular element was calculated in accordance with NTC 18 (figure 5.15):

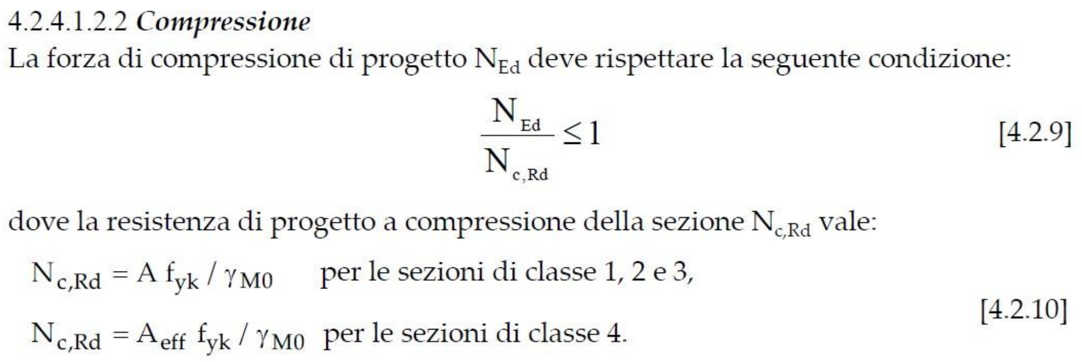

4.2.4.1.2.2 *Compressione*

La forza di compressione di progetto N_{Ed} deve rispettare la seguente condizione:

$$\frac{N_{Ed}}{N_{c,Rd}} \le 1 \qquad [4.2.9]$$

dove la resistenza di progetto a compressione della sezione $N_{c,Rd}$ vale:

$$N_{c,Rd} = A\, f_{yk} / \gamma_{M0} \quad \text{per le sezioni di classe 1, 2 e 3,}$$
$$N_{c,Rd} = A_{eff}\, f_{yk} / \gamma_{M0} \quad \text{per le sezioni di classe 4.} \qquad [4.2.10]$$

Fig. 5.15 – NTC18 specification for compressed members [40]

Where the class of the section is determined according to what is indicated in paragraph 4.2.3.1 of the NTC18 (figure 5.16):

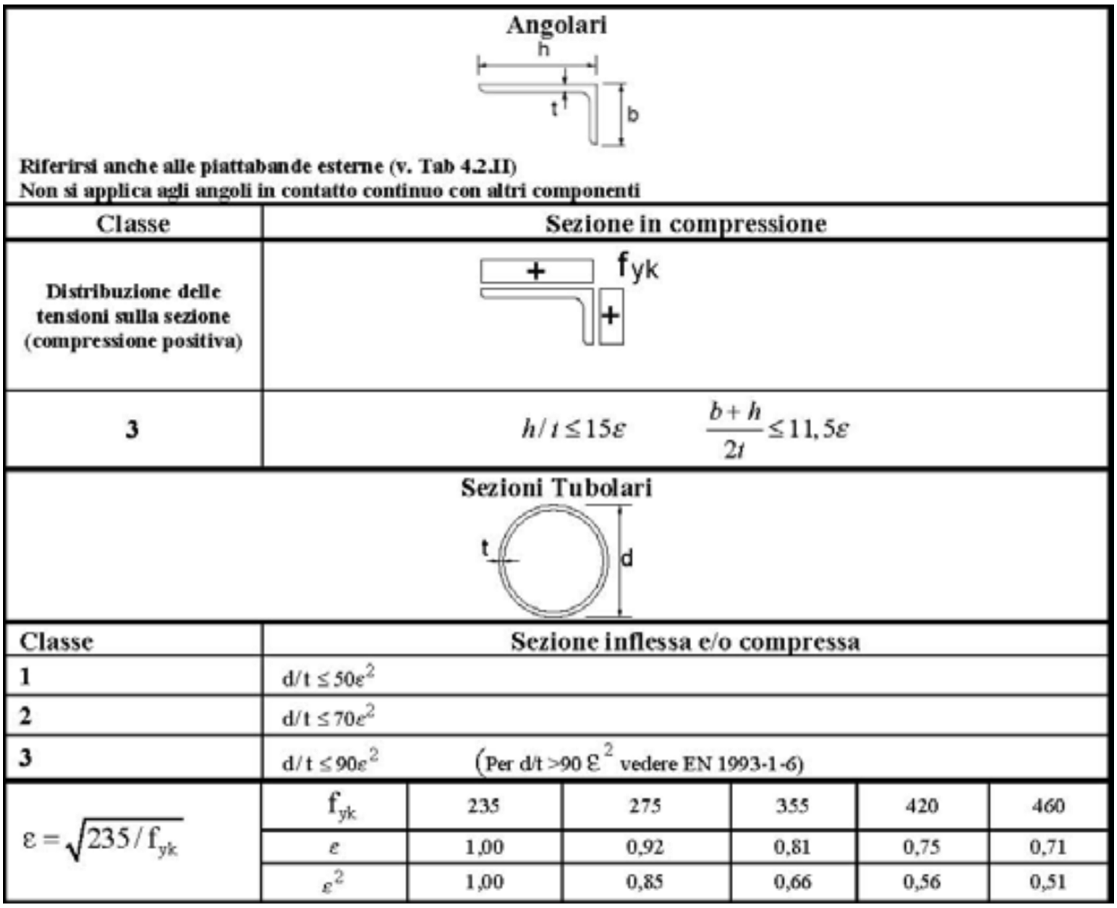

Angolari

Riferirsi anche alle piattabande esterne (v. Tab 4.2.II)
Non si applica agli angoli in contatto continuo con altri componenti

Classe	Sezione in compressione
Distribuzione delle tensioni sulla sezione (compressione positiva)	f_{yk}
3	$h/t \le 15\varepsilon$ $\quad \frac{b+h}{2t} \le 11,5\varepsilon$

Sezioni Tubolari

Classe	Sezione inflessa e/o compressa
1	$d/t \le 50\varepsilon^2$
2	$d/t \le 70\varepsilon^2$
3	$d/t \le 90\varepsilon^2$ (Per d/t >90 ε^2 vedere EN 1993-1-6)

$\varepsilon = \sqrt{235/f_{yk}}$	f_{yk}	235	275	355	420	460
	ε	1,00	0,92	0,81	0,75	0,71
	ε^2	1,00	0,85	0,66	0,56	0,51

Fig. 5.16 – NTC18 specification for tubular section classification [40]

It is therefore obtained (table 5.4):

t [mm]	80
d [mm]	2300
d/t	28.750

steel	SS316L
fyk [Mpa]	200
ε	1.084
50ε^2	58.750
classe	1
γ M0	1.05

Table 5.4 - Section classification

In the next tables are show the variation of N_{Rd} with increase of member thickness for four different Degree of Pitting (from table 5.5 to table 5.8):

DOP [%]	10					
t [mm]	20	30	40	50	60	70	80
A0 [mm^2]	143257	213942	284000	353429	422230	490403	557947
Ares [mm^2]	128931	192548	255600	318086	380007	441362	502152
Nrd [kN]	24558	36676	48686	60588	72382	84069	95648

Table 5.5 – Variation of resistance capacity for DOP=10%

DOP [%]	20						
t [mm]	20	30	40	50	60	70	80
A0 [mm^2]	143257	213942	284000	353429	422230	490403	557947
Ares [mm^2]	114605	171154	227200	282743	337784	392322	446357
Nrd [kN]	21830	32601	43276	53856	64340	74728	85020

Table 5.6 – Variation of resistance capacity for DOP=20%

DOP [%]	30						
t [mm]	20	30	40	50	60	70	80
A0 [mm^2]	143257	213942	284000	353429	422230	490403	557947
Ares [mm^2]	100280	149760	198800	247400	295561	343282	390563
Nrd [kN]	19101	28526	37867	47124	56297	65387	74393

Table 5.7 – Variation of resistance capacity for DOP=30%

DOP [%]	50					
t [mm]	20	30	40	50	60	70	80
A0 [mm^2]	143257	213942	284000	353429	422230	490403	557947
Ares [mm^2]	71628	106971	142000	176715	211115	245201	278973
Nrd [kN]	13643	20375	27048	33660	40212	46705	53138

Table 5.8 – Variation of resistance capacity for DOP=50%

For a better visualization and understanding of the results, the trends corresponding to the 4 different DOP values have been shown on the same graph (figure 5.17):

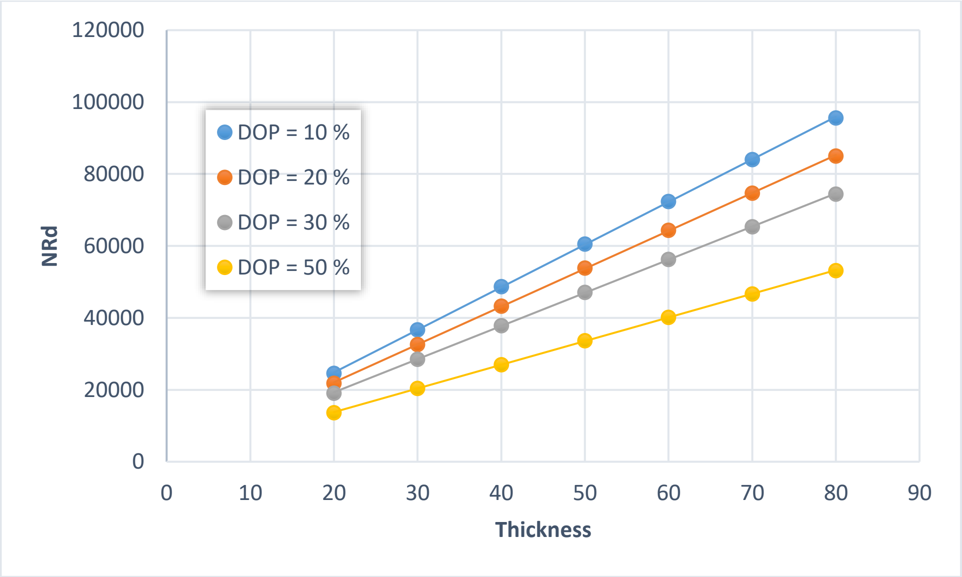

Fig. 5.17 – Trends comparison

It has been realized that the ultimate strength of a pitted specimen is governed by the DOP and its thickness. However the strength assessment may influence as changes of materials properties and aging effect is considered. The results presented in this study shows that corrosion monitoring for strength prediction is necessary and will be very useful for damage tolerant design of steel structures with pit corrosion.

5.2.4 Penalty factors for corroded welded joints

Usually, the go to solution when it comes to offshore fixed structures, jacket-type offshore structure is comprised of tubular structural elements (as they carry little wind load), in any pair combination of 4, 6 or 8 legs, extending from the connection to the topside, on the surface, to the piles attached to the sea bed. The tubular members of an offshore structure are interconnected by welded joints [31].

The primary basic parts of jacket type platforms, are created from circular hollow section (CHS) members by welding the prepared end of brace members onto the undisturbed surface of the chord, resulting in what is called a tubular joint (figure 5.17).

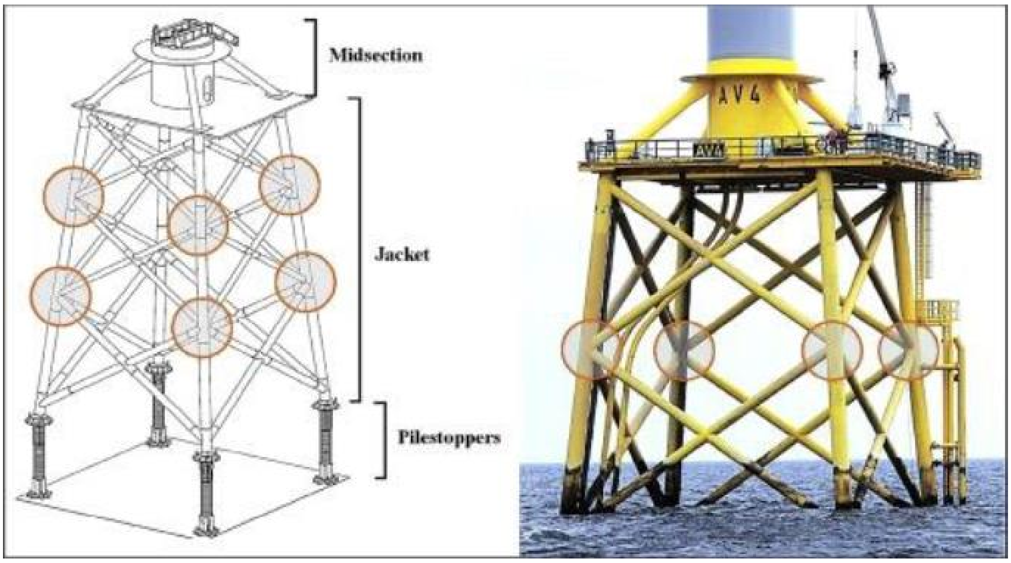

Fig. 5.17 - Example of offshore jacket structure with highlighted tubular joints [31]

Tubular sections are widely used because of their intrinsic properties consisting of the possession of high torsional rigidity and higher strength to weight ratio when compared to the conventional steel sections as well as the capability of minimizing the hydrodynamic forces with a great quality-cost balance.

However, the existing corrosion, especially near the welded parts of these structures is an aspect of extreme relevance with regard to resistance estimation in the context of tubular joints.

In fact, during the welding of stainless steels, regions susceptible to corrosion may develop. The process, called sensitization, is caused by the formation of chromium carbide along the grain boundaries. Sensitization depletes the chromium from the regions adjacent to the grain boundary, leading to the formation of localized galvanic cells.

If the chromium content drops below the 12% necessary to maintain a passive film, the region become susceptible to corrosion, and is likely to suffer intergranular attack. This attack results in weld decay and is most common in the HAZ (Heat-Affected Zones).

Furthermore, preferential weld corrosion occurs in welds when exposed to seawater and other corrosive environments. The weld metal compositions are usually optimized to enhance their mechanical properties; this makes them more anodic than the base steel, causing them to corrode at higher rates compared to their base metals [34].

The static strength and fatigue performance of tubular joints are the governing factors in the design of offshore steel structures. The welded joints may cause large stress concentrations, which severely affect the fatigue life. For offshore structures, which are subjected to considerable dynamic loading from the waves, fatigue is in many cases a dominating design criterion. The combined action of cyclic loading and aggressive environment often results in significant reduction in the fatigue performance compared with that obtained under cyclic loading in inert environments [41].

Fatigue cracks have been noticed in tubular joints during their service lives. Fatigue design recommendations for offshore structures are based on air-fatigue test results, whereas structural joints in offshore installations experience a range of environments for example, spray, full immersion under free corrosion and cathodic protection. Since sufficient corrosion fatigue data for tubular joints are not available, usually a penalty factor – knock down factors (KDF) or design fatigue factors (DFF) – is imposed to account for the effect of corrosion.

There are different DFF values assigned for different types of offshore structures, structural details, detail locations, and other considerations such as access and repair options. Different DFF values were also recommended

in different standards (ISO 19902, DNVGL, ABS). Table 5.9 lists some of the recommended values:

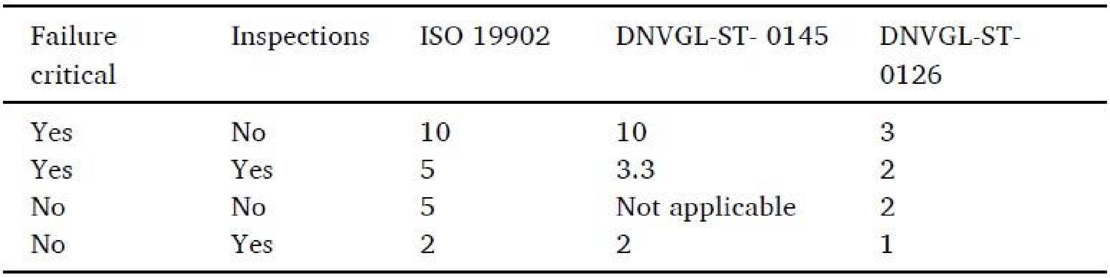

Failure critical	Inspections	ISO 19902	DNVGL-ST- 0145	DNVGL-ST-0126
Yes	No	10	10	3
Yes	Yes	5	3.3	2
No	No	5	Not applicable	2
No	Yes	2	2	1

Table 5.9 - Design Fatigue Factors from different standard [42]

DFFs have been used in fatigue design standards for offshore structures to ensure a desirable level of safety without elaborate reliability analysis.

5.2.5 Capacity loss of k-type joints

In figure 5.18 and 5.19 are shown the main types of tubular welded joints and component definition respectively.

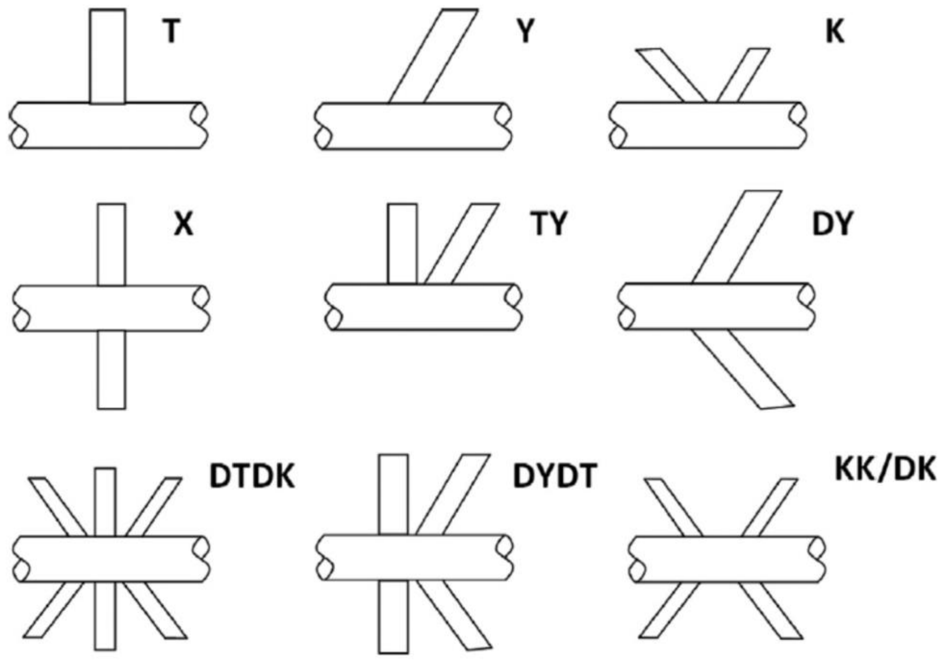

Fig. 5.18 - Types of tubular joints along with their nomenclature [31]

The welded joint consists of a chord (element of largest diameter) connected by one or more braces. These joint gives discontinuity to the structure which leads to stress concentration which in turn depends on joint configuration and loading type. Also it acts at a distance of almost half the diameter of the tubular member in both direction of the joints. Fig. 5.19 shows the region so formed around the joint having most of the stress concentration which is termed as Cans [37].

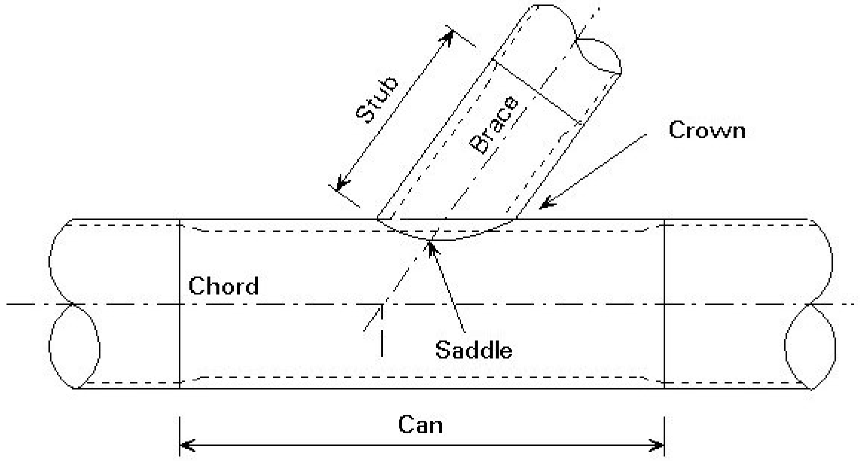

Fig. 5.19 – Component definition of generic tubular joint [35]

Whit reference to the figure 5.19 it is defined:

- The CHORD is the main member, receiving the other components. It is necessarily a through member. The other tubulars are welded to it, without piercing through the chord at the intersection. Other tubulars belonging to the joint assembly may be as large as the chord, but they can never be larger.
- The CAN is the section of the chord reinforced with an increased wall thickness, or stiffeners.
- The BRACES are the structural members which are welded to the chord. They physically terminate on the chord skin.
- The STUB is the extremity of the brace, locally reinforced with an increased wall thickness.

Different positions have to be identified along the brace - chord intersection line:

  - CROWN position is located where the brace to chord intersection crosses the plane containing the brace and chord.
  - SADDLE position is located where the brace to chord intersection crosses the plane perpendicular to the plane containing the brace and chord, which also contains the brace axis.

This study focuses on the static strength of K-type joints as can be seen from the j*acket view* in Figure 5.20.

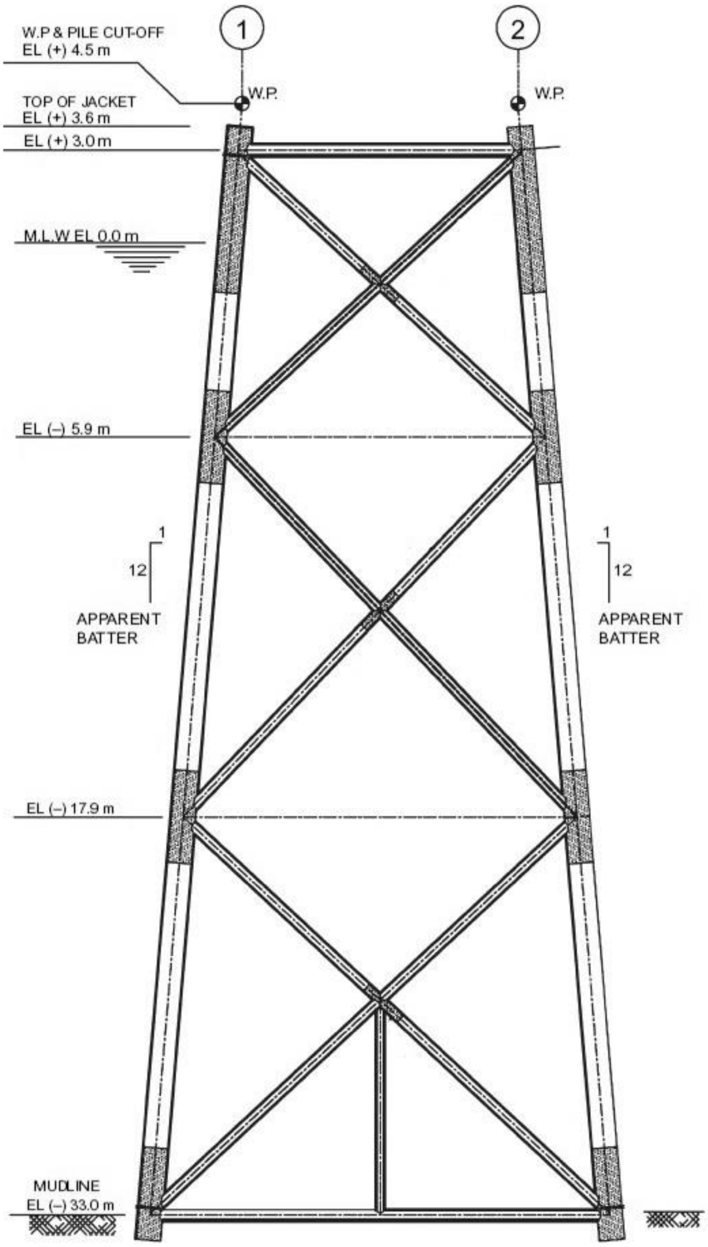

Fig. 5.20 - Jacket views [33]

The calculation of the joint strength is carried out in accordance with Eurocode 3 - Part 1-8 which specifies the following (table 5.10):

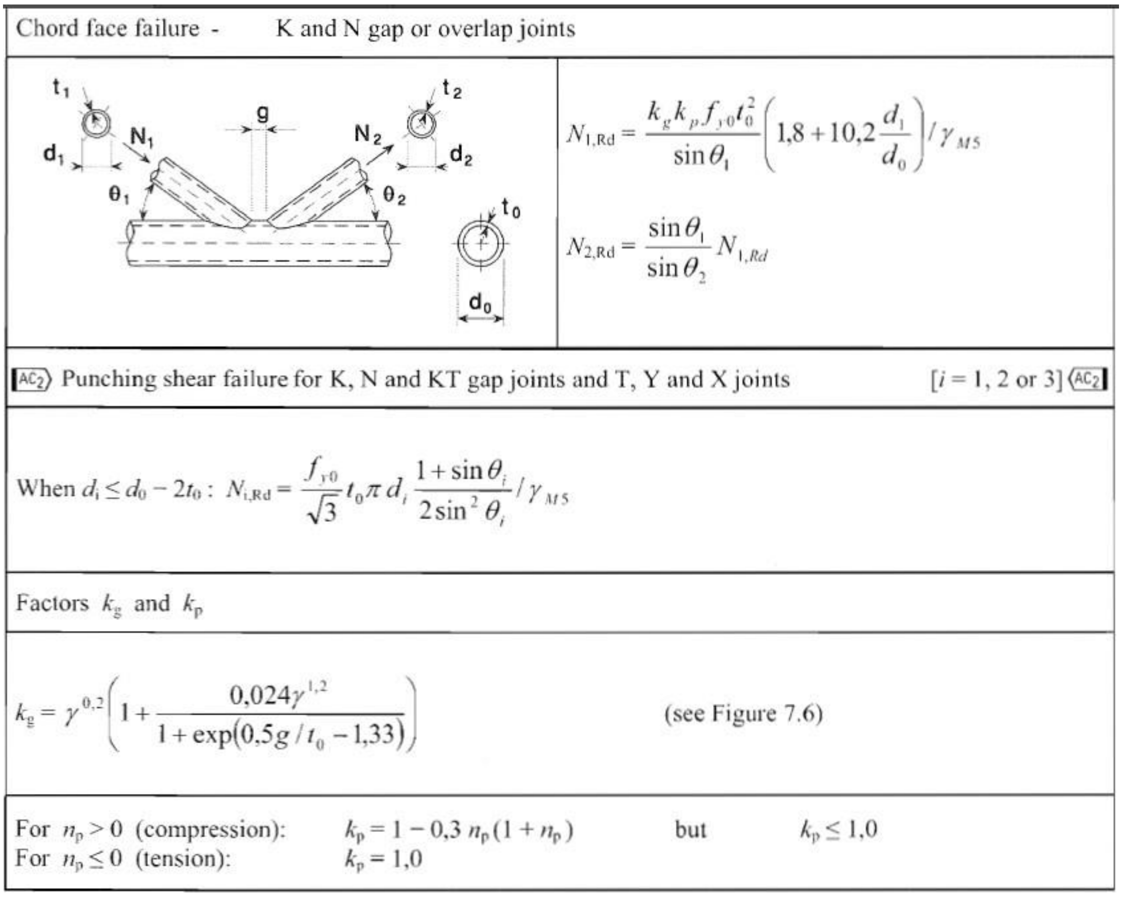

Chord face failure - K and N gap or overlap joints

$$N_{1,Rd} = \frac{k_g k_p f_{y0} t_0^2}{\sin\theta_1}\left(1,8+10,2\frac{d_1}{d_0}\right)/\gamma_{M5}$$

$$N_{2,Rd} = \frac{\sin\theta_1}{\sin\theta_2} N_{1,Rd}$$

AC2 Punching shear failure for K, N and KT gap joints and T, Y and X joints [i = 1, 2 or 3] AC2

When $d_i \le d_0 - 2t_0$: $N_{i,Rd} = \frac{f_{y0}}{\sqrt{3}} t_0 \pi d_i \frac{1+\sin\theta_i}{2\sin^2\theta_i}/\gamma_{M5}$

Factors k_g and k_p

$k_g = \gamma^{0,2}\left(1+\frac{0,024\gamma^{1,2}}{1+\exp(0,5g/t_0-1,33)}\right)$ (see Figure 7.6)

For $n_p > 0$ (compression): $k_p = 1 - 0,3\, n_p(1+n_p)$ but $k_p \le 1,0$

For $n_p \le 0$ (tension): $k_p = 1,0$

Table 5.10 - Design axial resistances of welded joints between CHS brace members and CHS chords [36]

The respective geometrical properties are included in Table 5.11 below.

t_0 initial [mm]	95
d_0 [mm]	2300
t_1 initial [mm]	40
d_1 [mm]	1200
g (gap) [mm]	90
θ_1 [°]	38.4185
θ_1 [rad]	0.6705
γ	12.1053
γ_{M5}	1
f_{y0} [Mpa]	200

Table 5.11 - Member dimensions and material properties

For joints within the range of validity given in Table 5.12, only chord face failure and punching shear need be considered. The design resistance of a connection should be taken as the minimum value for these two criteria.

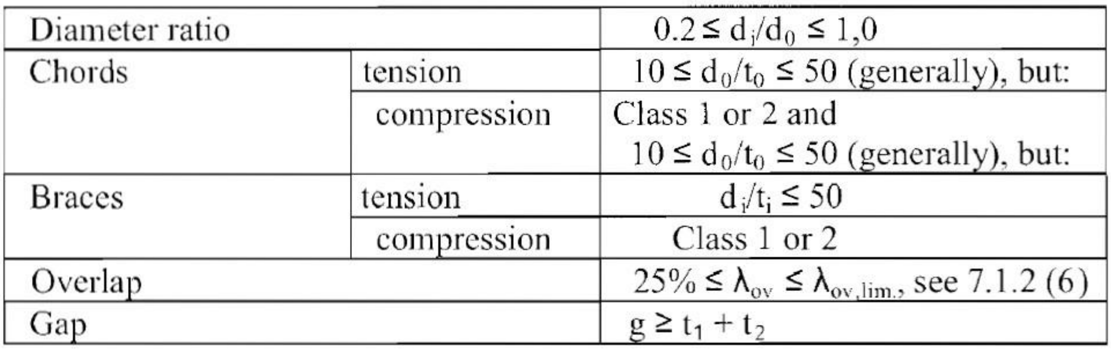

Diameter ratio		$0.2 \leq d_i/d_0 \leq 1,0$
Chords	tension	$10 \leq d_0/t_0 \leq 50$ (generally), but:
	compression	Class 1 or 2 and $10 \leq d_0/t_0 \leq 50$ (generally), but:
Braces	tension	$d_i/t_i \leq 50$
	compression	Class 1 or 2
Overlap		$25\% \leq \lambda_{ov} \leq \lambda_{ov,lim.}$, see 7.1.2 (6)
Gap		$g \geq t_1 + t_2$

Table 5.12 - Range of validity for welded joints between CHS brace members and CHS chords [36]

In this case all limits are respected (table 5.13):

Limits	
$0.2<d_1/d_0<1$	0.52173913
$10<d_0/t_0<50$	24.21052632
$d_1/t_1<50$	30
$g>2t_1$	80

Table 5.13 - Checking of geometric limits

The parametric study is carried out by varying years of deterioration (T) that is to say that is to say by varying the thickness of the tubular members as shown in table 5.14.

T [years]	0	5	10	15	20	25	30	35	40	45	50
c(T) [mm]	0.000	0.000	5.436	9.464	13.091	16.478	19.699	22.792	25.784	28.691	31.525
d(T) [mm]	95.000	95.000	89.564	85.536	81.909	78.522	75.301	72.208	69.216	66.309	63.475

Table 5.14 – Average thickness of the corroded tubular members

Having adopted the corrosion model presented in the previous chapter:

$$c\,(T) = 1.5\,(T-T_0)^{0.8} \qquad (5.15)$$

$$d\,(T) = t_0 - c\,(T) \qquad (5.16)$$

where c (T) is the corrosion wastage at age T; T_0 is the year when thickness of the plates starts to deviate from the as-built condition; d (T) is the remaining thickness at age T; t_o is the initial thickness of the tubular members.

The age when the corrosion starts, T_0, is itself a random variable. It can follow some distribution, like the lognormal distribution, the normal distribution, and the Weibull distribution. And T_0 can vary in a wide range. It is generally acknowledged that coating breakdown starts to take place in certain places when a structure is between 2 and 10 years old. Therefore, it can be expected that T_0 varies from 2 to 10 years [38].

In this case, the coating life T_0 is assumed to be a constant value, 5 years.

Finally, the following resistance values (table 5.15) of normal stress were obtained with reference to the plasticization of the chord face ($N_{Rd,ch}$) and to punching shear ($N_{Rd,ps}$):

T [years]	0	5	10	15	20	25	30	35	40	45	50
kg	2.200	2.200	2.195	2.191	2.187	2.183	2.179	2.174	2.169	2.164	2.159
$N_{Rd, ch}$ [kN]	45501	45501	40355	36740	33630	30849	28315	25984	23824	21814	19939
$N_{Rd, pu}$ [kN]	86824	86824	81856	78174	74860	71764	68821	65993	63259	60603	58012

Table 5.15 - Design axial resistances of welded joints

In this paper only parametric study has been considered.

Figure 5.21 gives the relationship between years of deterioration plotted on the x-axis with chord face failure along the y-axis. It is observed that with increase in time, ultimate strength decreases considerably.

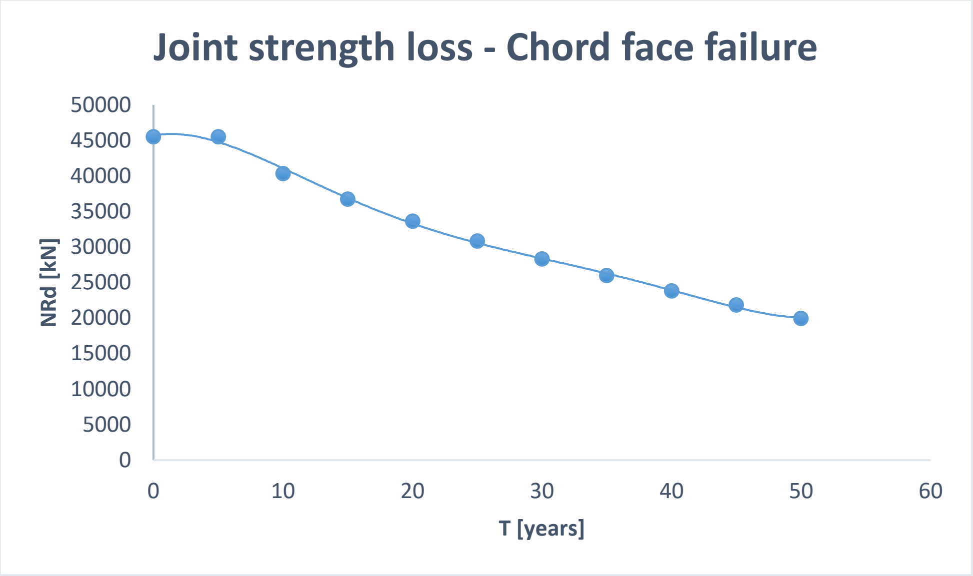

Figure 5.21 - $N_{Rd, ch}$ *evolution over time*

Figure 5.22 gives the relationship between years of deterioration plotted on the x-axis with punching shear failure along the y-axis. It is observed that with increase in time there is a remarkable decrease in ultimate strength.

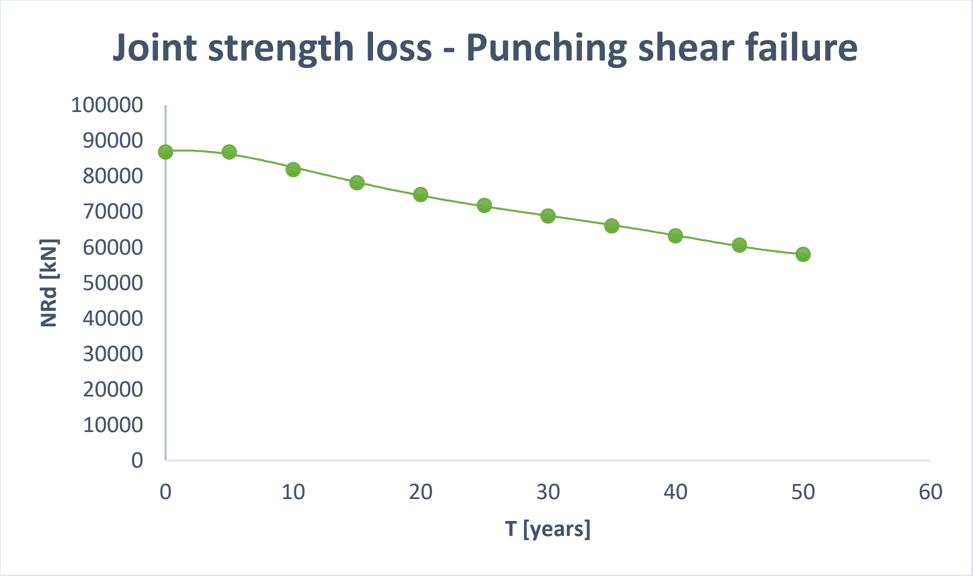

Figure 5.22 - $N_{Rd, pu}$ *evolution over time*

Comparing the two trends, it can be seen that $N_{Rd, ch}$ decreases faster than $N_{Rd, pu}$. This implies that the presence of long-term corrosion has a greater influence on the chord face failure of the tubular welded joint.

Conclusion

History shows that pitting corrosion is a dominant cause of structural failure in marine and offshore sectors. The reason for this is due to the well-known fact that seawater is an aggressive corrosive environment and the structures are generally fabricated with alloy steel which favours pitting corrosion.

In order to carry out the residual safety assessment of a corroded offshore structure, it is necessary to describe the loss of material due to corrosion or the depth of maximum depth pits. A good prediction of the strength reduction of steel structures is largely dependent on the quality of the corrosion prediction.

Pitting corrosion has been studied for several decades and considerable understanding of the pitting phenomenon has been generated. However it is a stochastic, probabilistic phenomenon that requires interdisciplinary concepts that incorporate surface science, metallurgy/material science, hydrodynamics and chemistry, so it is a complex problem which still arouses interest in many engineers.

In future research, one of the aims would be apply the prediction of capacity loss to understand at what level of corrosion it is necessary to implement intervention measures against damaged elements and which is the most performing repair technique for aging offshore steel structures.

References

[1] “Corrosion Engineering - Principles and Practice” - Pierre R. Roberge, Ph.D., P.Eng.

[2] https://theconstructor.org/structural-engg/steel/different-types-corrosion/35536/

[3] “Corrosion Control For Offshore Structures” - Ramesh Singh

[4] https://www.materialsperformance.com/articles/corrosion-basics/2020/12/corrosion-impact-of-offshore-platforms-structures-and-vessels

[5] "NOAA Ocean Explorer: Expedition to the Deep Slope" - https://oceanexplorer.noaa.gov/explorations/06mexico/background/oil/media/types_600.html

[6] https://www.google.az/search?q=Causes+for+failure+in+offshore+platforms

[7] “A review of offshore platform failure statistics” – Thesis - Kamran Abbasov

[8] “Corrosion in marine and offshore steel structures: Classification and overview” - Nour Eldeen M. A. Abo Nassar

[9] “Atmospheric and Marine Corrosion: Influential Environmental Factors and Models” - Y K Cai , Y Zhao , Z K Zhang , X B Ma and B Cheng

[10] “A Life at Sea and the Corrosion Fatigue Lives of Offshore Structures” - Daniel J. Thomas; https://doi.org/10.1007/s11668-021-01158-y

[11] “Predicting the future’ is essential to prevent damages to offshore structures” - Sam Tabahriti - https://www.offshore-

technology.com/analysis/ predict-future-prevent-damage-offshore-structure/

[12] “Expected implications of climate change on the corrosion of structures” - Joint Research Centre Technical report

[13] “Modelling of Pitting Corrosion in Marine and Offshore Steel Structures – A Technical Review” - Journal of Loss Prevention in the Process Industries

[14] “Modeling and Prediction of Long-Term Corrosion of Steel in Marine Environments” - Robert E. Melchers - Centre for Infrastructure Performance and Reliability, The University of Newcastle

[15] “Pitting Degradation Modeling of Ocean Steel Structures Using Bayesian Network” - Jyoti Bhandari, Faisal Khan, Rouzbeh Abbassi, Vikram Garaniya, Roberto Ojeda

[16] “An overview of maintenance management strategies for corroded 1 steel structures in extreme marine environments” - Muntazir Abbas, Mahmood Shafiee

[17] “Push Over Analysis Of Uniform Corrsion Damaged On Fixed-Jacket Strcuture” -Thesis - Zulhelmy Bin Za’aba

[18] “Long-term anticorrosion technology for steel structures, such as jackets, constructed in coastal areas” - https://www.jfe-eng.co.jp/en/products/bridge/kanren04.html

[19] https://flowergarden.noaa.gov/science/toolstech.html

[20] https://en.wikipedia.org/wiki/Autonomous_underwater_vehicle#/media/File:BPAUV-MP_from_HSV-.jpg

[21] https://www.metengr.com/testing-services/metallurgical/metallographic-exam

[22] https://www.twi-global.com/technical-knowledge/faqs/what-is-non-destructive-testing

[23] “Progress in developing realistic corrosion models” - Robert E. Melchers - Centre for Infrastructure Performance and Reliability, The University of Newcastle, Newcastle, Australia

[24] “The Effect of Pitting Corrosion on the Strength Capacity of Steel Offshore Structures” - R. Abdel-Ghany, S. Saad-Eldeen, H. Leheta

[25] “The effect of corrosion on the structural reliability of steel offshore structures” - Robert E. Melchers

[26] “Reliability And Integrity Management Of Ocean Structures” - Jyoti Prasad Bhandari, B.Eng. (Hons) Ocean Engineering

[27] “Marine Structural Design Calculations” - Mohamed A. El-Reedy, Ph.D.

[28] “Welding of Offshore Structures” - John du Plessis, Chief Executive Officer, Spesmet Technology

[29] “A Review of Trends for Corrosion Loss and Pit Depth in Longer-Term Exposures” - Robert E. Melchers

[30] https://en.wikipedia.org/wiki/Eurocodes

[31] “Analysis Of A Typical Offshore Tubular Kt-Joint To Evaluate The Scf And Sif Values” - João Nuno da Silva Pedro Castanheira da Costa

[32] “Condition Assessment Techniques for Aged Fixed-Type Offshore Platforms Considering Decommissioning: a Historical Review” - Mohamed Mubarak Abdul Wahab & V. John Kurian & Mohd Shahir Liew & Do Kyun Kim

[33] “Marine Structural Design Calculations” - Mohamed A. El-Reedy, Ph.D

[34] “Causes and Prevention of Corrosion on Welded Joints” - Kasay Mwiks

[35] “Tubular Joints in Offshore Structures” - http://fgg-web.fgg.uni-lj.si/~/pmoze/ESDEP/master/wg15a/l0700.htm

[36] EN 1993-1-8 – “Eurocode 3: Design of steel structures - Part 1-8: Design of Joints”

[37] “A Parametric Study On Efficiency Of Tubular Joint Cans In Offshore Structures” - Aswindas. M, Venugopal. S.V, I. Yamini Sreevalli

[38] “Time-varying ultimate strength of aging tanker deck plate considering corrosion effect” - Jinting Guo, Ge Wang, Lyuben Ivanov, Anastassios N. Perakis

[39] “Compressive Strength of Tubular Members with Localized Pitting Damage Considering Variation of Corrosion Features” - Renhua Wang, Haichao Guo, R Ajit Shenoi.

[40] Norme tecniche per le costruzioni (NTC) – Aggiornamento del 17 Gennaio 2018

[41] “Fatigue crack growth in stiffened steel tubular joints in seawater environment” - P. Gandhi, D.S. Ramachandra Murthy, G. Raghava, A.G. Madhava Rao

[42] “Calibration of design fatigue factors for offshore structures based on fatigue test database” - Wangwen Zhao